



Fall 1977

Geology and Mineral Deposits of the Southwest Quarter of the Tanacross D-1 Quadrangle, Alaska

Roger Douglas Gill
Western Washington University

Follow this and additional works at: <https://cedar.wwu.edu/wwuet>



Part of the [Geology Commons](#)

Recommended Citation

Gill, Roger Douglas, "Geology and Mineral Deposits of the Southwest Quarter of the Tanacross D-1 Quadrangle, Alaska" (1977).
WWU Graduate School Collection. 824.
<https://cedar.wwu.edu/wwuet/824>

This Masters Thesis is brought to you for free and open access by the WWU Graduate and Undergraduate Scholarship at Western CEDAR. It has been accepted for inclusion in WWU Graduate School Collection by an authorized administrator of Western CEDAR. For more information, please contact westerncedar@wwu.edu.

GEOLOGY AND MINERAL DEPOSITS OF THE SOUTHWEST QUARTER
OF THE TANACROSS D-1 QUADRANGLE, ALASKA

A Thesis
Presented to
the Faculty of
Western Washington University

In Partial Fulfillment
of the Requirements for the Degree
Master of Science

by
Roger D. Gill
October 1977

GEOLOGY AND MINERAL DEPOSITS OF THE SOUTHWEST QUARTER
OF THE TANACROSS D-1 QUADRANGLE, ALASKA

by

Roger D. Gill

Accepted in Partial Completion
of the Requirements for the Degree
Master of Science

Dean of Graduate School

Advisory Committee

Chairman

MASTER'S THESIS

In presenting this thesis in partial fulfillment of the requirements for a master's degree at Western Washington University, I grant to Western Washington University the non-exclusive royalty-free right to archive, reproduce, distribute, and display the thesis in any and all forms, including electronic format, via any digital library mechanisms maintained by WWU.

I represent and warrant this is my original work and does not infringe or violate any rights of others. I warrant that I have obtained written permissions from the owner of any third party copyrighted material included in these files.

I acknowledge that I retain ownership rights to the copyright of this work, including but not limited to the right to use all or part of this work in future works, such as articles or books.

Library users are granted permission for individual, research and non-commercial reproduction of this work for educational purposes only. Any further digital posting of this document requires specific permission from the author.

Any copying or publication of this thesis for commercial purposes, or for financial gain, is not allowed without my written permission.

Name: Robert Gill

Signature: [Handwritten Signature]

Date: 5-16-18

TABLE OF CONTENTS

	Page
ABSTRACT	1
INTRODUCTION	2
Purpose	2
Procedure	2
Geographic Setting	3
Geologic Setting	3
Regional Structures	6
Porphyry Belt	9
Acknowledgements	11
LITHOLOGY	13
Metamorphic Rock Units	13
Greenschist Unit	13
Greenschist Unit 1	14
Greenschist Unit 2	14
Mica Schist Unit	14
Marble Unit	14
Skarn-like Rock	14
Meta-quartzdiorite	15
Pelly Gneiss (Augen Gneiss)	15
Igneous Rock Units	15
Diorite	17
Monzodiorite and Monzonite	17
Granodiorite	18
Gabbro	18
Andesite	18

TABLE OF CONTENTS (contd.)

	Page
Hornblende Andesite	19
Pyroxene Andesite	19
Hornblende-Pyroxene Andesite Porphyry	19
Basalt	19
STRUCTURE	23
Local Structure	23
Landsat Imagery	26
Magnetics	28
Aeromagnetics	28
Ground Magnetics	30
MINERAL DEPOSITS	35
Alteration	35
Propylitic Alteration	37
Phyllic Alteration	37
Potassic Alteration	38
Silicification	39
Alteration Zoning Patterns	40
Carbonatization	42
Economic Mineralization	43
Geochemistry	44
Analytical Procedure	45
Statistical Methods	45
Interpretation	60
Geochemistry of the Pika Canyon Claim Block Area	66
Geochemistry of the Fishhook Prospect Area	73

TABLE OF CONTENTS (contd.)

	Page
Geochemistry of the NE Pika Canyon Claim Block Area	73
Economic Evaluation and Comparison of the Map Area Prospects with Known Mineral Deposits in the Interior Porphyry Belt	80
SUMMARY AND CONCLUSIONS	84
REFERENCES	89
APPENDIX A - Mineral assemblages observed in thin section	92
APPENDIX B - Raw geochemical and magnetic data	104
PLATES	
PLATE 1 - Index map showing petrography sample locations	Pocket
PLATE 2 - Bedrock geology map of the thesis area	Pocket
PLATE 3 - Reconnaissance alteration map of the thesis area	Pocket
PLATE 4 - Index map showing reconnaissance soil sample localities	Pocket
PLATE 4a - Map showing Cu/Mo geochemistry from the recon- naissance soil samples	Pocket
PLATE 4b - Map showing Zn/Ag geochemistry from the recon- naissance soil samples	Pocket
PLATE 5 - Index map showing reconnaissance rock-chip sample localities	Pocket
PLATE 5a - Map showing Cu/Mo geochemistry from the recon- naissance rock-chip samples	Pocket
PLATE 5b - Map showing Zn/Ag geochemistry from the recon- naissance rock-chip samples	Pocket
PLATE 6 - Index map showing reconnaissance stream-sediment sample localities	Pocket
PLATE 6a - Map showing Cu/Mo geochemistry from the recon- naissance stream-sediment samples	Pocket
PLATE 6b - Map showing Zn/Ag geochemistry from the recon- naissance stream-sediment samples	Pocket

FIGURES

Figure	Page
1. Location of the study area.	4
2. Topographic map of the study area showing claim blocks and prospects.	5
3. Reconnaissance geologic map of the study area.	7
4. Map of major transcurrent dextral faults of Alaska.	8
5. Map showing Interior Porphyry copper belt of Alaska.	10
6. Pelly Gneiss with augen of K-feldspar.	16
7. Dike of alkaline basalt.	20
8. Generalized cross sections through the Pika Canyon, NE Pika Canyon, and Fishhook prospect areas.	25
9. Lineaments and mapped faults of the study area.	27
10. Aeromagnetic map of the study area.	29
11. Magnetic contour map of the Pika Canyon claim block.	31
12. Magnetic contour map of the NE Pika Canyon claim block.	33
13. Alteration zoning in a typical porphyry copper-type ore deposit.	36
14. Frequency histogram of copper concentrations based on 955 soil samples.	47
15. Frequency histogram of molybdenum concentrations based on 955 soil samples.	48
16. Frequency histogram of zinc concentrations based on 955 soil samples.	49
17. Frequency histogram of silver concentrations based on 955 soil samples.	50
18. Frequency histogram of copper concentrations based on 97 rock-chip samples.	51
19. Frequency histogram of molybdenum concentrations based on 97 rock-chip samples.	52
20. Frequency histogram of zinc concentrations based on 97 rock-chip samples.	53

FIGURES (contd.)

Figure	Page
21. Frequency histogram of silver concentrations based on 97 rock-chip samples.	54
22. Frequency histogram of copper concentrations based on 53 stream-sediment samples.	55
23. Frequency histogram of molybdenum concentrations based on 53 stream-sediment samples.	56
24. Frequency histogram of zinc concentrations based on 53 stream-sediment samples.	57
25. Frequency histogram of silver concentrations based on 53 stream-sediment samples.	58
26. Distribution of copper based on anomalous values from reconnaissance soil, rock-chip, and stream-sediment samples.	62
27. Distribution of molybdenum based on anomalous values from reconnaissance soil, rock-chip, and stream-sediment samples.	63
28. Distribution of zinc based on anomalous values from reconnaissance soil, rock-chip, and stream-sediment samples.	64
29. Distribution of silver based on anomalous values from reconnaissance soil, rock-chip, and stream-sediment samples.	65
30. Sample index map for the Pika Canyon claim block soil grid.	67
31. Pika Canyon geochemical contour map for copper based on soil grid samples.	68
32. Pika Canyon geochemical contour map for molybdenum based on soil grid samples.	69
33. Pika Canyon geochemical contour map for zinc based on soil grid samples.	70
34. Pika Canyon geochemical contour map for silver based on soil grid samples.	71
35. Schematic vertical cross section of mineralization in a typical porphyry copper-type ore deposit.	72
36. Sample index map for the NE Pika Canyon claim block soil grid.	75

FIGURES (contd.)

Figure		Page
37.	NE Pika Canyon geochemical contour map for copper based on soil grid samples.	76
38.	NE Pika Canyon geochemical contour map for molybdenum based on soil grid samples.	77
39.	NE Pika Canyon geochemical contour map for zinc based on soil grid samples.	78
40.	NE Pika Canyon geochemical contour map for silver based on soil grid samples.	79
41.	Location of major mineral deposits and thesis area within the interior porphyry belt.	81

TABLES

Table	Page
1. Whole rock geochemical analysis and C. I. P. W. norm of alkaline basalt.	21
2. Table showing how the elements copper, molybdenum, zinc, and silver for soil, rock-chip, and stream-sediment samples are classed into the anomalous groups.	59
3. General description of mineral deposits within the interior porphyry belt.	82

ABSTRACT

The study area is in the northeast corner of the Tanacross quadrangle, east-central Alaska. Known as the Interior Porphyry belt, it lies between the Tintina fault to the north and the Denali fault to the south. Seven major porphyry copper-type deposits have been found within the belt since 1969. Because much of the belt was unglaciated during Pleistocene time, the probability of finding a zone of supergene enrichment is enhanced. In Alaska a porphyry copper-type deposit with a supergene zone may improve the current economic status by helping to facilitate amortization of production capital costs.

The rocks within the study area consist mainly of Paleozoic or older schists and gneiss units that have been intruded by late Cretaceous-early Tertiary igneous rocks.

Limited exposures, residual soils, and thick brush in the Tanacross area have necessitated the use of reconnaissance geochemistry, aeromagnetism, and Landsat imagery to locate areas of potential mineralization. Three such areas were found within the study area; they have been named Pika Canyon, NE Pika Canyon, and Fishhook prospects. The Pika Canyon and NE Pika Canyon prospects have been studied by detailed soil geochemistry, ground magnetism, and geologic and alteration mapping. Only the geology and alteration have been mapped at the Fishhook prospect. Work completed at the three prospects indicates that Pika Canyon and Fishhook prospects represent potential porphyry copper-type deposits, and that NE Pika Canyon is possibly a structurally controlled copper-zinc deposit.

At the present stage of exploration the economic potential of these prospects cannot be determined.

INTRODUCTION

Purpose

Since 1969 three major porphyry-type copper-molybdenum deposits and numerous prospects have been discovered in the area between the Denali and Tintina faults in the Tanacross quadrangle. The quadrangle was not glaciated, partly because of the arid climate during Pleistocene time (Gleeson and Brummer, 1976). This type of climate can result in deep oxidation, with the formation of a blanket of supergene chalcocite to yield enriched porphyry-type deposits. High costs of production in Alaska require finding a substantial high-grade zone of supergene enrichment which could be produced early in the life of a mine to facilitate amortization of production capital costs. Therefore, the purpose of this study is to describe the lithology, alteration and structure of the rocks, and, with the aid of geochemical, magnetic, and Landsat imagery data, to outline areas for further mineral exploration in the southwest quarter of the Tanacross D-1, Alaska quadrangle.

Procedure

Approximately 3½ weeks were spent in the field. Geology was plotted on the Tanacross D-1 Alaska 15-minute quadrangle map enlarged to the scale of 1:24,000. The best exposures are found mainly at higher elevations and along ridge crests; exposures are poor elsewhere. Approximately 200 thin sections were made and studied using the flat stage, and a few rocks were studied by X-ray diffraction techniques.

A total of 1105 samples were collected during the years 1974, 1975, and 1976, and of these 955 are soil, 97 rock-chip, and 53 stream-sediment samples. Two claim blocks, Pika Canyon and NE Pika Canyon are within the map area and are currently held by Cities Service Minerals Corporation. Both were sampled for soil geochemistry on a grid 200 by 500 feet.

A ground magnetic survey was conducted on both claim blocks along the same grid coordinates as the geochemical survey.

Geographic Setting

The Tanacross D-1 Alaska quadrangle (U. S. G. S. map, 1:63,360) is in the Yukon-Tanana Upland; the thesis area includes the southwest quarter of the quadrangle, and includes approximately 36 square miles (Fig. 1). Fig. 2 shows the location of Pika Canyon and NE Pika Canyon claim blocks, and Fishhook and NE Fishhook prospects, all of which will be referred to throughout the text.

Accessibility is limited. The southeast corner of the map area can be approached from the east or south via Winter Trail by all-terrain vehicles, but the main mode of transportation is by helicopter.

The study area is more or less bordered by streams. Sixtymile River flows north along the eastern edge, Dude Creek flows north along the western edge, Liberty Creek flows northwest along the northern edge, and the East Fork Dennison Fork flows south from the southern edge of the map area.

A maximum elevation of 4,810 feet is located on a ridge in the south-central part of the map area, but most ridge crests average between 3,000 and 4,000 feet. Most valleys drop to 2,500 feet or less in elevation, therefore, maximum relief is about 2,000 feet.

Geologic Setting

The Tanacross quadrangle is in an area of erosional maturity that escaped Pleistocene glaciation. Drainages are characterized by V-shaped valleys and an absence of lakes.

The soils in this unglaciated area are residual and thickness varies according to slope and rarely exceeds two feet on hill tops. The upper soil layers are often water-saturated and poorly drained during the summer

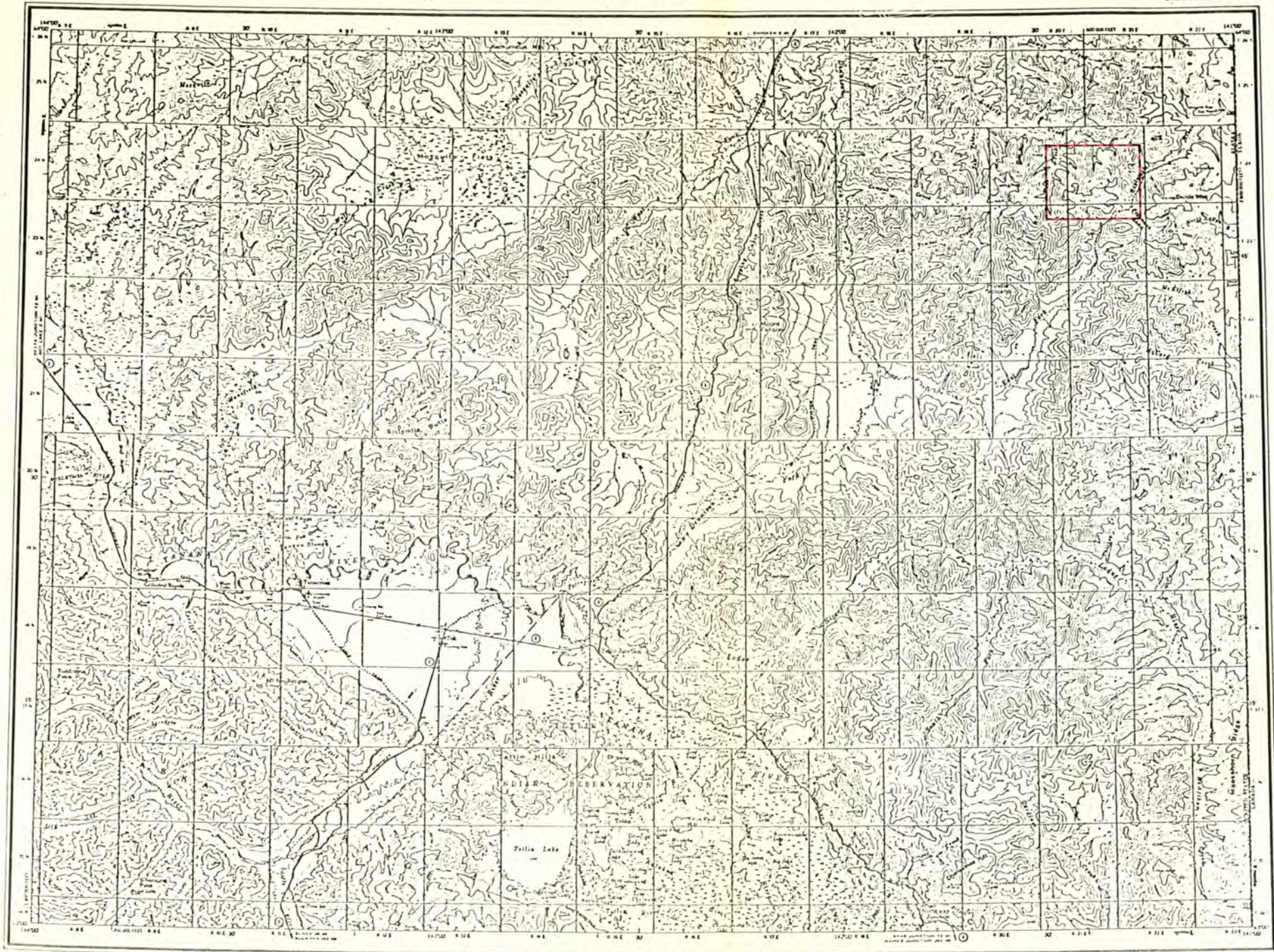


Fig. 1. Location of the study area (outlined in red).

MAILED (EDIT) AND PUBLISHED BY THE GEOLOGICAL SURVEY
 DESIGN BY MISS LUCAS, AND REVISIONS BY MISS LUCAS
 CONTROL BY MISS LUCAS, AND REVISIONS BY MISS LUCAS
 CONTROL BY MISS LUCAS, AND REVISIONS BY MISS LUCAS
 CONTROL BY MISS LUCAS, AND REVISIONS BY MISS LUCAS
 CONTROL BY MISS LUCAS, AND REVISIONS BY MISS LUCAS

ALASKA

SCALE 1 : 500,000

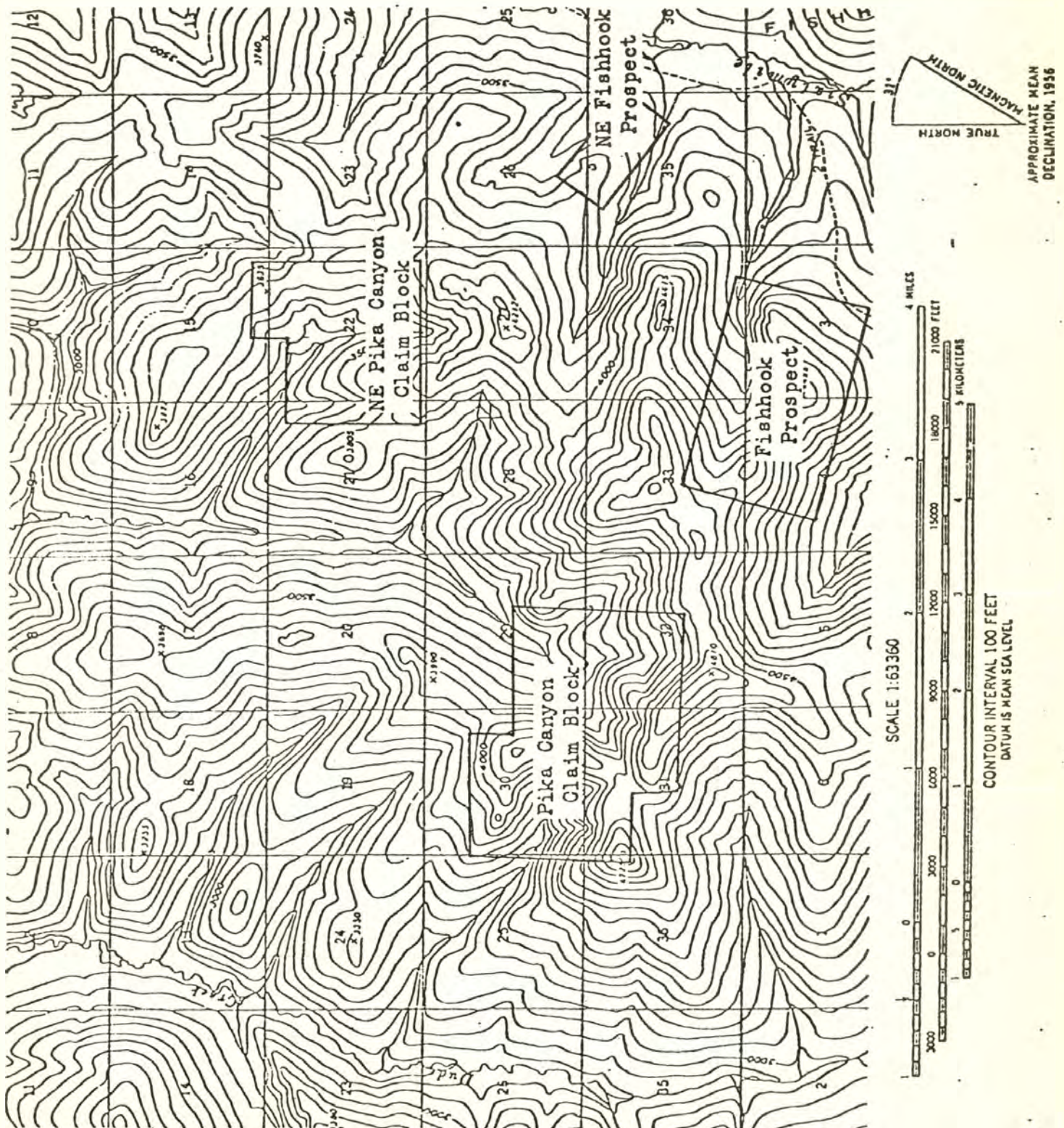
CONTOUR INTERVAL, 200 FEET
 SPOT ELEVATIONS AT 100 FEET INTERVALS
 SPOTS IN RED ARE SPOT ELEVATIONS
 SPOTS IN BLUE ARE SPOT ELEVATIONS
 SPOTS IN GREEN ARE SPOT ELEVATIONS
 SPOTS IN YELLOW ARE SPOT ELEVATIONS
 SPOTS IN ORANGE ARE SPOT ELEVATIONS
 SPOTS IN PURPLE ARE SPOT ELEVATIONS
 SPOTS IN BROWN ARE SPOT ELEVATIONS
 SPOTS IN GREY ARE SPOT ELEVATIONS
 SPOTS IN BLACK ARE SPOT ELEVATIONS

LOCATION INDEX

ROAD CLASSIFICATION
 HIGHWAY
 RAILROAD
 CANAL
 RIVER
 STREAM
 LAKE
 OCEAN

TANACROSS, ALASKA

Fig. 2. Topographic map of the study area, showing locations of Pika Canyon and NE Pika Canyon claim blocks and Fishhook and NE Fishhook prospects.

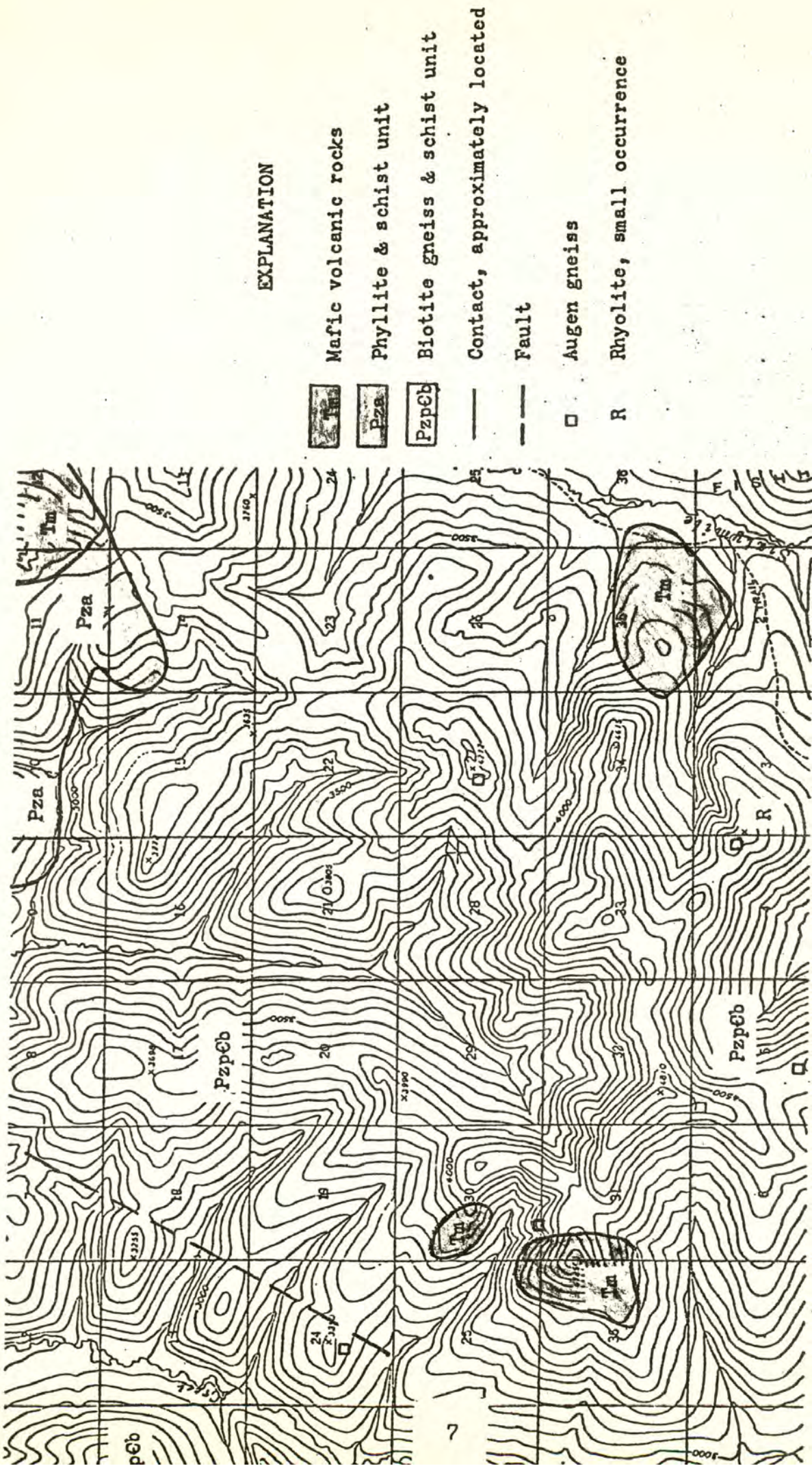


due to a thin, impermeable layer of permafrost. A typical soil section in the map area comprises 3 to 12 inches of poorly decomposed organic material overlying a poorly developed light-brown soil from a few inches to several feet in thickness, which, in turn, overlies frost broken bed-rock detritus.








A reconnaissance geologic map of the Tanacross quadrangle (Foster, 1970) shows three major rock units within the thesis area (Fig. 3). Two metamorphic rock units are recognized, one a Precambrian or early Paleozoic biotite gneiss and schist; and the second a Paleozoic phyllite and schist. The third is a Tertiary mafic volcanic rock unit. The oldest rock unit is characterized primarily by assemblages of quartz-biotite gneiss and schist, quartz-hornblende gneiss, quartz-feldspar-biotite gneiss, augen gneiss, quartz-muscovite-garnet gneiss and quartzite. The phyllite and schist unit consists of light-pink, light-green, tan, and gray phyllite, quartz-sericite schist, quartz-sericite-chlorite schist, quartzite and marble. The mafic volcanic rocks have been described as dark-gray, dark-greenish-gray, and dark-maroon lava, breccia, and tuff, mostly of andesitic composition. The texture varies from uniformly fine-grained to coarsely porphyritic.

Regional structures

The thesis area is located between the Denali and Tintina faults (Fig. 4). Freeland and Dietz (1973) have described the faults as trans-current dextral faults of assumed Paleozoic age, and postulate that the area between them is part of the North American Craton. They have suggested that the faults formed as Alaska rotated counterclockwise around poles near the eastern end of the faults. As the blocks rotated, each moved to the right with respect to the next block south. A second interpretation has been proposed by Foster and Keith (1974), who have



EXPLANATION

-  Mafic volcanic rocks
-  Phyllite & schist unit
-  Biotite gneiss & schist unit
-  Contact, approximately located
-  Fault
-  Augen gneiss
-  Rhyolite, small occurrence

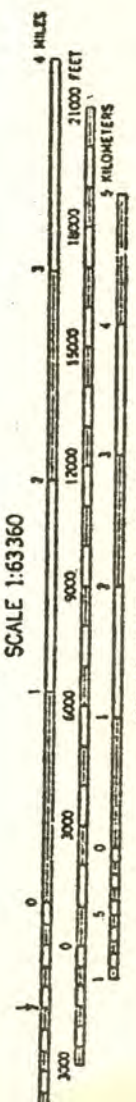


Fig. 3. Reconnaissance geologic map of the study area (modified after Foster, 1970).

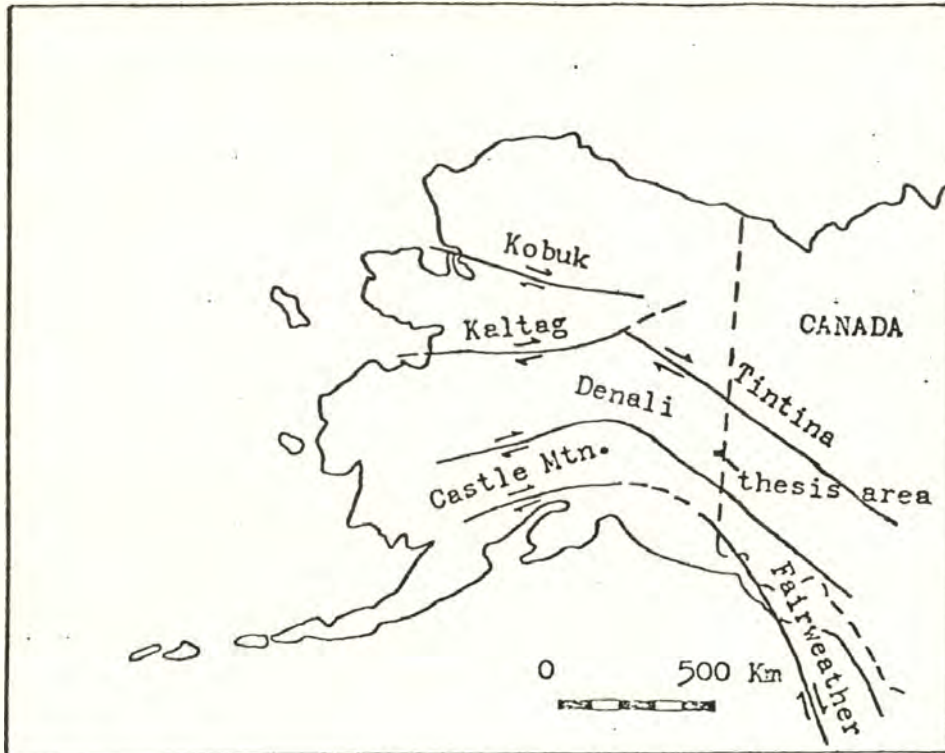


Fig. 4. Sketch map showing the major transcurrent dextral faults of Alaskā and their relation to the thesis area (modified after Freeland and Dietz, 1973).

suggested that the metamorphic terrain between the two faults is an allochthonous slice of continental material that has moved northward, and that the Tintina fault system may represent a late Paleozoic plate boundary. They also consider that the Denali fault may represent a suture zone between the allochthonous slice and an island arc complex.

Prindle Volcano, a small inactive basaltic cone of Quaternary age, is located about eight miles southwest of the thesis area (Fig. 1). The alkali-olivine basalt in places contains abundant ultramafic and granulite inclusions (Foster, and others, 1966). The occurrence of this rock assemblage suggests a mantle source, possibly a deep seated tear fault resulting from movement along the Denali or Tintina fault system, or both.

Foster and Keith (1974) have mapped numerous occurrences of ultramafic rocks north of the thesis area and south of the Tintina fault. They believe that some of the ultramafics are alpine-type peridotites and possibly dismembered ophiolite. The Tintina fault system may have provided a zone of weakness along which mantle material was tectonically emplaced or it may have been a plate boundary in Paleozoic time.

Porphyry Belts

Hollister and others (1974) suggest that porphyry copper deposits in southern Alaska and contiguous Yukon Territory occur in two broad, but relatively distinct belts. Only the interior belt will be considered in this report. The interior belt lies between the Denali and Tintina faults, and includes the map area (Fig. 5). Hollister and others (1974) noted that the porphyry mineral deposits within this belt are genetically associated with the youngest period of plutonic activity (late Cretaceous-early Tertiary) and that no deposits are known to be related to older plutons. Moreover, all deposits now known in the interior belt are as-

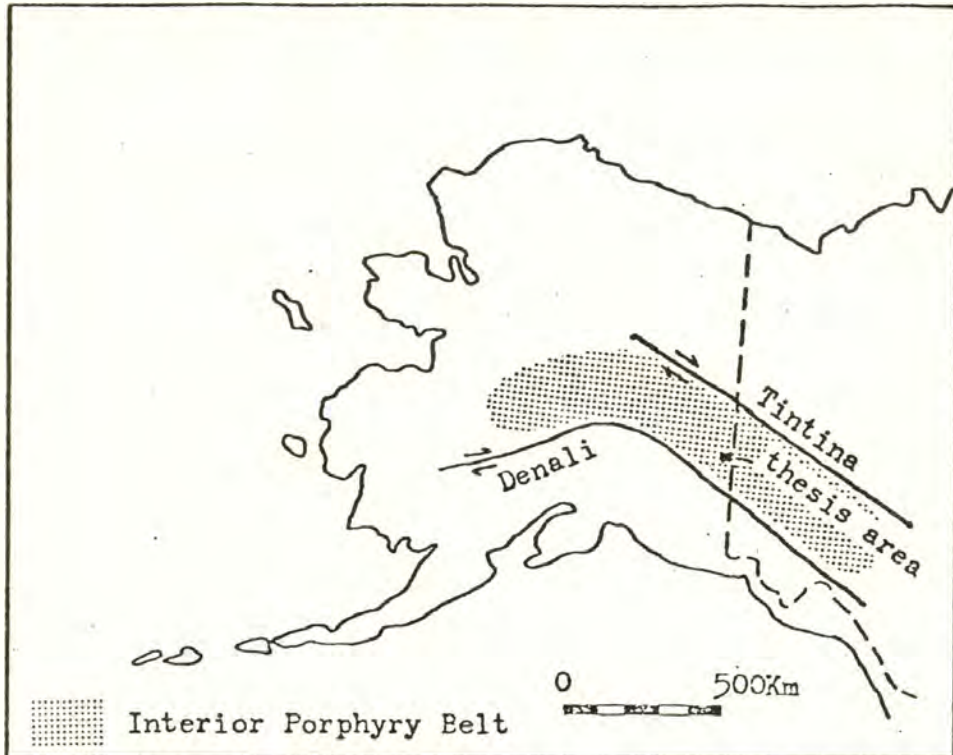


Fig. 5. Sketch map showing the general area of the interior porphyry belt and its relation to the thesis area.

sociated with quartz monzonite porphyry intrusions, and generally exhibit a zoned arrangement of potassic, phyllic, argillic, and propylitic alteration outward from the central core.

Assuming that Freeland and Dietz (1973) were correct in their interpretation that the area between the Denali and Tintina faults represents part of the North American Craton, then a possible correlation could be made between the porphyry copper-type deposits of the interior belt with those of southwestern United States. Lowell and Guilbert (1970) have shown that typical porphyry copper-type deposits of the southwestern United States are generally late Cretaceous or early Tertiary in age, associated with quartz monzonite intrusions, exhibit a zoned arrangement of potassic, phyllic, argillic, and propylitic alteration outward from the central core, and that southwestern United States is part of the North American Craton. The origin of porphyry copper-type deposits of the southwestern United States has been disputed recently and two major theories have been proposed. Sillitoe (1972) suggests that the deposits are due to subduction of exceptionally copper-rich oceanic crust. Alternatively, Lowell (1974) suggests that metals are derived directly from a source in the lower crust or upper mantle and that an ore deposit is produced from a pluton migrating upward along a zone of crustal weakness. The occurrence within North America of two genetically similar but spatially separated porphyry copper-type provinces is of considerable interest, and continued work in both areas may solve the disputed problem of origin, which will aid in future exploration for this type of ore deposit.

Acknowledgements

Sincere gratitude is extended to Cities Service Minerals Corporation of Alaska, who encouraged me to make this study, supplied all geochemical samples, analyses, and provided total financial support and equipment

for the field work.

I am indebted to David Hedderly-Smith, formerly of Cities Service Minerals Corporation for initially suggesting this study, and for his help in drafting the geologic and alteration maps.

Appreciation is extended to Drs. D. R. Pevear, R. S. Babcock, and A. Swineford for their helpful criticism and critical reading of the manuscript.

LITHOLOGY

Lithology within the map area consists mainly of metamorphic rocks that have been intruded by numerous igneous stocks and dikes of various compositions.

Approximately 200 rock samples were collected in the field for petrographic analysis. The sample locations are shown in Plate 1, and the mineral assemblages observed in thin section are given in Appendix A. The geologic map is shown in Plate 2.

Metamorphic Rock Units

Stratigraphic relations, thicknesses, and relative ages of the metamorphic units are obscure because primary layering is lacking and contacts between the metamorphic units are complicated by structural mixing of the rocks during deformation and metamorphism. This does not imply or negate a close stratigraphic relationship among the metamorphic rock units. This section describes the macroscopic and microscopic properties of the metamorphic units within the map area.

The term greenschist was used in the field to classify schist containing greater than 5 percent mafic minerals and was retained in the same context during the petrographic classification. Greenschist has not been used to imply metamorphic grade. The term mica schist was used in both field mapping and petrographic classification to distinguish schists with less than 5 percent mafic minerals. The metamorphic grade of both greenschist and mica schist units is transitional from greenschist to lower amphibolite facies.

Greenschist Unit

The greenschist unit consists dominantly of light-greenish-gray schists that in places show segregation layering. The unit is a heterogeneous metamorphic assemblage that may represent several structurally mixed

stratigraphic units, or it may represent a single assemblage of meta-sedimentary and metavolcanic rocks.

Greenschist Unit 1

Greenschist unit 1 is a dark-greenish-black, feldspar-quartz-biotite schist. Exposures of this unit are small and generally conform to the regional trend of foliation, and probably represent a former thin bed of andesitic or basaltic tuff.

Greenschist Unit 2

Greenschist unit 2 is a dark-greenish, biotite-cordierite-anthophyllite schist which may be genetically related to the skarn-like rock observed near the northeast corner of the NE Pika Canyon claim block. Two occurrences of an apple-green, magnesite-talc-antigorite schist were also noted. They occur as small (500 to several 1,000 square feet) lens-like bodies, and possibly represent small ultramafic bodies that were originally faulted into place and then later metamorphosed.

Mica Schist Unit

The schists range in color from light-green and light-gray to tan, and in places show segregation layering. The mica schist unit is a heterogeneous metamorphic assemblage that may represent several structurally mixed stratigraphic units, or it may represent a single assemblage of metasedimentary and metavolcanic rocks.

Marble Unit

A subordinate marble unit of cream-colored, recrystallized calcite is found at two locations in the map area. Both exposures are small (500 to several 1,000 square feet) elongate bodies parallel to the foliation.

Skarn-Like Rock

Two outcrops of skarn-like rock are found within the mica schist unit. One is located at the northeast corner of the NE Pika Canyon claim

block. It is small (1,000 square feet) and elongate, and possibly represents an impure calcareous quartzite that has been altered by a small concealed intrusive body. The second occurrence is located near the northwest corner of the Fishhook prospect, and possibly represents a contact between the mica schist unit and the Pelly Gneiss, i.e., (the mica schist unit at this location is thought to represent a roof pendant within the Pelly Gneiss).

Meta-Quartzdiorite

The meta-quartzdiorite is dark-greenish-gray metamorphosed rock of quartzdioritic composition. The rock shows a slight schistosity, and metamorphic grade of the epidote-amphibolite facies.

Pelly Gneiss (Augen Gneiss)

The Pelly Gneiss is typically light-colored and characterized by many augen, usually of K-feldspar, rarely of quartz, which range from 2 inches in diameter downward to microscopic dimensions (Fig. 6). The term Pelly Gneiss was first introduced by Brooks (1900) to refer to a rock assemblage of distinct metamorphic lithology found near the mouth of the Pelly river in the Yukon. The term is still used today but it does not imply age or stratigraphic position.

The gneiss has been described by Cockfield (1921) and Mertie (1937) to be derived from metamorphism of a granitic plutonic parent rock. The age of this unit is not known, but Cockfield (1921) was convinced that this gneiss intruded all the Precambrian crystalline rocks, even though he was unable to determine its position in the stratigraphic column.

Igneous Rock Units

The igneous rocks of the thesis area range in composition from silicic to mafic and in texture from fine-grained to porphyritic. The youngest plutonic event of the Tanacross quadrangle was intrusion of small isolated



Fig. 6. Pelly Gneiss with augen of large white to light-gray potassium feldspar crystals.

plutons, including hypabyssal stocks, and eruption of silicic and mafic volcanic rocks during Paleocene time (Foster, and others, 1976). A small andesite plug approximately 3 miles southwest of the thesis area was dated by potassium-argon methods at 64.5 ± 3 and 67.4 ± 3 million years (Foster, and others, 1976). The stocks and dikes within the map area have not been dated but are probably also early Tertiary in age.

The intrusive rocks of the map area range in composition from gabbro to granodiorite, and probably represent small stocks connected in the subsurface to a large pluton.

The extrusive and subvolcanic rocks are mainly andesitic in composition and similar dikes appear to have intruded both the granitic stocks and metamorphic rocks.

Three isolated exposures of basalt are thought to be late Tertiary or Quaternary in age (Foster, 1970).

Diorite

The diorite is dark-blackish-gray and medium to fine-grained. The rock texture is holocrystalline. Most of the plagioclase is zoned and hypidiomorphic, but in several thin sections it is panidiomorphic. The plagioclase is generally incompletely saussuritized, and fine-grained sericite is found throughout the thin sections. Hornblende is generally more abundant than biotite, and in some thin sections primary biotite and much of the primary hornblende are replaced by chlorite. Small amounts of secondary carbonate are evident in a few thin sections.

Monzodiorite and Monzonite

The rocks are dark-gray and medium-grained. When compared to the diorite these rocks are higher in K-feldspar, biotite, and quartz, and lower in hornblende. The rock texture is holocrystalline. Most of the plagioclase is hypidiomorphic and oscillatory zoning is common. Many

of the plagioclase crystals are saussuritized. The other constituents are generally allotriomorphic. Some of the rocks exhibit propylitic or phyllic stages of alteration. At the Pika Canyon claim block, the geologic map (Plate 2) shows rocks of this unit surrounding the granodiorite; suggesting that the rocks may represent the more mafic outer rim of a concentrically zoned stock.

Granodiorite

The granodiorite is light-gray and medium-grained. When compared to the monzodiorite and monzonite unit the granodiorite is higher in quartz, K-feldspar, and biotite, and significantly lower in hornblende and pyroxene. The texture is holocrystalline. Most of the plagioclase is hypidiomorphic and some shows oscillatory zoning. Many of the plagioclase crystals are saussuritized. Biotite is partly altered to chlorite in many of the thin sections. Most of the outcrops are altered and exhibit either propylitic or phyllic alteration, and there is one occurrence of potassic alteration.

Gabbro

The rock is dark-gray to black and fine-grained. The texture is holocrystalline. Most of the plagioclase and biotite is hypidiomorphic and most of the pyroxene allotriomorphic.

Andesite

The andesite is light-gray and porphyritic. The rock has a hyalopilitic groundmass. Most of the plagioclase phenocrysts are hypidiomorphic and have been replaced by sericite. Oscillatory zoning is also characteristic of many plagioclase phenocrysts. Secondary quartz is found throughout most thin sections as anhedral blebs, and some exhibit embayment. Most of the rocks in this unit have been sericitized and, due to strong alteration, generally lack mafic minerals.

Hornblende Andesite

The hornblende andesite is greenish-gray and porphyritic. The rock has a hyalopilitic groundmass. Most of the plagioclase phenocrysts are hypidiomorphic, and in some thin sections the plagioclase has been completely sericitized. The hornblende phenocrysts are generally replaced by chlorite and vary from hypidiomorphic to allotriomorphic and a few thin sections show reaction rims of magnetite. Most of the thin sections examined show either a propylitic or phyllic stage of alteration.

Pyroxene Andesite

The pyroxene andesite varies in color from maroon to blackish-gray, and is porphyritic. The rock has a trachytic to felty groundmass.

Hornblende-Pyroxene Andesite Porphyry

This rock is dark-gray and porphyritic. The plagioclase, hornblende, and pyroxene phenocrysts are hypidiomorphic. Plagioclase phenocrysts are slightly sericitized and some show oscillatory zoning.

Basalt

The rock is dark-gray, porphyritic, and in places vesicular. The rock has a pilotaxitic groundmass. Phenocrysts of hypidiomorphic pyroxene and allitriomorphic olivine lie in a groundmass of granular pyroxene, plagioclase laths, magnetite, and black glass.

One exposure and two small frost boils were located in the field. The exposure (Fig. 7) is a small discordant dike which trends north-south, and the rocks at the frost boils probably represent a similar type of occurrence.

A whole rock chemical analysis of the basalt (sample 51) is shown in table 1, with the C. I. P. W. norm. The analysis was obtained by X-ray fluorescence methods on an EDAX-EXAM, Model 704, energy dispersive spectrophotometer. The rock is low in silica and contains 8.31 percent



Fig. 7. Dike of alkaline basalt trending north-south and intruding the mica schist unit.

Table 1. Chemical composition (oxides, wt %) and C. I. P. W. norm for basalt (sample 51) from study area. Analyst: G. Mustoe, Western Washington State College, Bellingham, WA, 1977.

CHEMICAL COMPOSITION		NORM (C. I. P. W.)	
SiO ₂	45.54		
TiO ₂	3.05	Orthoclase	11.57
Al ₂ O ₃	12.94	Albite	10.96
FeO*	14.51	Anorthite	13.99
MnO	.22	Nepheline	8.31
MgO	10.57	Diopside	26.97
CaO	9.79	Olivine	12.95
Na ₂ O	3.41	Magnetite	8.32
K ₂ O	1.98	Ilmenite	5.73
Total	102.01		98.80

FeO* = total iron calculated as FeO

normative nepheline. Because of the presence of both nepheline and olivine in the norm the rock should probably be classified as a basanitoid. Although nepheline is present in the norm, it has not been detected in thin sections.

STRUCTURE

The area described in this report is a small part of an extensive and structurally complex metamorphic terrain which is sharply bounded on both the north and the south by major faults (Fig. 4). On the north the northwest-trending Tintina fault separates the metamorphic rocks of the Yukon-Tanana Upland from unmetamorphosed Precambrian and Paleozoic rock (Foster, 1969). On the south the metamorphic rocks of the Alaska Range are separated from unmetamorphosed rocks by the northwest-trending Denali fault (St. Amand, 1957). The amount of displacement along these right lateral strike-slip faults is controversial.

Local Structure

The faults within the study area have a general northeast trend, and were mapped by the use of topographic or geomorphic lineaments, scarps or slope breaks (Plate 2). Relative movement and attitude are generally difficult to appraise. The largest fault recognized in the map area is a northeast-trending, left lateral strike-slip fault. The amount of displacement on this fault is not known but offset of the intrusive complex at the Pika Canyon claim block suggests 1,000 to 1,500 feet. Another large fault in the northwest corner of the map area was recognized by Foster (1970), but she did not indicate the type of displacement. Because the units on the west side of this fault correspond to the units of the north limb of the inferred fold on the east side, it may have left lateral displacement. The latter may be part of a more complex fault system trending along Dude Creek. The majority of the other mapped faults are small and of minimal displacement.

The map area has been roughly divided in half by the contact between the schist units and the Pelly Gneiss (Plate 2). The north half consists of two schist units and the south half is mostly Pelly Gneiss. Cockfield

(1921) suggested that prior to metamorphism the Pelly Gneiss intruded all the Precambrian crystalline rocks of the Sixtymile district, which includes the present study area. His conclusions are supported by the observation that schist units in contact with the gneiss have a garnet assemblage along the contact. In the map area garnetiferous schists were observed at the contact with the Pelly Gneiss (Plate 2). The foliation of these schists generally dips away from the gneiss. If the foliation is parallel to the original bedding, then it would further suggest that prior to metamorphism the gneiss intruded the schists. The Pelly Gneiss now represents a large pluton that has been metamorphosed, faulted and intruded by rocks of Tertiary age.

The structure of the metamorphic terrain between the Denali and Tintina faults has been thought to represent a northwest-trending geanticline (Eardley, 1962); and in the map area the general strike of the foliation is northwest with northeast dip. This suggests that if Eardley's hypothesis is correct and if the foliation is parallel to bedding, then the rocks probably represent units of the northern limb of the proposed geanticline. Because of limited exposure and the lack of a working stratigraphic column the small folds common throughout the map area could not be clearly identified.

Three generalized cross sections have been constructed to show the structural relations of rocks within the map area (Fig. 8). Cross section A-A' trends north-south through the Pika Canyon claim block, B-B' trends northwest-southeast through the Fishhook prospect, and C-C' trends north-south through the NE Pika Canyon claim block. The greenschist units and the mica schist unit shown in cross section B-B' are thought to represent meta-volcanic or meta-sedimentary septa within the Pelly Gneiss.

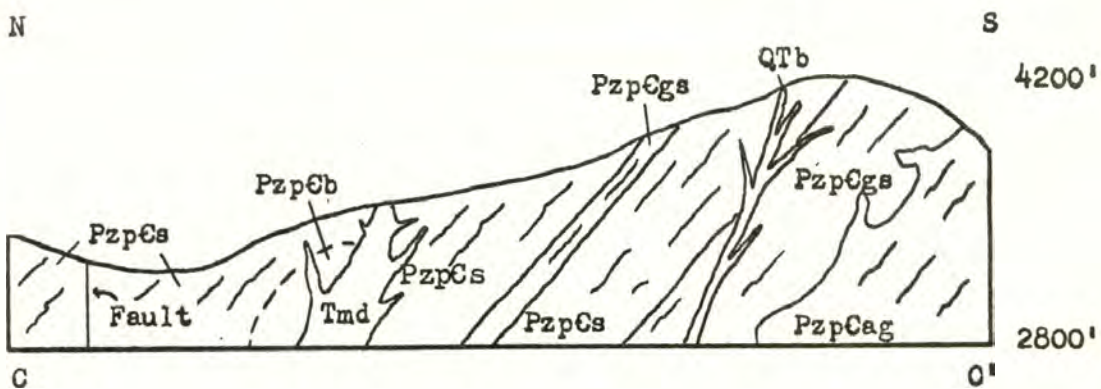
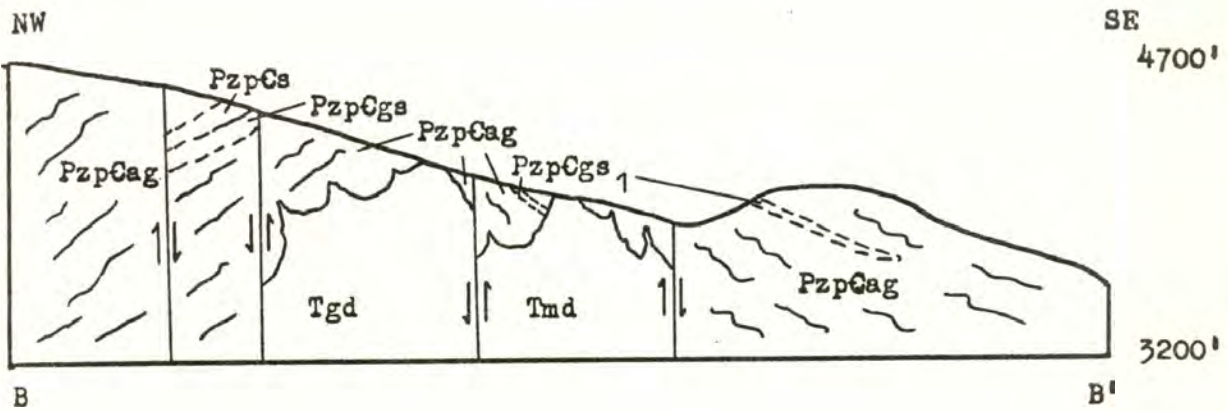
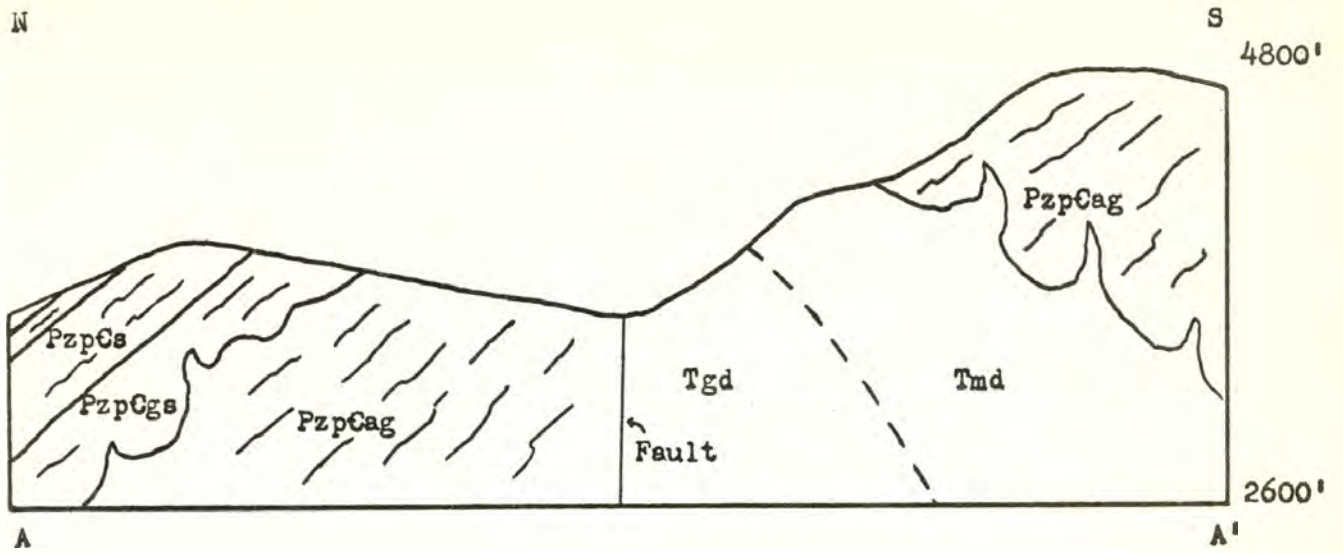


Fig. 8. Three generalized cross sections. A-A', Pika Canyon area; B-B', Fishhook prospect area; C-C', NE Pika Canyon area. For precise location and explanation see Plate 2.

Landsat Imagery

An interpretation of Landsat imagery of the Tanacross quadrangle made by Albert and Steele (1976) has been used in this report to help define structures and to correlate lineaments with areas of potential mineralization.

The term lineament has been defined by O'Leary and others (1976) as "a mappable, simple or composite linear feature of a surface, whose parts are aligned in a rectilinear or slightly curvilinear relationship and which differs distinctly from the patterns of adjacent features and presumably reflects a subsurface phenomenon".

Previous studies of Nimbus and ERTS (now Landsat) imagery by E. H. Lathram and others (1973) resulted in the formulation of an hypothesis that mineralized areas in Alaska may be spatially related to a regional set of northeast and northwest-trending lineaments, many previously unrecognized, that possibly reflect crustal fractures. They have suggested that lineaments representative of this set are clearly apparent on an ERTS mosaic of the Yukon-Tanana Upland, which includes the study area. Lathram (1974) postulated that favorable areas would form belts parallel to major northwest and northeast-trending fractures, and deposits would be more abundant where such fractures crossed. Albert and Steele (1976) in their interpretation have identified lineaments, arcuate, and circular features within the Tanacross quadrangle, but no arcuate or circular features were defined within the study area. The lineaments as determined by Albert and Steele (1976) and faults mapped by the writer are shown in (Fig. 9). Five lineaments and one inferred lineament are shown to pass through the study area. Two of the lineaments labeled A and B have been described by Albert and Steele (1976), as follows: lineament A, with an approximate N 55° E trend, is over 850 km long and can be traced from

EXPLANATION

- -- Linear Feature, dashed where uncertain
- - - Mapped Faults

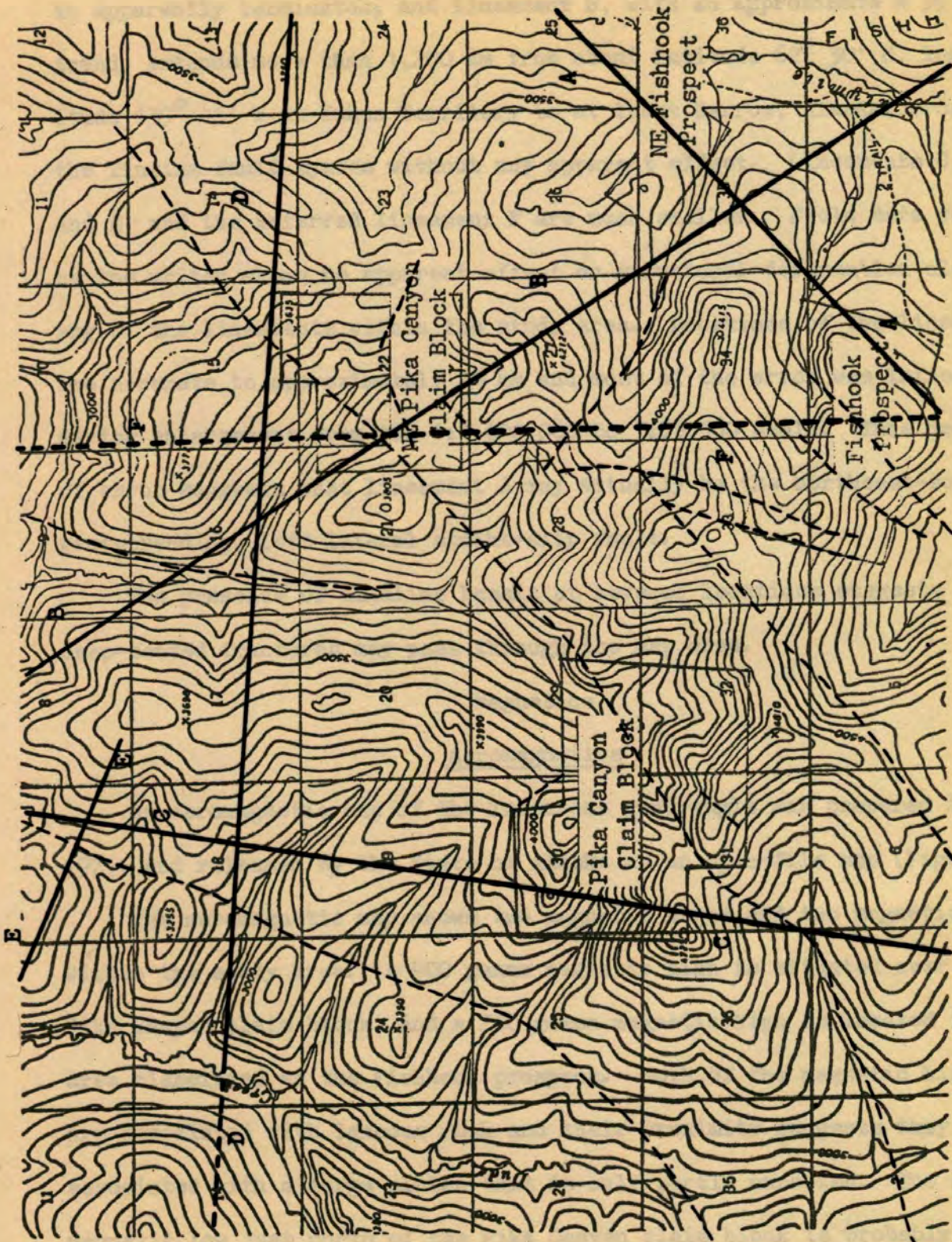
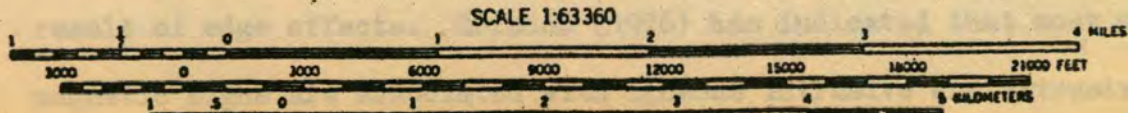
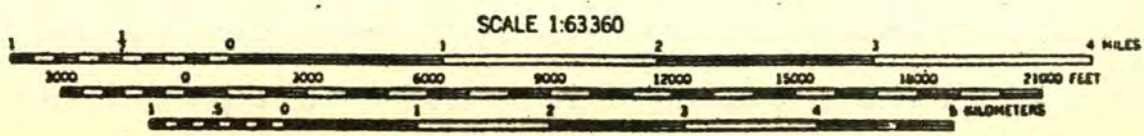
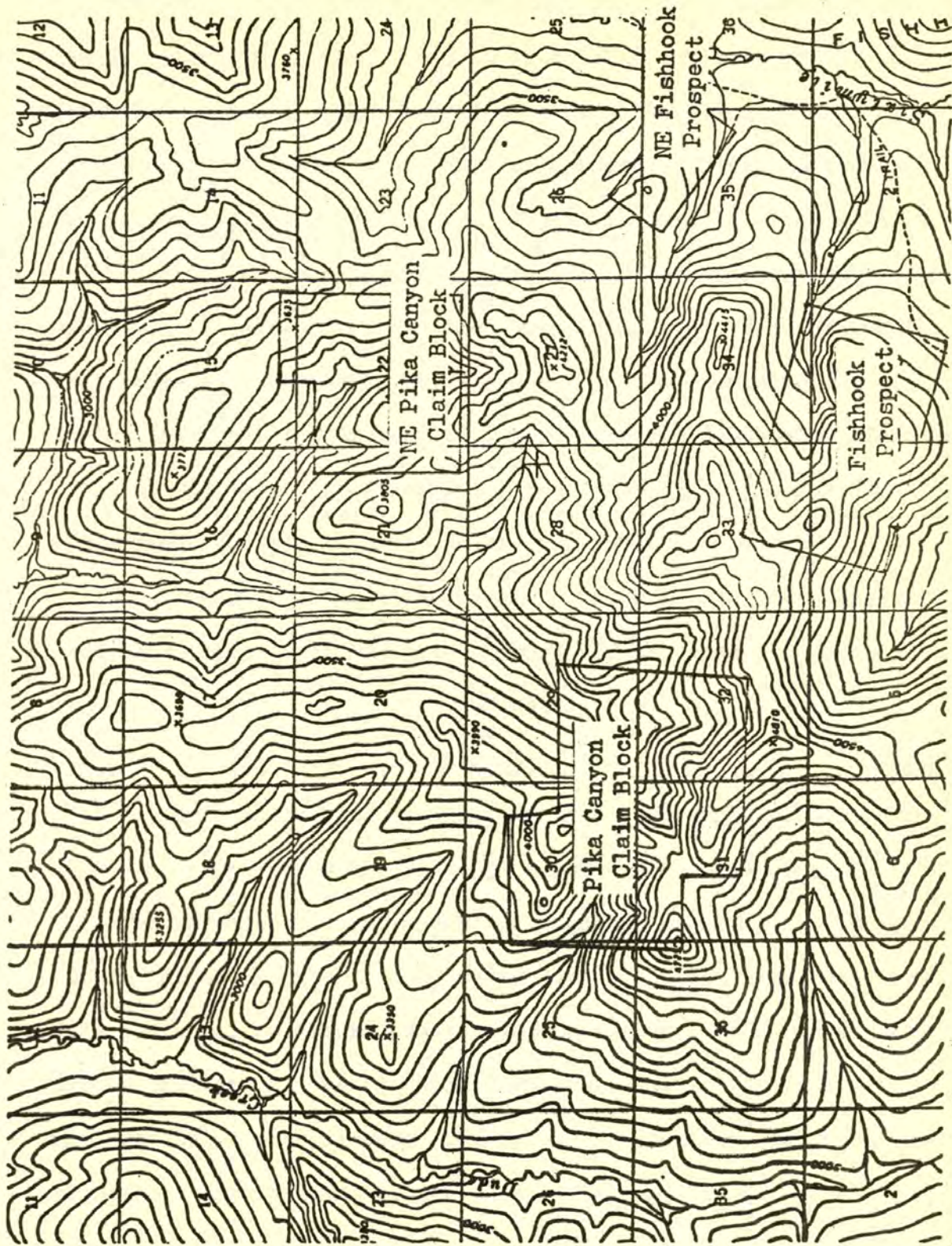


Fig. 9. Lineaments determined by Landsat imagery in relation to mapped faults within the thesis area (lineaments modified after Albert and Steele, 1976).

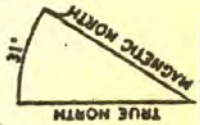


SCALE 1:63360
CONTOUR INTERVAL 100 FEET
DATUM IS MEAN SEA LEVEL





CONTOUR INTERVAL 100 FEET
 DATUM IS MEAN SEA LEVEL



APPROXIMATE MEAN
 MAGNETIC NORTH
 TRUE NORTH
 DECLINATION, 1956

the southwestern tip of Kenai Peninsula, across the Denali fault without any apparent offset, to the Tintina fault in Yukon Territory where it apparently terminates; and lineament B, with an approximate N 35° W trend, extends more than 1,200 km from about latitude 62° 30' N, longitude 139° 45' W in Yukon Territory to at least Barrow, Alaska, crossing the Tintina fault system without any apparent offset. Lineaments C, D, and E, and the inferred lineament F are much smaller. Field data collected by the writer shows no apparent offset or structural deformation along any of the lineaments within the study area. Locations of the lineaments are accurate to approximately 1½ km and most of the error was introduced during enlargement from the 1:1,000,000 to 1:63,360 scale. This amount of error suggests that lineament A may actually be the northeast-southwest-trending, left lateral strike-slip fault.

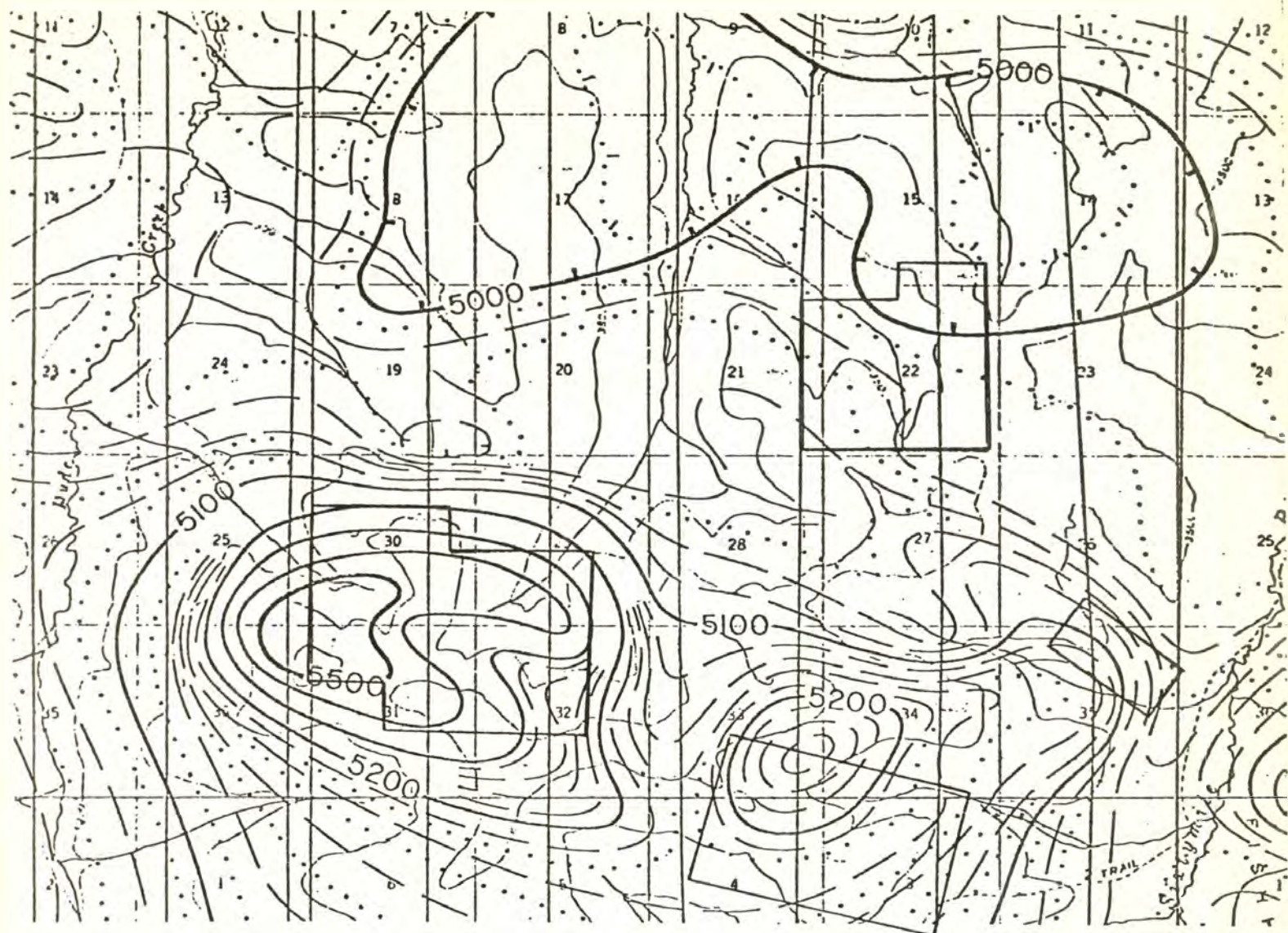
The presence of alkaline basalt at several locations suggests that deep-seated fractures may pass through the map area.

Magnetics

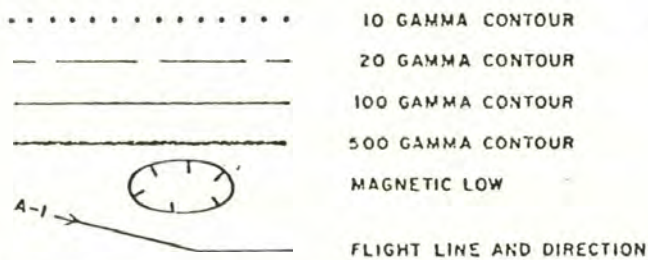
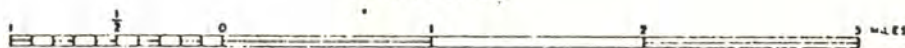
Aeromagnetics

An aeromagnetic map of the Tanacross quadrangle was prepared in 1971, and released by the State of Alaska as an open-file map (Fig. 10).

The aeromagnetic map shows two magnetic highs and two magnetic lows within the study area. A 400 gamma magnetic high is situated over the Pika Canyon claim block, and a 200 gamma magnetic high is located in an area classified as the Fishhook prospect. Both of the magnetic highs are associated with igneous rock and their proximity suggests they are associated with a large pluton that is only partly unroofed. The small magnetic low just north of the Pika Canyon claim block is probably the result of edge effects. Griscom (1976) has indicated that most of the magnetic highs are associated with igneous intrusive and extrusive rocks,



SCALE 1:63360



FLIGHT LINE SPACING 3/4 MILES

FLIGHT ALTITUDE NOMINALLY 1000 FEET ABOVE GROUND

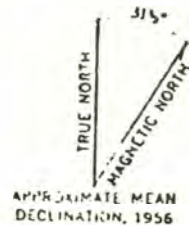


Fig. 10. Aeromagnetic map of the study area. The claim blocks and prospects are outlined as follows: Pika Canyon claim block in red, NE Pika Canyon claim block in orange, Fishhook prospect in blue, and NE Fishhook prospect in green (from Griscom, 1976).

and that magnetic lows on the north and northeast sides of major magnetic highs are the result of edge effects, and not the result of reverse remanent magnetization. The large magnetic low situated on the northern flank of the NE Pika Canyon claim block may represent metamorphic rocks of uniform and weak magnetization.

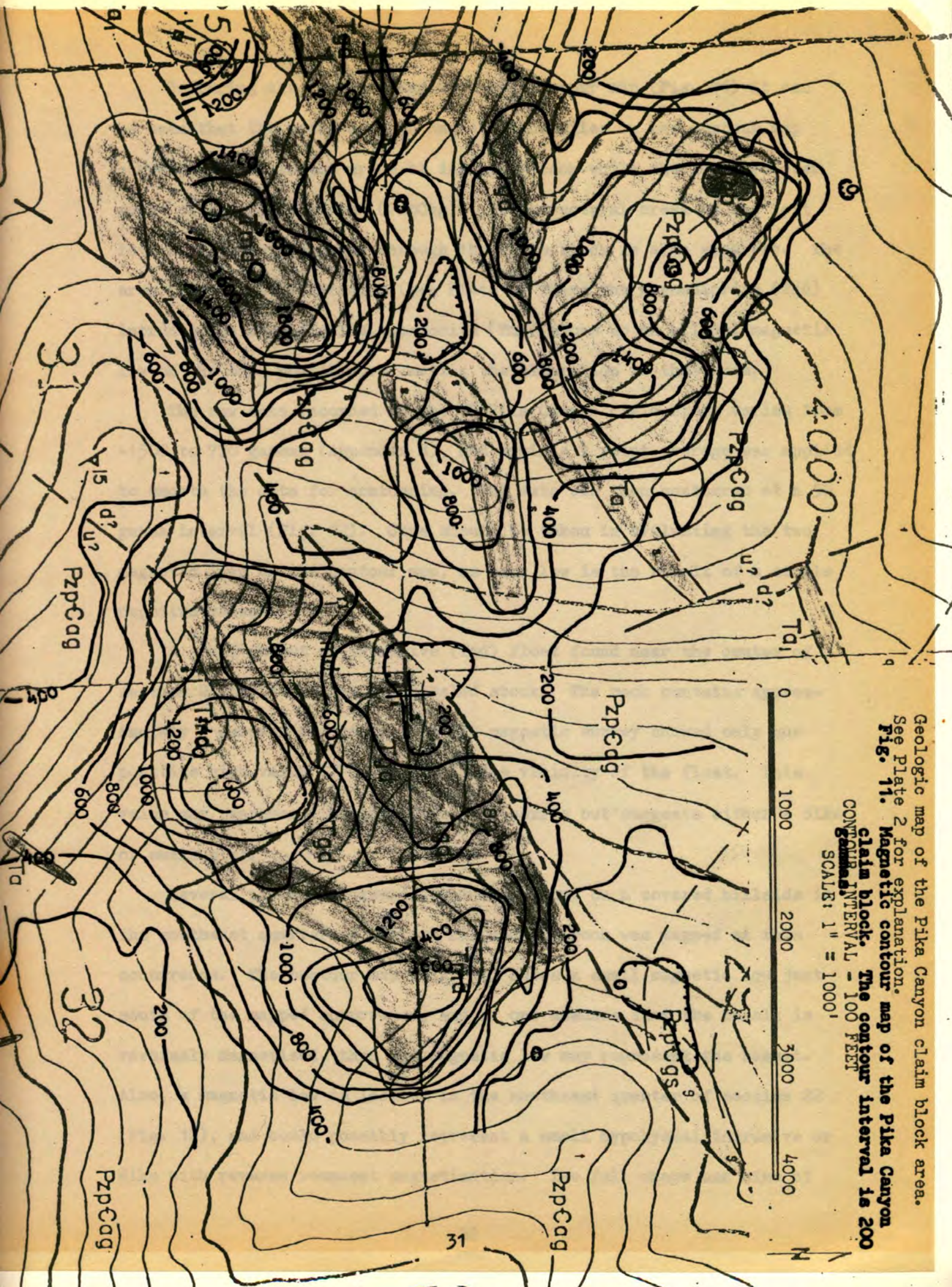
In the Tanacross quadrangle the metamorphic rocks are generally less magnetized than the igneous rock. This has made aeromagnetics very useful in interpreting the bedrock geology in an area of thick vegetation, residual soils, and limited outcrop exposure.

Ground Magnetics

During the summer of 1976, a reconnaissance ground magnetic survey was conducted on the Pika Canyon and NE Pika Canyon claim blocks. The main purpose of the survey was to aid in preparation of the geologic map, particularly by locating igneous rocks in areas of limited outcrop.

The magnetometer used was a Scintrix MF-2 flux-gate model, which measured the vertical field with a precision of 5 gammas. A base station was established at each claim block and a line of secondary base stations was run east-west down the center of both claim blocks. The purpose of the secondary base stations was to eliminate returning to the primary base station periodically to check for drift.

The raw data recorded at the Pika Canyon claim block varies from -1700 to 2150 gammas (Appendix B). To smooth the data, so that it could be easily contoured, a 7 point average was employed, (i.e., each station value plus the 6 closest station values were averaged and that value represents the 7 point average). The 7 point average data was then contoured at a 200 gamma interval. To eliminate negative contour values a positive value equal to the largest negative value was added to each contour (Fig. 11).



Geologic map of the Pika Canyon claim block area.

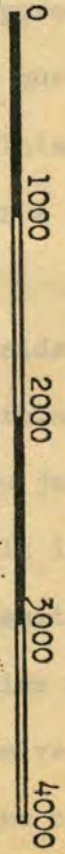
See Plate 2 for explanation.

Fig. 11. Magnetic contour map of the Pika Canyon

claim block. The contour interval is 200

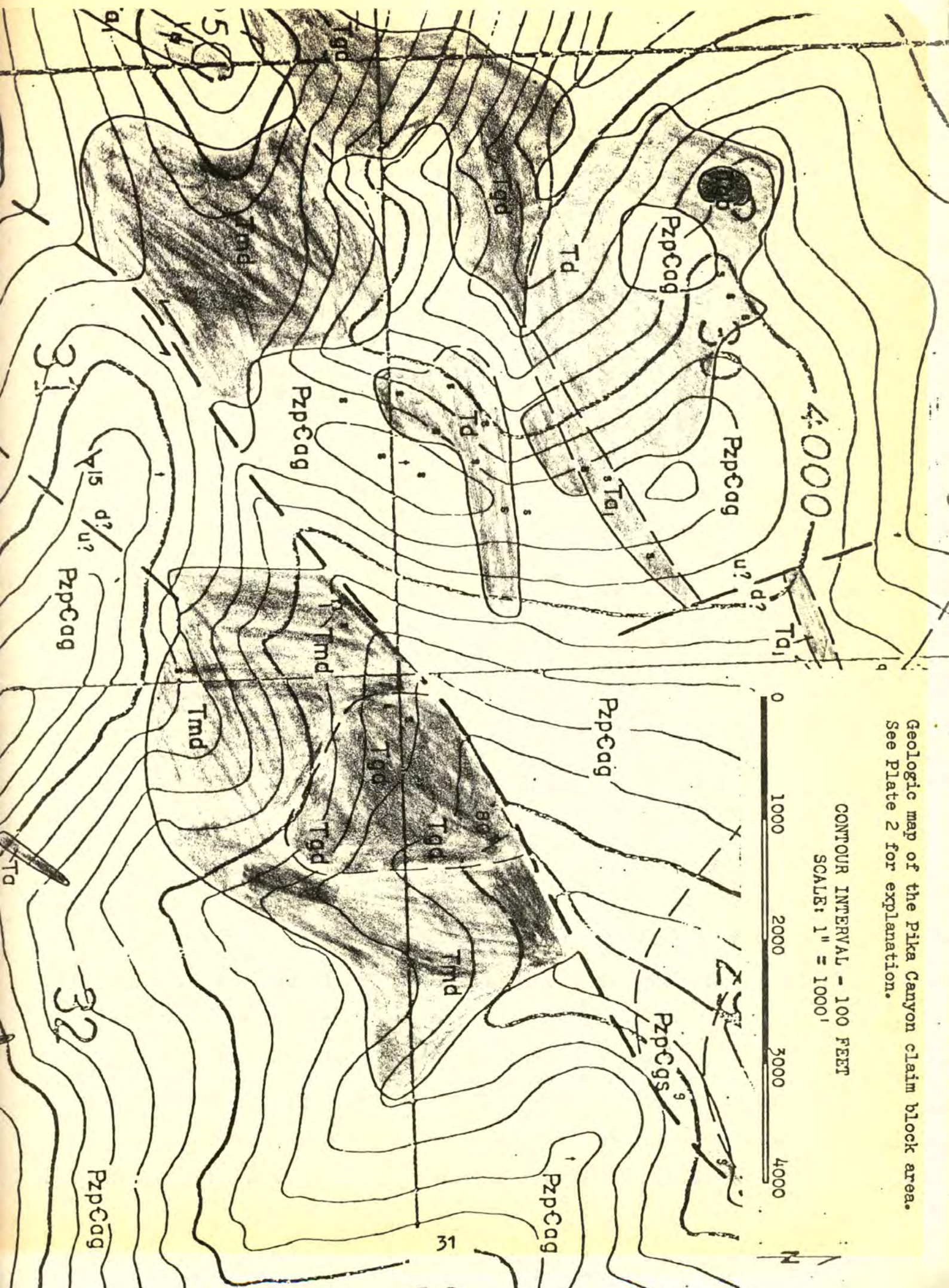
feet. CONTOUR INTERVAL - 100 FEET

SCALE: 1" = 1000'



Geologic map of the Pika Canyon claim block area.
See Plate 2 for explanation.

CONTOUR INTERVAL - 100 FEET
SCALE: 1" = 1000'

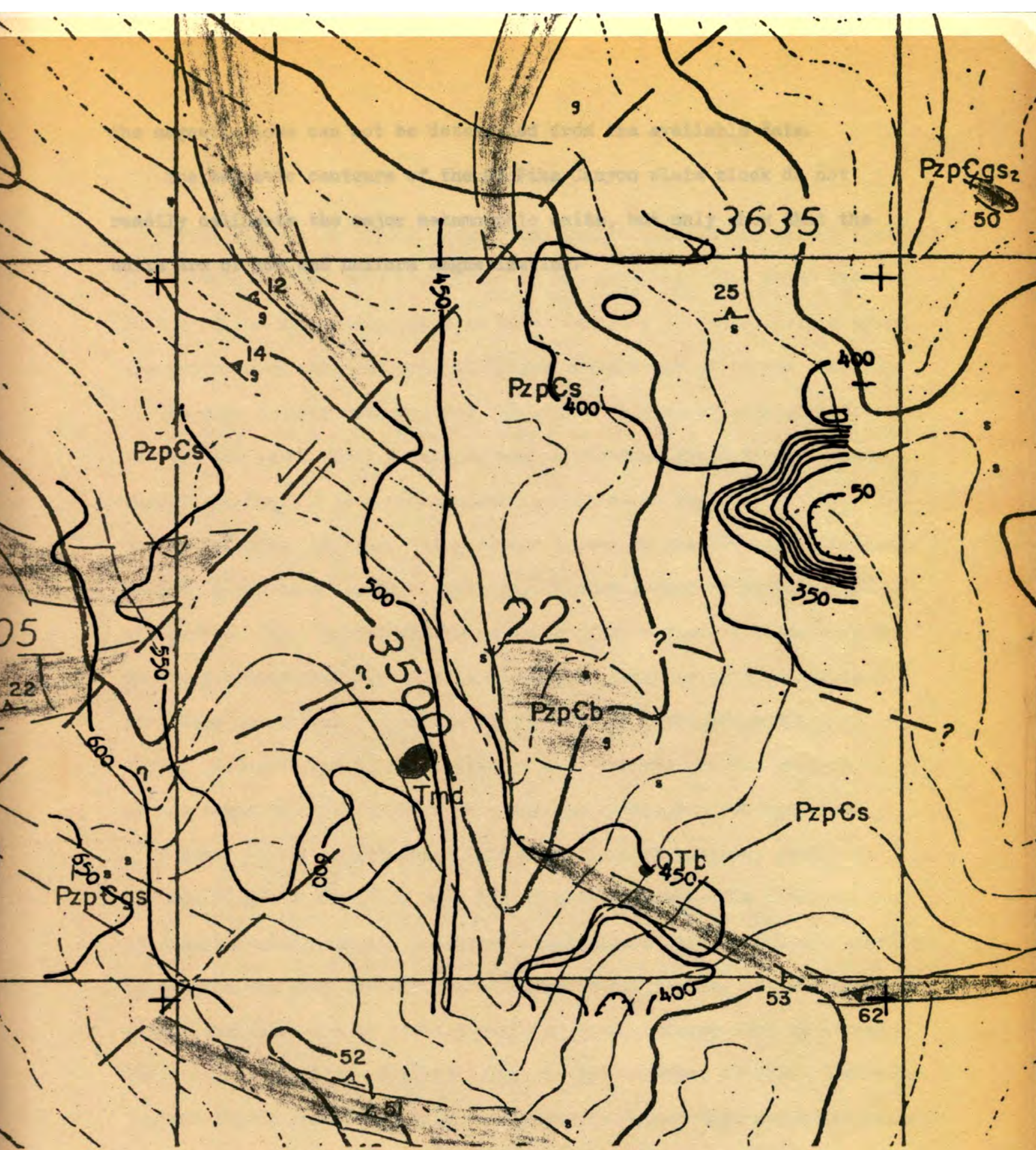


Comparing the geologic map with the contour map (Fig. 11) it can be seen that the areas of high magnetic anomalies on the contour map correspond well to the areas of intrusive rock while the lows are over areas of the Pelly Gneiss (PzpCag). The structural break of the left lateral strike-slip fault through the claim block is also apparent. The area of potassic alteration (see Plate 3) where the granodiorite (Tgd) intrudes the monzodiorite, monzonite (Tmd) shows up as a local magnetic low on the map, possibly reflecting the alteration in that area.

The raw data recorded at the NE Pika Canyon claim block varies from -1500 to 770 gammas (Appendix B), and again a 7 point average was applied to smooth the data for contouring. The data was then contoured at a 50 gamma interval (Fig. 12). Care should be taken in evaluating the two magnetic lows on the contour map, as each low is the result of a single negative value.

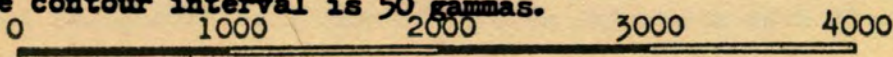
A small amount of intrusive (Tmd) float found near the center of section 22 may represent a concealed stock. The rock contains approximately 1 percent magnetite, but the magnetic survey showed only one positive high value (770 gammas) in the vicinity of the float. This value may represent the intrusive rock source but suggests either a dike or small plug.

Several pieces of basalt float were found on a covered hillside in the southeast quarter of section 22, and the rock was mapped at this occurrence. The contour map (Fig. 12) shows a small magnetic low just south of the mapped occurrence, and if one assumes that the basalt is reversely magnetized, then the magnetic low may represent the basalt. Also, a magnetic low is located in the northeast quarter of section 22 (Fig. 12), and could possibly represent a small hypabyssal intrusive or dike with reverse remanent magnetization. The full shape and size of

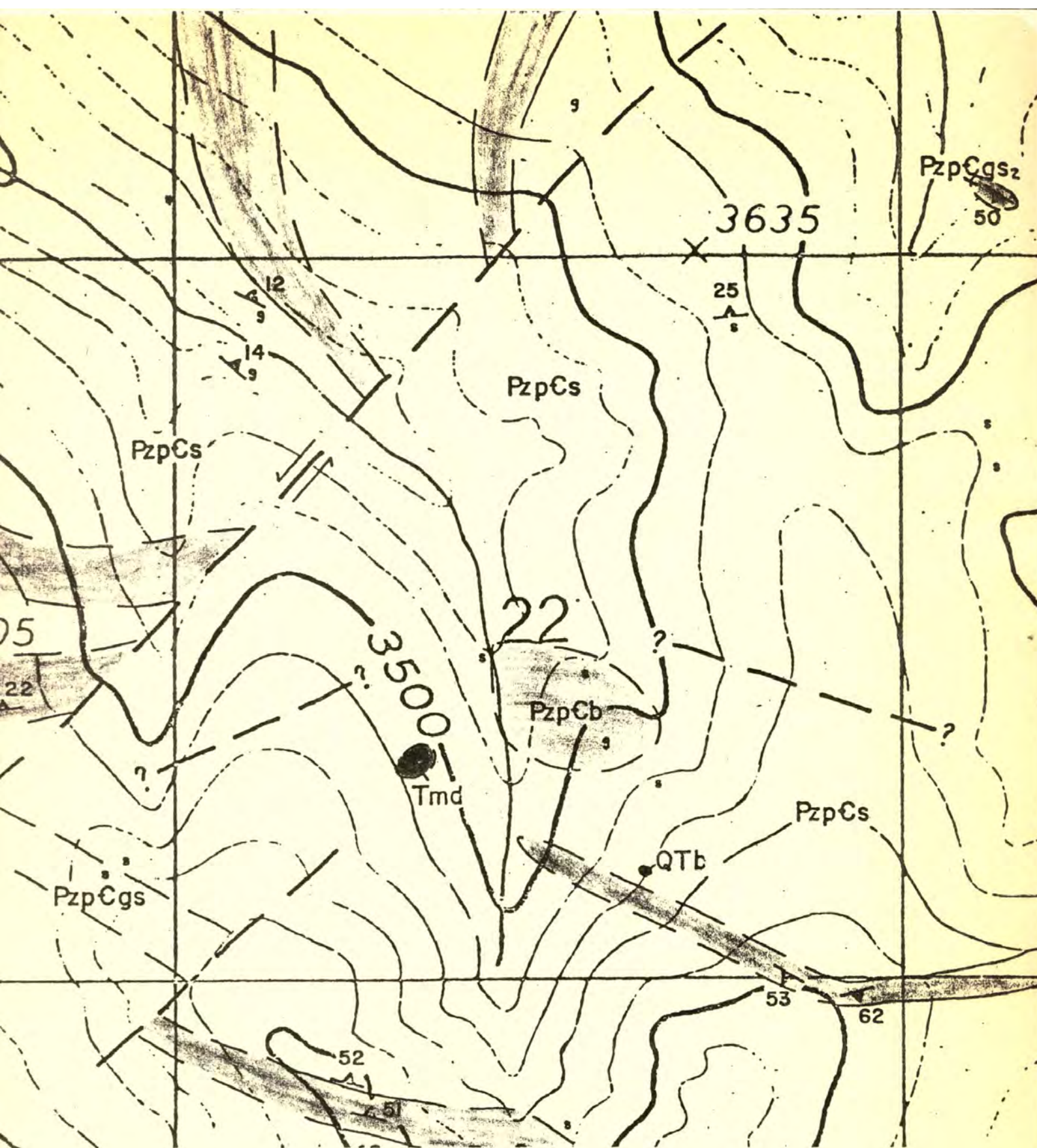


CONTOUR INTERVAL - 100 FEET

Fig. 12. Magnetic contour map of the NE Pike Canyon claim block. The contour interval is 50 gammas.



Geologic map of the NE Pike Canyon claim block area. See Plate 2 for explanation.



CONTOUR INTERVAL - 100 FEET

SCALE: 1" = 1000'

0 1000 2000 3000 4000

Geologic map of the NE Pika Canyon claim block area. See Plate 2 for explanation.

the magnetic lows can not be determined from the available data.

The magnetic contours of the NE Pika Canyon claim block do not readily delineate the major metamorphic units, but only show that the units are of low and uniform magnetization.

MINERAL DEPOSITS

Alteration

Five alteration types: propylitic, phyllic, potassic, silicification, and carbonatization were recognized in the map area. The areal distribution of the alteration zones is shown in Plate 3. Both field mapping and petrography were employed to define the alteration zones. Because of the poor outcrop exposure and the limited number of rock samples collected, the exact areal extent of most alteration zones is not known. Therefore, Plate 3 is a reconnaissance alteration map.

Propylitic, phyllic, and potassic appear in the literature as terms used to describe zones of mineral assemblages formed by hydrothermal alteration. The typical zoning sequence of hydrothermal alteration in porphyry copper-type deposits is an outward progression from a potassic core to a peripheral propylitic zone (Fig. 13) (Guilbert and Lowell, 1974). Potassic can be classified as high temperature and propylitic as low temperature alteration with phyllic alteration between them.

White (1974) has proposed that magmatic heat has been essential in supplying the energy of most hydrothermal systems. He inferred that localized heating results in thermal expansion of pore fluid and promotes convection and deep circulation of hydrothermal fluids. During convection, either the intrusive or country rock, or both, undergo weak to strong addition and leaching of elements by the hydrothermal fluids. The hydrothermal fluids associated with most porphyry copper-type deposits generally consist of magmatic volatiles and meteoric water (White, 1974).

As the convection system cools, Taylor (1974) has demonstrated that the external (meteoric) hydrothermal system interacts with the hydrothermally altered rocks formed by the internal (magmatic) system which results in a retrograde alteration system where low temperature alter-

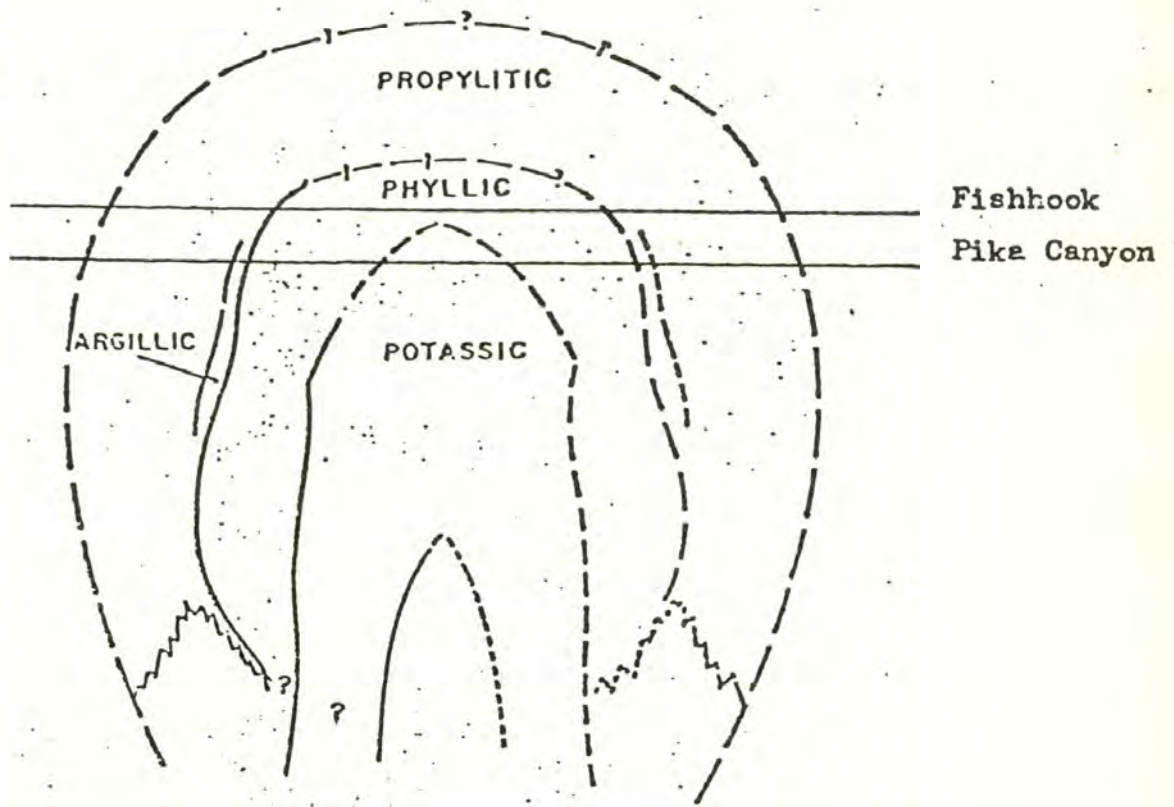


Fig. 13. Schematic drawing of alteration zoning in a typical porphyry copper-type ore deposit. Also shown are the possible vertical levels of alteration exposed at the Pike Canyon and Fishhook areas (modified after Guilbert and Lowell, 1974).

ation phases are superimposed upon high temperature phases, (i.e., potassic with retrograde propylitic alteration).

Propylitic Alteration

Within the map area propylitic alteration is confined to small zones, generally near zones of phyllic alteration.

Lowell and Guilbert (1970) define the propylitic zone as the most widely distributed and least distinctive of the alteration assemblages. Minerals characteristic of this zone are chlorite, epidote, carbonates, albite, and adularia. Minerals generally characteristic of the propylitic zones in the map area are epidote, chlorite, calcite, sericite, and pyrite. The most common mineral alteration reactions are: 1) biotite altering to chlorite, 2) hornblende altering to chlorite plus epidote, and 3) feldspar altering to sericite. Most occurrences of propylitic alteration within the map area are associated with igneous rocks and are visible in outcrop.

Phyllic Alteration

Phyllic alteration is, by definition, characterized by the mineral assemblage quartz-sericite-pyrite (Guilbert and Lowell, 1974), and generally occurs in an intermediate position between the outer propylitic and inner potassic zone of most porphyry copper-type deposits (Fig. 13). Several thin sections of rocks from the map area have shown a clay-sericite-quartz assemblage, which is characteristic of argillic alteration (Guilbert and Lowell, 1974). Due to the lack of samples the areal extent of the argillic alteration was not discernable; it has therefore been included with the phyllic alteration assemblage on Plate 3.

Petrographic study has shown that plagioclase generally is replaced by a felted mat of fine-grained sericite; but traces of cleavage, zoning,

and twin planes are generally retained. Orthoclase may or may not be totally sericitized, depending on the rock type. For example, the orthoclase in the intrusive rocks varies in the degree of sericitization; whereas, orthoclase in the Pelly Gneiss is generally completely sericitized. Primary quartz is unaffected but generally overgrown. Pyrite is abundant in most thin sections, generally occurring as disseminated euhedral crystals.

Within the map area, phyllic alteration is found in three general areas. The first is located in the Pika Canyon claim block area and the second and third are located in the Fishhook and NE Fishhook prospects (Plate 3). At each locality the alteration is associated with igneous rocks, and as mentioned before, the result of a hydrothermal system.

Another feature of interest is the relationship between the phyllic alteration, igneous intrusive and subvolcanic rocks, and the country rocks. The intrusive rocks that exhibit phyllic alteration are usually granodioritic in composition and the subvolcanic rocks andesitic. In general the intrusive rocks show phyllic alteration within the intrusive rock itself, but also extending out into the country rock; whereas, the andesitic rocks, which are generally dikes, show phyllic alteration confined to the igneous rock. This could possibly be explained by the rate of cooling, as the andesitic dikes would cool faster than the larger intrusive stocks, therefore, the hydrothermal system would not have time to affect the country rock.

Potassic Alteration

Potassic alteration is distinguished by the presence of fine-grained secondary biotite and (or) orthoclase, and is generally associated with the central core of a vertical cylinder of alteration in typical porphyry copper-type deposits (Fig. 13) (Guilbert and Lowell, 1974).

Within the map area, potassic alteration is confined to a small area in the Pika Canyon claim block (Plate 3), first identified by Hederly-Smith (1975). He described the rock as a granodiorite which had undergone potassic alteration and retrograde propylitization, and suggested that a large percentage of quartz in the rock suggested a period of silicification. The potassic alteration also occurs in the best mineralized rock found on the surface at the Pika Canyon claim block (the hand sample contains approximately 1 percent chalcopyrite).

In a thin section of the potassically altered granodiorite, plagioclase appears to have been almost completely replaced, predominately by orthoclase with lesser amounts of sericite, epidote, and carbonate. Sulfides are disseminated throughout the sample and are generally associated with chlorite. Biotite has been replaced by chlorite, and tourmaline is found in small rosettes. The presence of tourmaline in the rock is due to minor boron in the hydrothermal fluids, and suggests that this alteration is clearly metasomatic rather than isochemical.

Silicification

Silicification is the deposition of secondary quartz introduced by hydrothermal solutions, or it may recrystallize from silica already present in the rock. Within the map area there are small, isolated occurrences of silicification, but the main concentration was recognized at the Fishhook prospect. At this prospect silicification is generally closely associated with the phyllic alteration, and the quartz has formed a maze of veins and veinlets (stockwork) throughout the rocks. The veins cut one another indicating two and possibly three phases of silicification. There was one occurrence of molybdenite as disseminated grains in a stockwork of quartz veins. At the Fishhook prospect the quartz stockwork

usually averages about 20 percent of the total rock, but in places it may represent 50 percent or more. The increased silicification of the Fishhook area in relation to other areas can probably be attributed to intense structural deformation and intrusive activity. In the previous discussion on structure it was shown that faults and lineaments pass through the prospect area (Fig. 9). The faults, lineaments, and intrusive activity would have provided many fractures and fissures to allow migrating fluids to deposit the quartz. The Fishhook prospect is in contrast with the Pika Canyon area where silicification is mainly confined to the zone of phyllic alteration. This suggests that the Pika Canyon complex was intruded rather passively and structural deformation limited.

Veins of quartz are present in nearly all the rocks of the map area, but the crystalline schists, because of their age, have been acted upon by vein-making processes of every period, and consequently contain more quartz veins than any of the other rocks. Much of the quartz is white and vitreous and ranges from small seams to veins and lenses several feet thick, but some of it, particularly in the smaller seams is colorless and transparent. Some of the quartz veins may be mineralized with pyrite, but in general most of the older quartz veins of the crystalline schists are barren.

Alteration Zoning Patterns

Propylitic, phyllic and potassic alteration and silicification are associated with many hydrothermal ore deposits. The propylitic, phyllic, and potassic alteration zones are shown as circular in Fig. 13, but Gilbert and Lowell (1974) have noted that expression of zoning is affected by exposure, structural and compositional homogeneity, and post-intrusive

faulting or intrusive activity, and that the larger the occurrence the more regular and well developed the zoning is in terms of both mineralization and alteration. They have also found that the reverse is equally true, that smaller deposits even of ore grade are inclined to show significantly less regular alteration patterns.

At the Pika Canyon claim block the alteration zones (Plate 3) roughly resemble a horizontal section through the typical southwestern United States porphyry copper-type deposit shown in vertical section in Fig. 13. But at Pika Canyon the zones of alteration are in patches which suggests that if Guilbert and Lowell are correct in their interpretation, then the deposit is probably small.

To explain the patchy nature of the alteration zones several ideas have been suggested. Taylor (1974) has implied that the permeability of Precambrian crystalline rocks is somewhat limited, which suggests that the Pelly Gneiss could possibly have restricted the flow of migrating hydrothermal fluids, especially if the rocks were not structurally deformed prior to and during intrusive emplacement. In the discussion on phyllic alteration it was suggested that emplacement may have been passive with limited deformation of the country rock.

The vertical extent of the alteration system may in fact be the main reason for the patchy alteration zones. The small size and patchy distribution of potassic alteration suggest that the alteration system is just beginning to be exposed by erosion. The possible vertical level of exposure currently observed is shown in Fig. 13. Level of erosion, in conjunction with limited permeability and limited structural deformation may explain the patchy alteration zoning at the Pika Canyon claim block.

At the two Fishhook prospects, phyllic alteration and silicification

are the predominant alteration phases. Phyllic alteration at these prospects forms several small cores with silicification stockwork throughout the cores and extending outward from the phyllic zones. Several small zones of propylitic alteration surround the phyllic cores, but are not very extensive.

Of the two prospects, Fishhook is probably the most interesting. Silicification covers a broad area beyond the small intrusive bodies (see Plate 3), which may represent the top of a large stock. The phyllic alteration is closely associated with the intrusives. The probable vertical level of alteration currently exposed at this porphyry copper-type prospect is shown in Fig. 13. The lack of propylitic alteration around this prospect may in part be due to the lack of samples and poor field notes.

Carbonatization

Carbonatization is confined to the andesitic rocks in the northeastern corner of the map area (Plate 3). Carbonatization consists of the formation of secondary carbonates in the host rocks of epigenetic deposits. Boyle (1970) explains that ankeritization of mafic volcanics appears to require only the introduction of CO_2 , the other constituents of ankerite such as Ca, Fe, Mg, and Mn come from the chemical breakdown of amphiboles, pyroxenes, and feldspar. During this process much SiO_2 is removed and probably transferred to the veins where it crystallizes as quartz. Boyle (1970) has explained that gold-quartz deposits such as the Yellowknife, are associated with carbonatization, and that extensive carbonatization releases large quantities of silica.

In thin section the andesitic rocks from the carbonatized area are thoroughly altered. Carbonates have replaced most of the feldspar, pyroxene and hornblende, and there are many veinlets of both quartz and calcite

throughout the thin sections.

Economic Mineralization

Within the map area only a limited amount of mineralized rock has been found on the surface. Archer and Main (1971) have indicated that surface mineralization at the Casino deposit in the Yukon was also very limited, and that no chalcopyrite or molybdenite were recognized on the surface although malachite and occasionally azurite were found coating fractures on leached fragments. The map area prospects are in basically the same geologic environment as the Casino deposit and neither area was glaciated during Pleistocene time.

A drilling program at Casino has shown that 50 to 70 percent of the copper and about 70 percent of the molybdenite have been removed from the leached zone; and that a zone of secondary copper enrichment between 100 and 300 feet thick lies below the leached zone (Archer and Main, 1971). The enrichment is due to replacement of chalcopyrite and pyrite by chalcocite. The limited surface mineralization at both Pika Canyon and Fishhook areas suggests a mineralization profile similar to the Casino deposit.

At the Pika Canyon prospect the best mineralized rock is represented by petrography sample number 201 (see Plate 1 for sample location) and the geochemistry is represented by sample numbers 23700 and 27621 (see Appendix B for geochemical data). The rock is a potassically altered granodiorite with disseminated pyrite and chalcopyrite, and minor amounts of malachite coating fractures.

At the Fishhook prospect area three occurrences of mineralized rock were noted. The petrography sample number and geochemical sample number for each sample are given respectively 209/27615, 212/27616, and 122/27617. The petrography sample locations are shown on Plate 1 and the geochemical data in Appendix B.

Sample 209/27615 is Pelly Gneiss that has been altered to the phyllic stage and then silicified. In this rock fine-grained molybdenite was found associated with the quartz stockwork. The rock consists of approximately 40 percent quartz stockwork.

Sample 122/27617 is a granodiorite that has been altered to the phyllic stage, and contains approximately 2 percent disseminated pyrite.

Sample 212/27616 represents one of several pieces of float. Petrographically the rock is similar to greenschist unit 1 and is thought to represent a metamorphosed andesitic or basaltic tuff. The sulfides in this rock are in bands and consist mainly of pyrite with minor chalcopyrite. The pyrite is in two forms, massive fine-grained and fractured euhedral to subhedral cubes approximately 1 millimeter in size. Sangster (1973) has stated that pyrite with this type of texture forms during metamorphism and that with increasing metamorphic grade the pyrite crystals grow larger. This suggests that the sulfides were syngenetic (volcano-sedimentary) and remobilized during low-grade metamorphism. This occurrence is therefore fundamentally different than the porphyry copper-type mineralization common to this area. During emplacement of the intrusive rock sulfides from this probable syngenetic volcano-sedimentary occurrence could have been mobilized and redeposited.

Geochemistry

A total of 1105 soil, rock-chip, and stream-sediment samples were collected in the study area. Of these, 268 were reconnaissance soil, 97 reconnaissance rock-chip, 53 reconnaissance stream-sediment, 378 soil grid samples at the Pika Canyon claim block, and 309 soil grid samples at the NE Pika Canyon claim block. The soil samples were collected by the use of an auger; and if permafrost permitted, the soil collected for analysis was that just below the organic layer. Stream-sediment samples consisted

of silt and fine-grained material taken from several locations at each sample site. Rock-chip samples were collected from float as well as outcrops. However, the geochemical results for each sample will be considered to be representative of the rock at that location. All samples were analyzed for the trace elements copper, molybdenum, zinc, and silver.

Analytical Procedure

Geochemical analyses were carried out at Acme Analytical Laboratories Ltd., Burnaby, British Columbia. The analytical procedure is as follows (Acme Analytical Laboratories Pamphlet, 1975):

The soil and stream-sediment samples were reduced by screening, and the rock-chip samples were pulverized to minus 80-mesh. A 0.5 gram cut of minus 80-mesh sample was digested with mixed concentrated nitric acid and perchloric acid until all the organics were decomposed. This solution was diluted with water to 10 milliliters and analyzed by a Perkin-Elmer 305 Atomic Absorption Spectrophotometer for copper, molybdenum, and zinc in parts per million. Silver was analyzed by the same procedure, except that a deuterium-arc background corrector was used with the spectrophotometer to reduce molecular absorption interference and enhance the detection limit to 0.1 parts per million.

Samples collected during the summer 1974, and analyzed for silver, did not have a background correction. These have been identified by an asterisk on the geochemical maps.

Statistical Methods

The statistical method used for data treatment is that described by Levinson (1974). To establish the local background values for each element, the median value of the data distribution has been used. One disadvantage of this method is that it does not take into account very large or very small values, and is therefore relatively insensitive to large fluctuations in the data. This problem only occurred with two rock samples in which the copper and molybdenum values were very large, and these

samples were omitted from the statistical interpretation.

To determine which of the values or range of values occur most frequently, the data can be subdivided into specific intervals. A common formula for choosing the number of intervals into which data are to be subdivided is given by $(k=10 \cdot \log_{10} N)$ where k is the largest interval contained in the right hand expression and N is the number of samples. To obtain the interval width, the largest elemental value is divided by k and then rounded to the nearest whole number. For example: there are 955 soil samples, therefore, the number of intervals is equal to $k=10 \cdot \log_{10} 955$ which equals 29.8, or rounded to 30. To compute the histogram interval width for copper, the value of the largest sample (305 parts per million), is divided by k (30), $(305/30=10.16)$, or rounded to 10). A histogram can now be constructed by plotting frequency (number of samples) versus the midpoint of each class interval. Figs. 14 thru 25 are histograms of the four trace elements: Figs. 14 thru 17 represent soil samples, Figs. 18 thru 21 rock-chip samples, and Figs. 22 thru 25 stream-sediment samples. The median, mean average, and standard deviation have been listed on each figure.

The median has been established as the background value, therefore, any larger value will have the potential to be anomalous. For each type of sample, (i.e., soil, rock-chip, and stream-sediment) I have grouped the "anomalous" values of each element into three arbitrarily established groups: 1) potentially anomalous, 2) probably anomalous, and 3) definitely anomalous. Table 2 lists the anomalous group values for each element of the three types of samples. For each type of sample the threshold of anomalous values may vary. For example, soil samples with a copper value greater than 65 ppm are definitely anomalous; whereas, rock-chip samples require a copper value greater than 105 ppm to be considered definitely

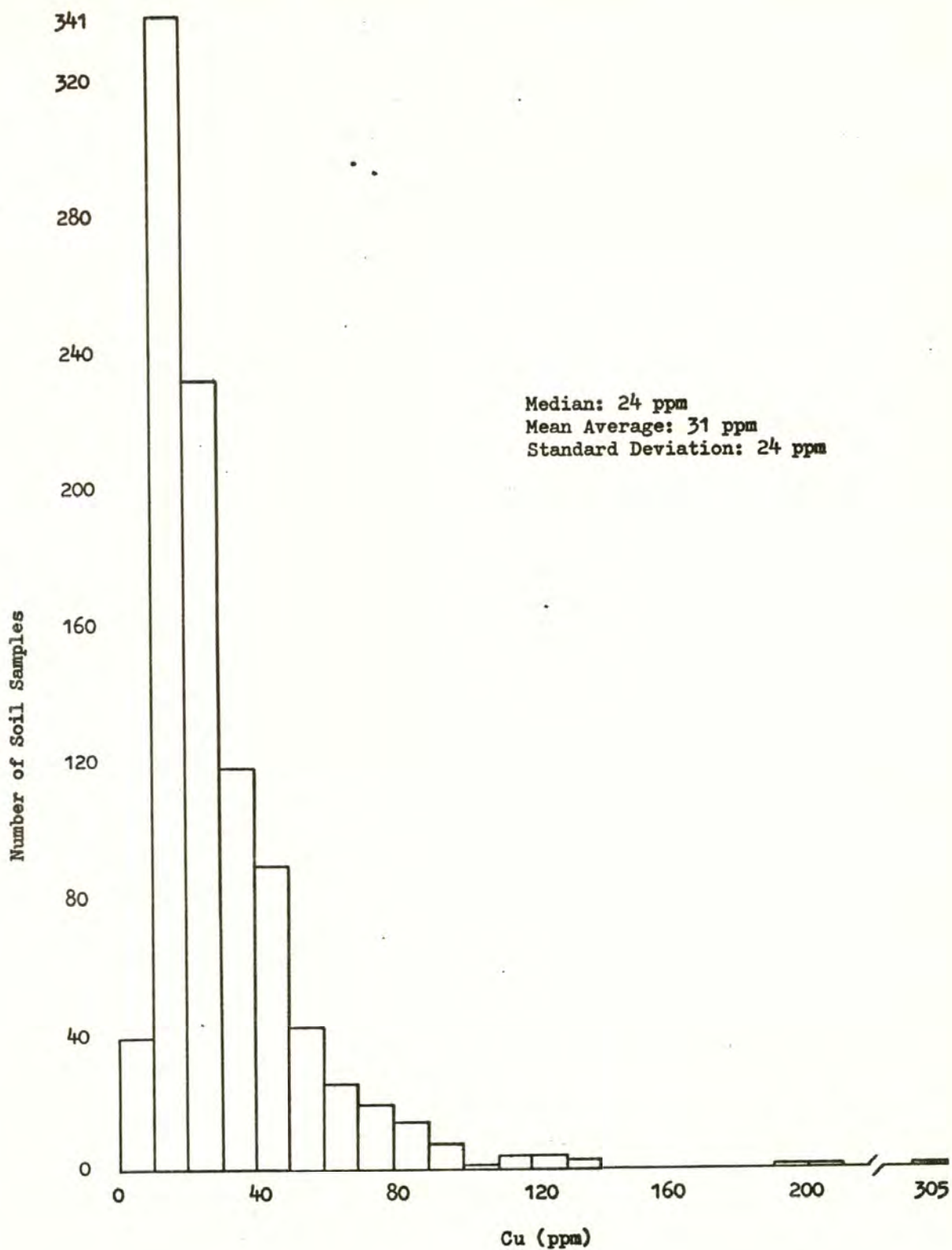


Fig. 14. Histogram and statistical data of copper concentrations based on 955 soil samples. The ppm scale has been expanded past 210 ppm to accommodate the 305 ppm value.

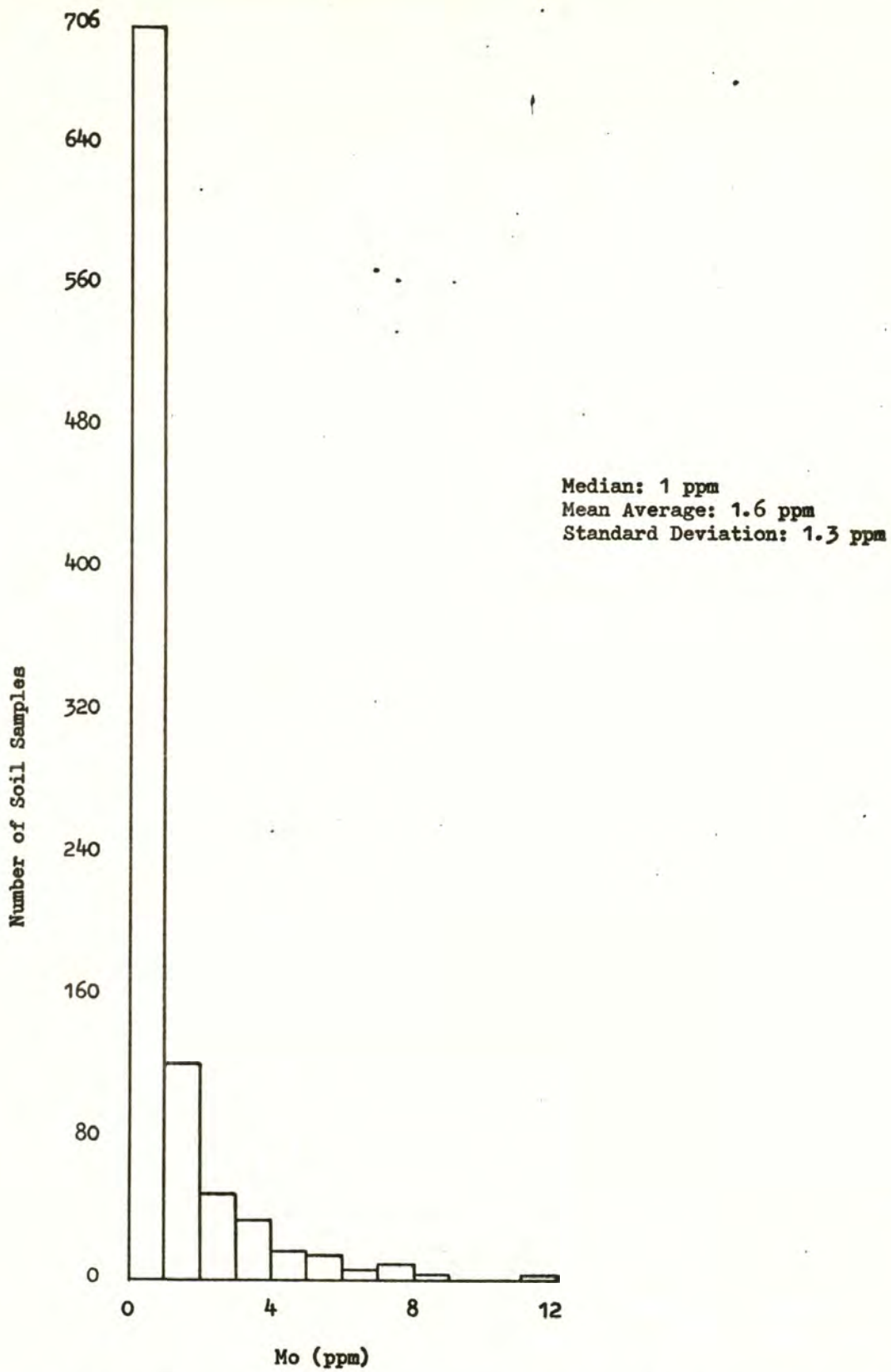


Fig. 15. Histogram and statistical data of molybdenum concentrations based on 955 soil samples.

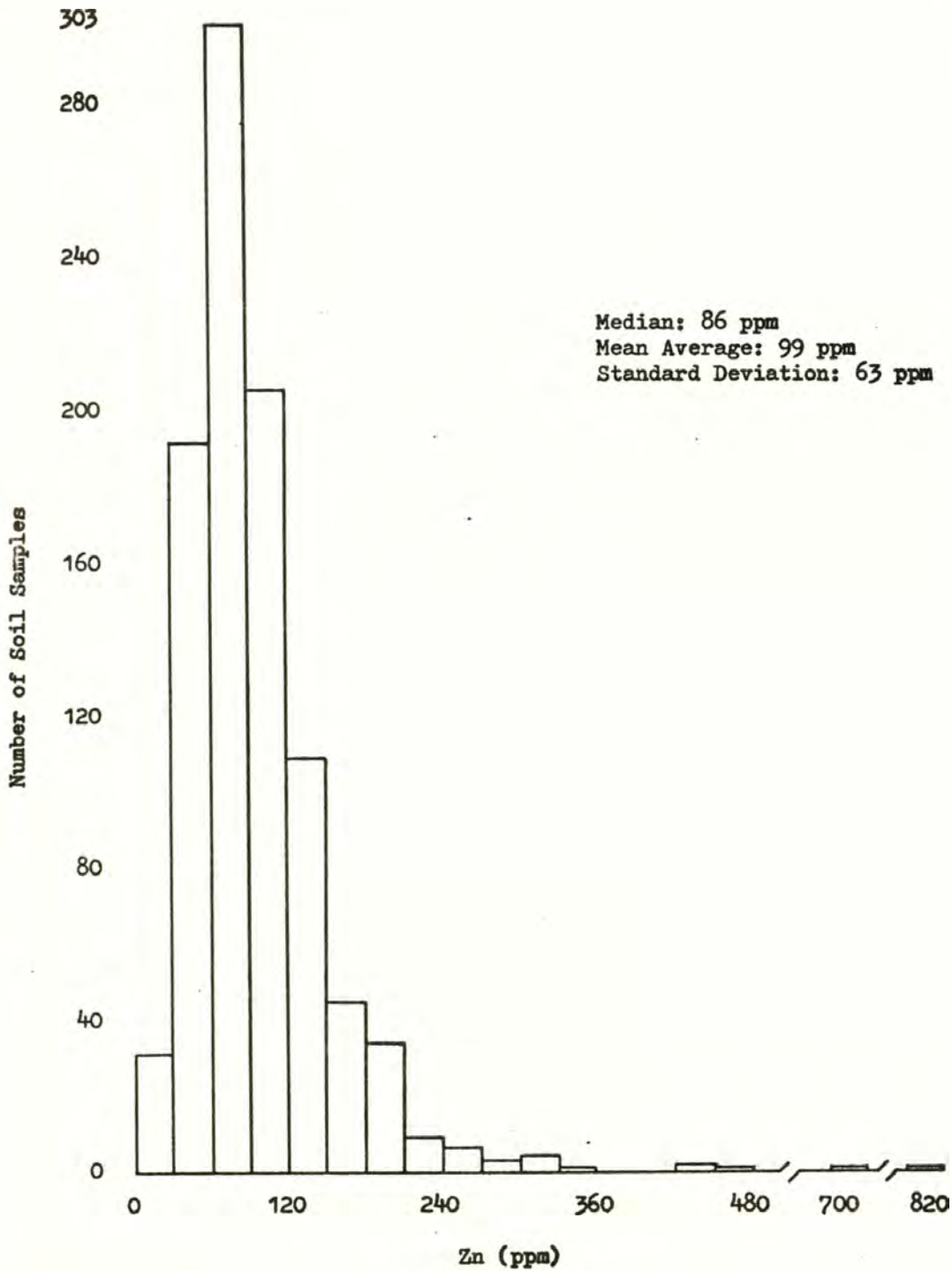


Fig. 16. Histogram and statistical data of zinc concentrations based on 955 soil samples. The ppm scale has been expanded past 480 ppm to accommodate the two larger values.

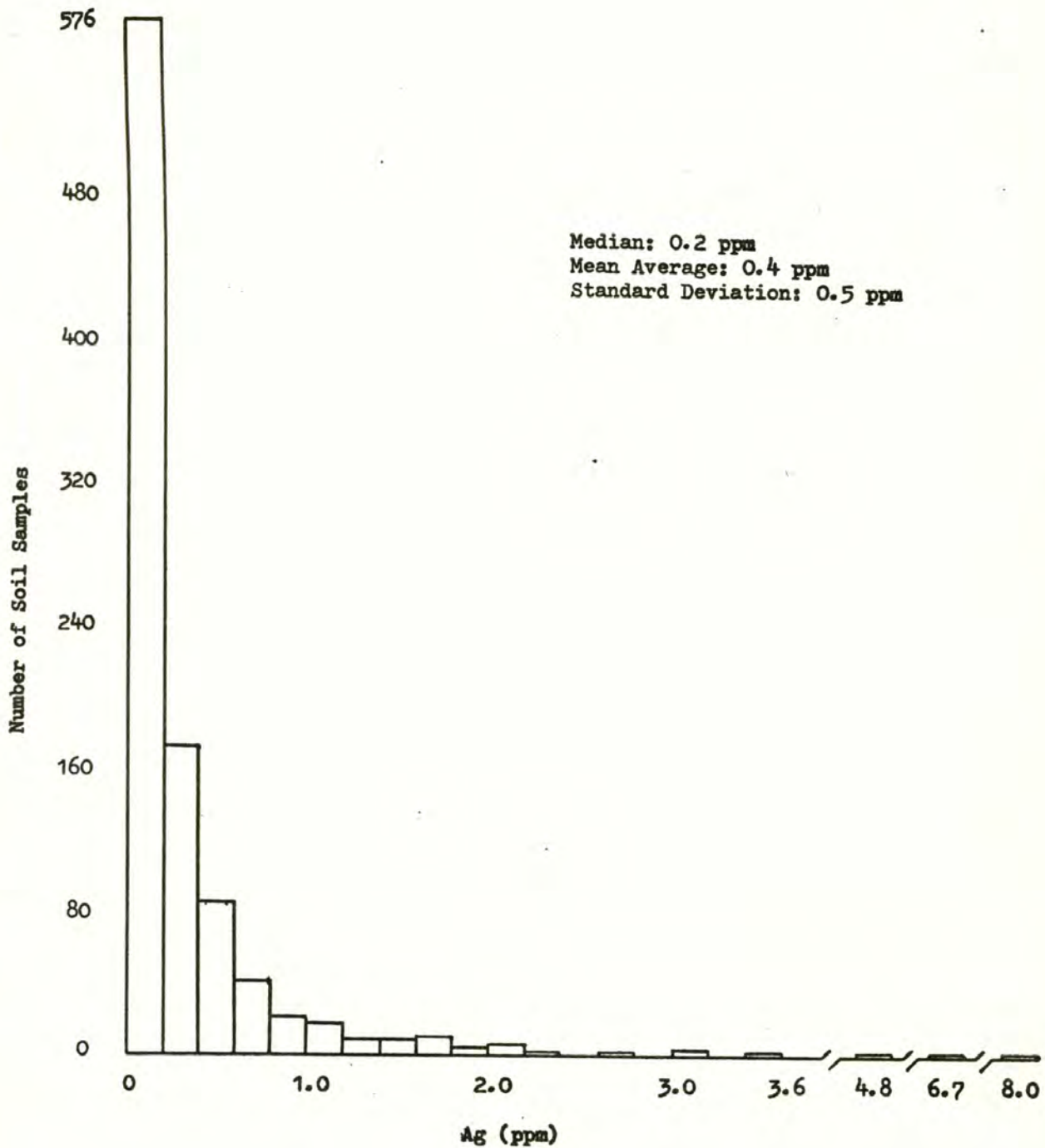


Fig. 17. Histogram and statistical data of silver concentrations based on 955 soil samples. The ppm scale has been expanded past 3.6 ppm to accommodate the three larger values.

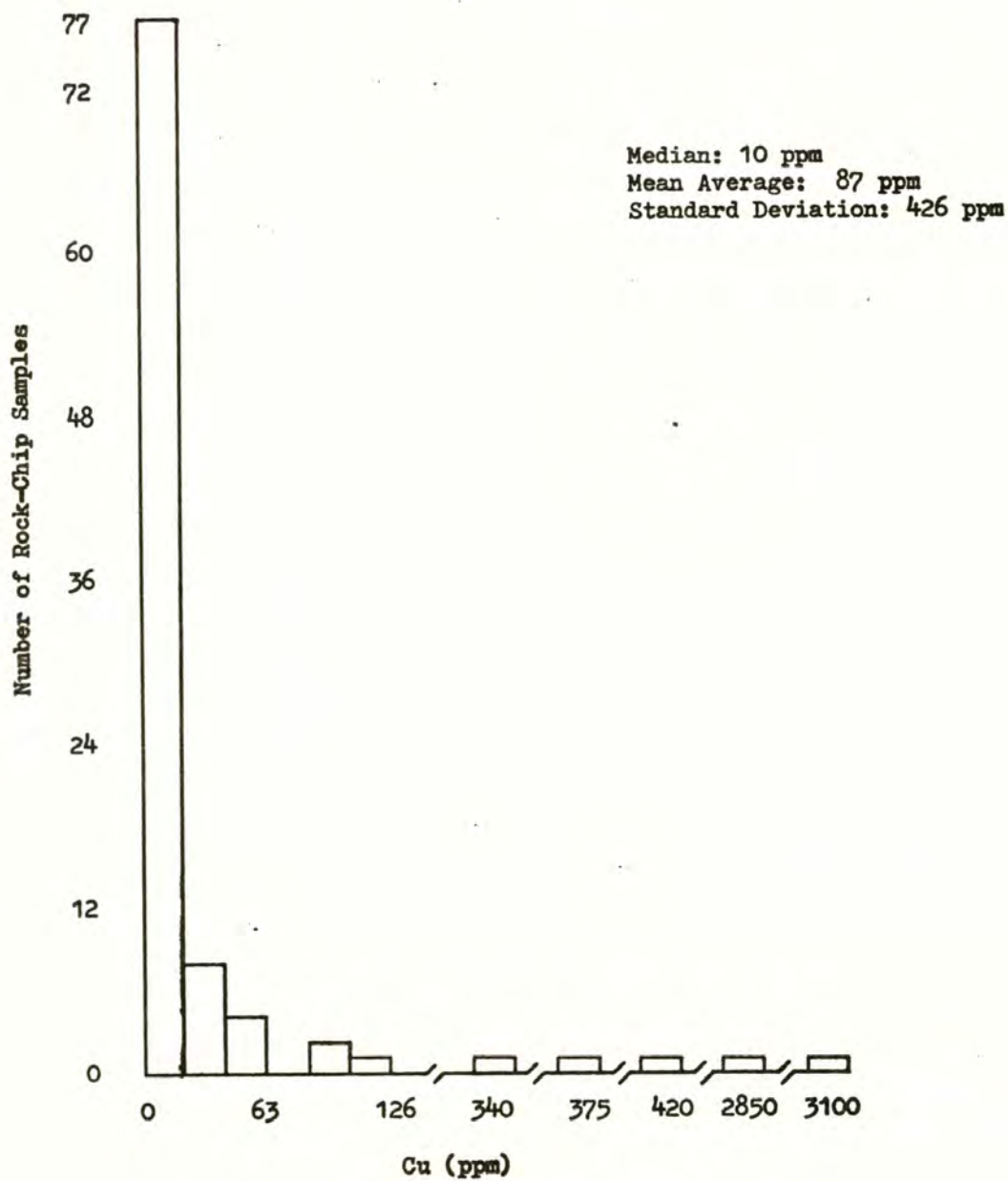


Fig. 18. Histogram and statistical data of copper concentrations based on 97 rock-chip samples. The ppm scale has been expanded past 126 ppm to accommodate the five larger values.

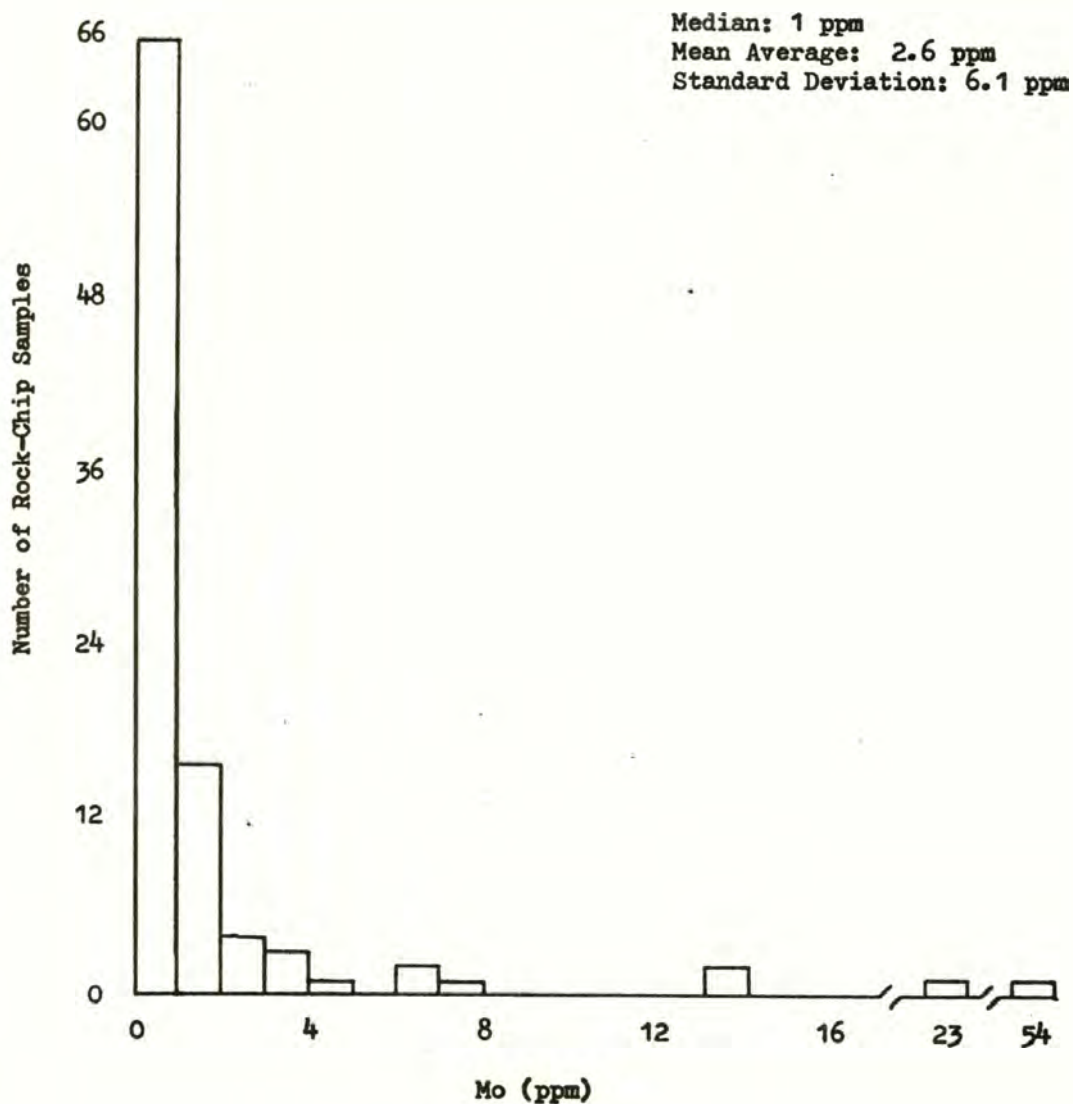


Fig. 19. Histogram and statistical data of molybdenum concentrations based on 97 rock-chip samples. The ppm scale has been expanded past 16 ppm to accommodate the two larger values.

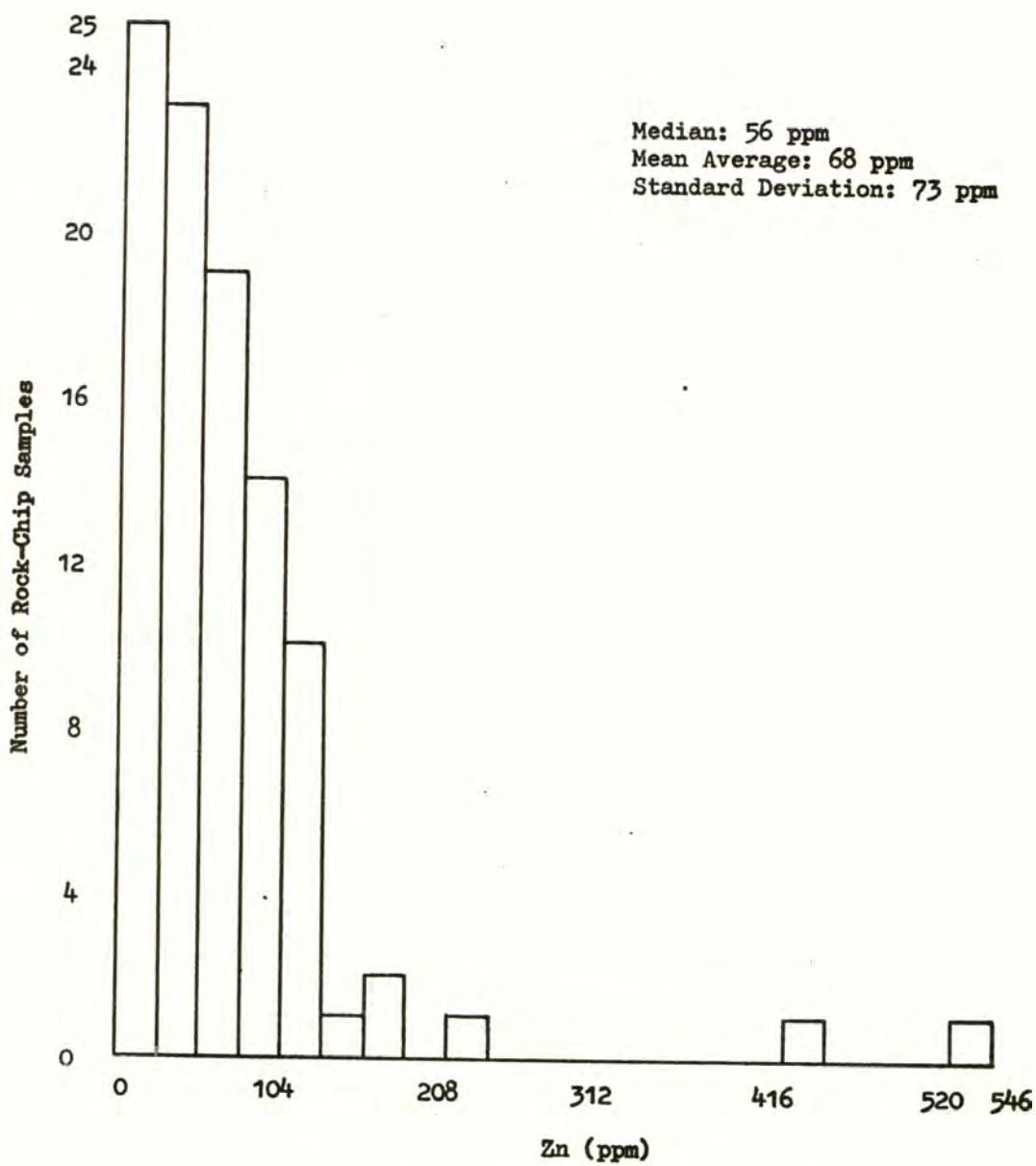


Fig. 20. Histogram and statistical data of zinc concentrations based on 97 rock-chip samples.

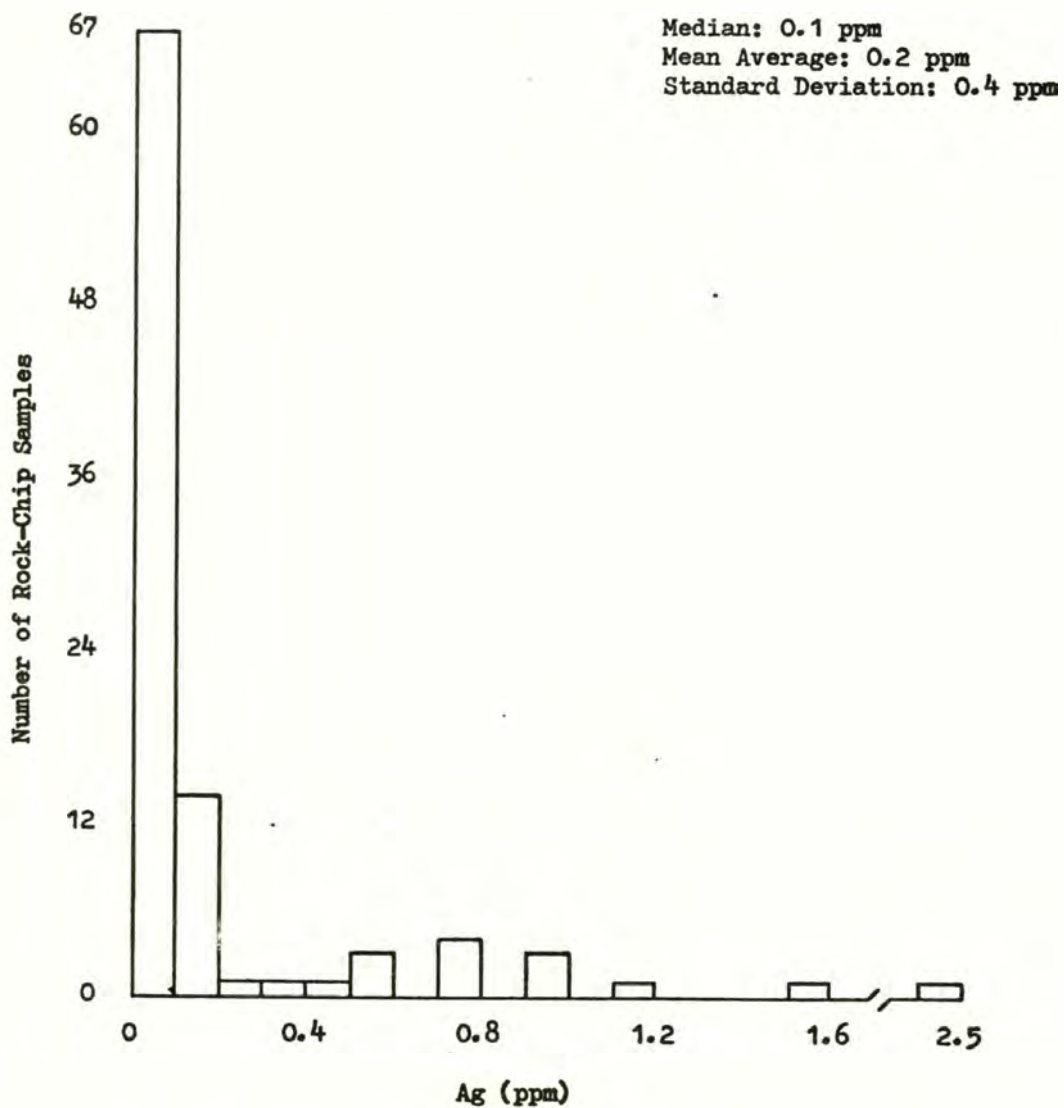


Fig. 21. Histogram and statistical data of silver concentrations based on 97 rock-chip samples. The ppm scale has been expanded past 1.6 ppm to accommodate the 2.5 ppm value.

Median: 16 ppm
Mean Average: 19
Standard Deviation: 14 ppm

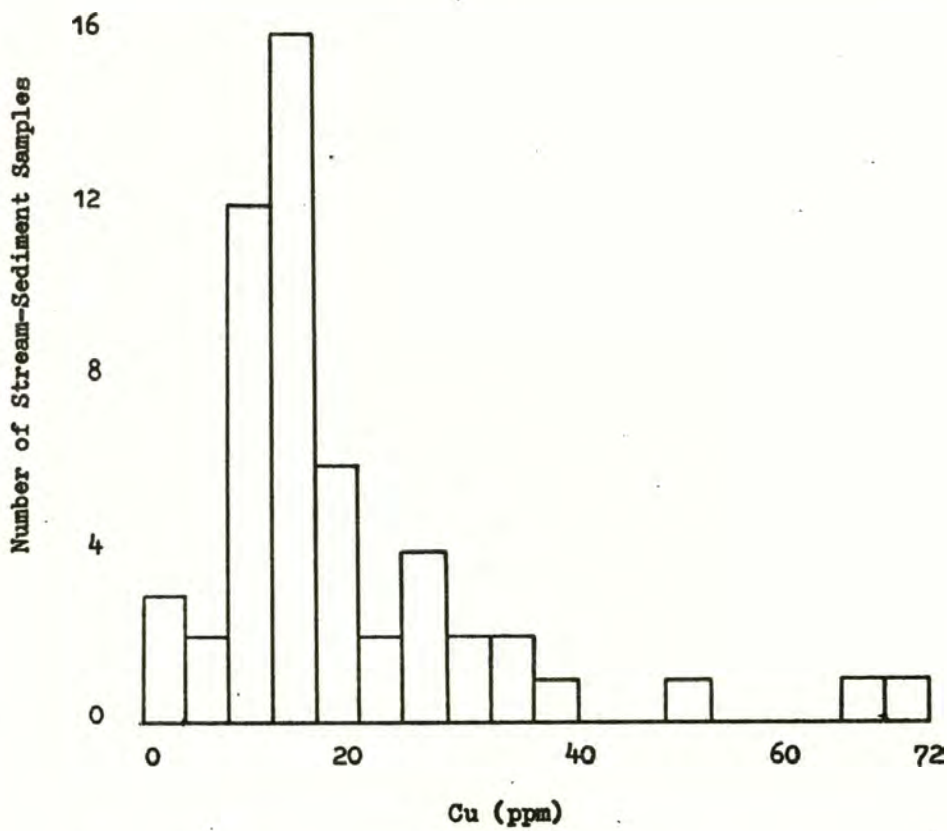


Fig. 22. Histogram and statistical data of copper concentrations based on 53 stream-sediment samples.

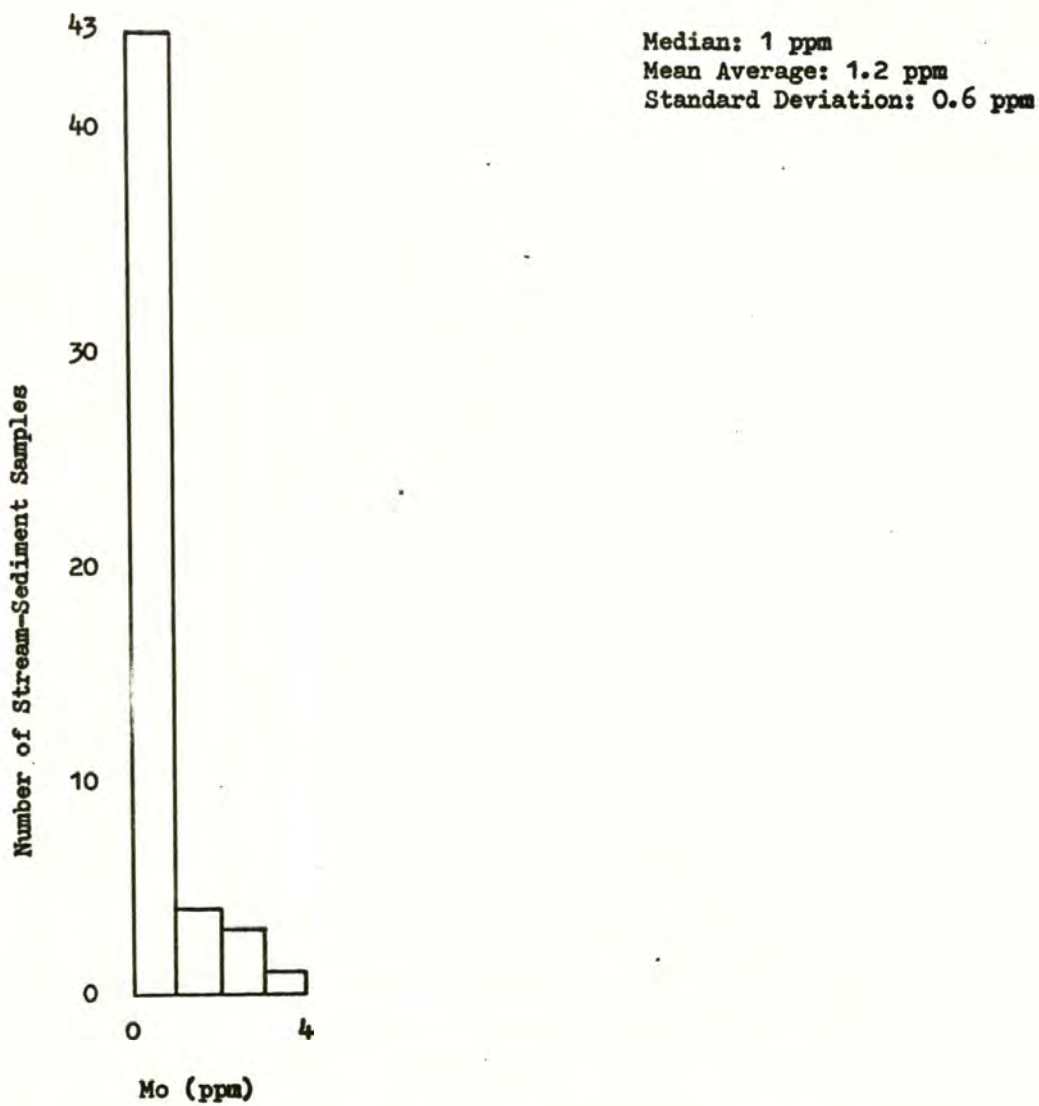


Fig. 23. Histogram and statistical data of molybdenum concentrations based on 53 stream-sediment samples.

Median: 90 ppm
Mean Average: 100 ppm
Standard Deviation: 69 ppm

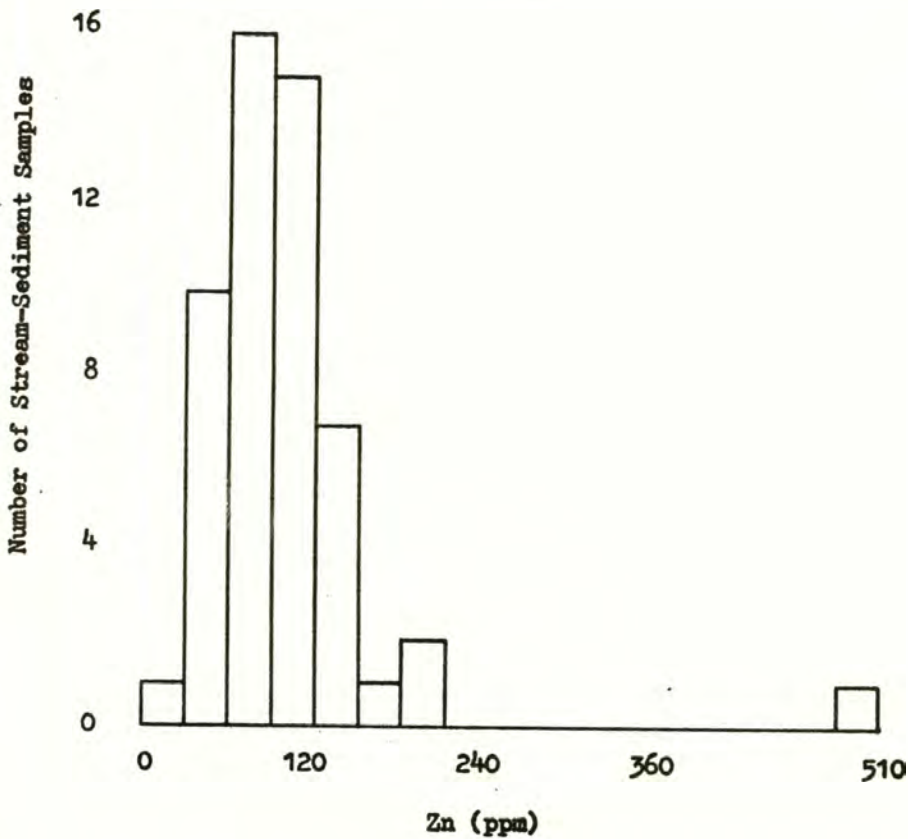


Fig. 24. Histogram and statistical data of zinc concentrations based on 53 stream-sediment samples.

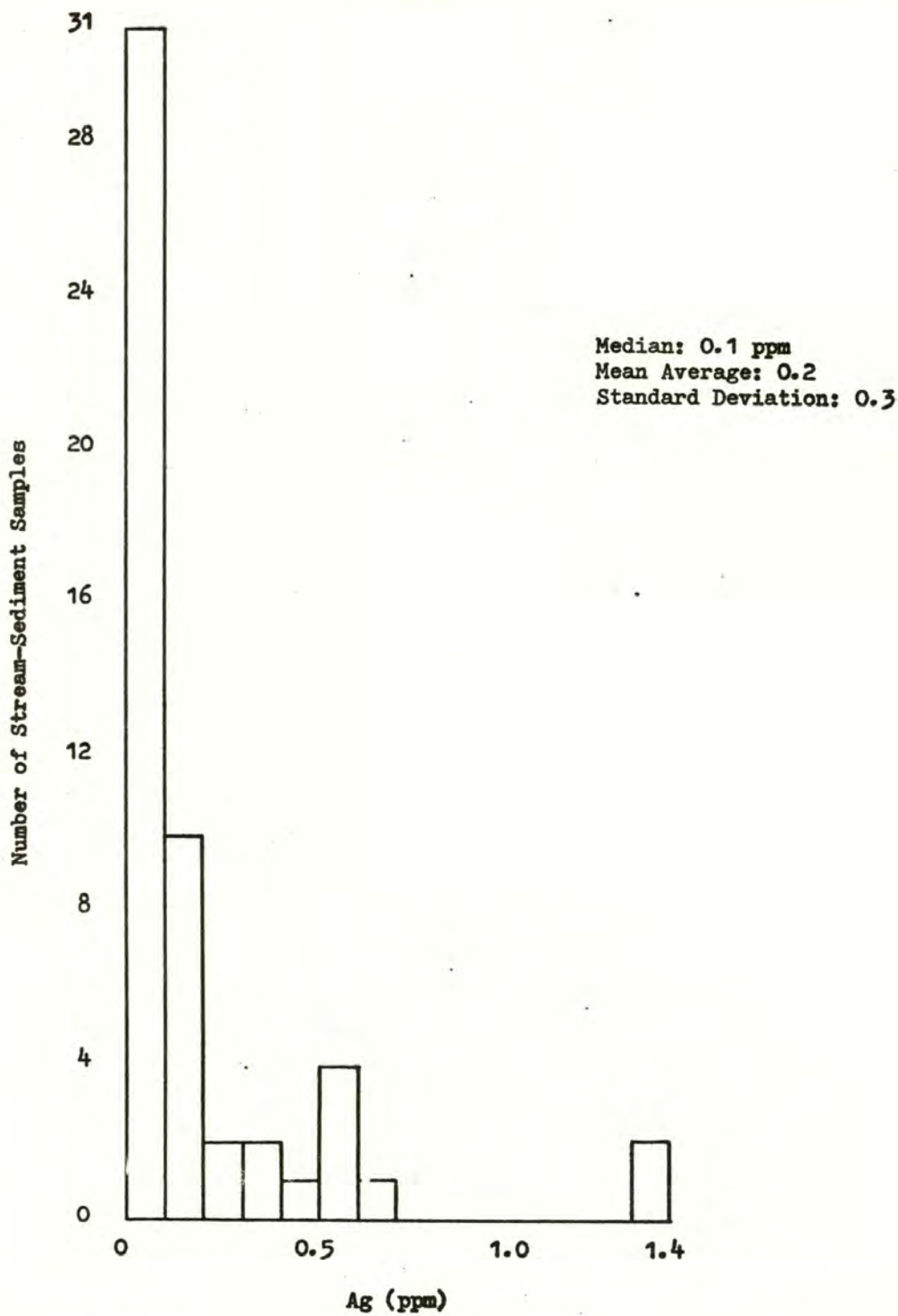


Fig. 25. Histogram and statistical data of silver concentrations based on 53 stream-sediment samples.

Table 2. This table shows how the elements copper, molybdenum, zinc, and silver for soil, rock-chip, and stream-sediment samples are classed into the anomalous groups (all values in parts per million).

SOIL	ROCK-CHIP	STREAM-SEDIMENT	ANOMALOUS GROUPS
<u>Copper</u>			
25 to 45	11 to 42	16 to 24	Potentially
46 to 65	43 to 105	25 to 36	Probably
greater than 65	greater than 105	greater than 36	Definitely
<u>Molybdenum</u>			
2 to 4	2 to 3	2	Potentially
5 to 7	4 to 5	3	Probably
greater than 7	greater than 5	greater than 3	Definitely
<u>Zinc</u>			
87 to 117	57 to 104	91 to 120	Potentially
118 to 148	105 to 156	121 to 150	Probably
greater than 148	greater than 156	greater than 150	Definitely
<u>Silver</u>			
0.3 to 0.7	0.2 to 0.4	0.2 to 0.4	Potentially
0.8 to 1.2	0.5 to 0.7	0.5 to 0.7	Probably
greater than 1.2	greater than 0.7	greater than 0.7	Definitely

anomalous.

Interpretation

Locations of reconnaissance soil samples, sample numbers, Cu/Mo values, and Zn/Ag values are given on Plates 4, 4a, and 4b respectively. Locations of rock-chip samples, sample numbers, Cu/Mo values, and Zn/Ag values are given on Plates 5, 5a, and 5b respectively. Locations of stream-sediment samples, sample numbers, Cu/Mo values, and Zn/Ag values are given on Plates 6, 6a, and 6b respectively.

Before evaluating the geochemical results it should be emphasized that the map area was unglaciated during Pleistocene time and is presently in a zone of discontinuous permafrost. These conditions have affected the secondary dispersion of certain elements and must be taken into consideration when interpreting soil and stream-sediment geochemistry.

Horsnail and Fox (1974) have noted that chemical and physical weathering as well as hydromorphic and clastic dispersion in permafrost terrains affect secondary dispersion of certain elements. They have suggested that hydromorphic dispersion within the seasonally thawed active zone of permafrost is widespread, and that the water in this zone is generally enriched in metals. To explain this, Horsnail and Fox (1974) noted that low temperatures tend to increase the concentration of elements in soil and groundwater solutions by a process of partial freezing. In the Dawson Range, Yukon Territory, Coope (1966) noted that zinc is strongly affected by hydromorphic dispersion. He attributes this to leaching from the more acidic near-surface soil horizon.

Horsnail and Fox (1974) observed that chemical weathering is more intense on south-facing slopes than those facing north, and that drainage channels on the southerly slopes are likely to receive a considerable influx of dissolved metals. This phenomenon was also noted by Archer

and Main (1971) when describing drainage anomalies associated with the Casino deposit, Yukon Territory (see Fig. 41 for location). They found that streams on south-facing slopes are moderately acid and anomalous in copper. In marked contrast, north-facing drainage systems are nearly neutral and contain only background copper.

Physical weathering is mainly characterized by the freeze-thaw cycle which provides material for clastic dispersion. The characteristic features of clastic dispersion are downslope migration of anomalies under the influence of solifluction and the occurrence of frost boils within which mineral fragments may be brought to the surface from depths of several feet (Horsnail and Fox, 1974).

Rock-chip samples were collected throughout the map area but the sample density was not large enough to determine primary dispersion patterns for the four trace elements.

To locate areas of potential mineralization and show geochemical trends I constructed four reconnaissance anomaly maps, one for each trace element. The maps were compiled by using geochemical values from the previously established groups "probably anomalous and definitely anomalous". Values of the two anomalous groups from the soil, rock-chip, and stream-sediment samples were combined for each element and plotted on maps. The anomalous values on each map were enclosed to show the general areas of trace element concentration (Figs. 26 thru 29).

The four trace element maps show a general relationship in geochemical trends but copper is more erratic than the other elements, and is anomalous throughout the north-half of the map area in the greenschist and mica schist units. The rocks of these two metamorphic units may be derived from both sediments and volcanics, and it has been noted by Levinson (1974) that sediments (shales) and mafic volcanics are generally higher

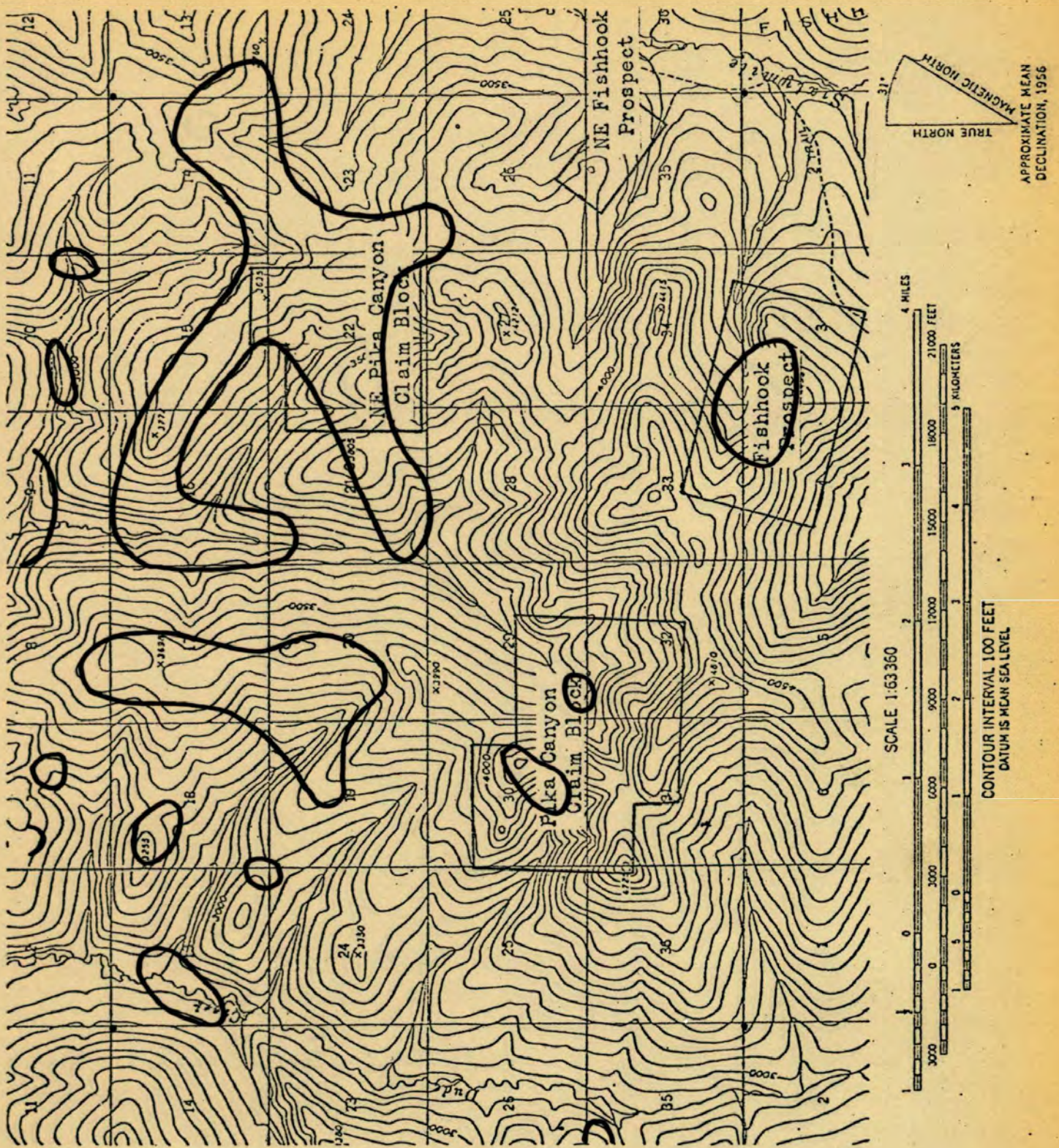
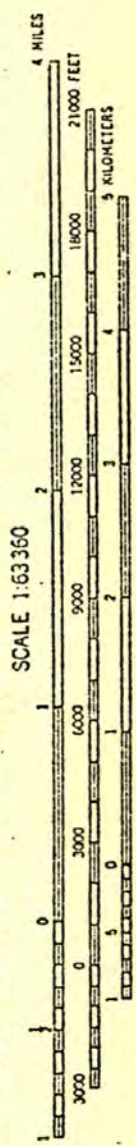
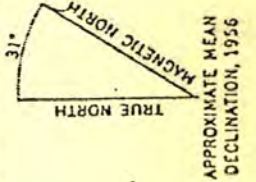
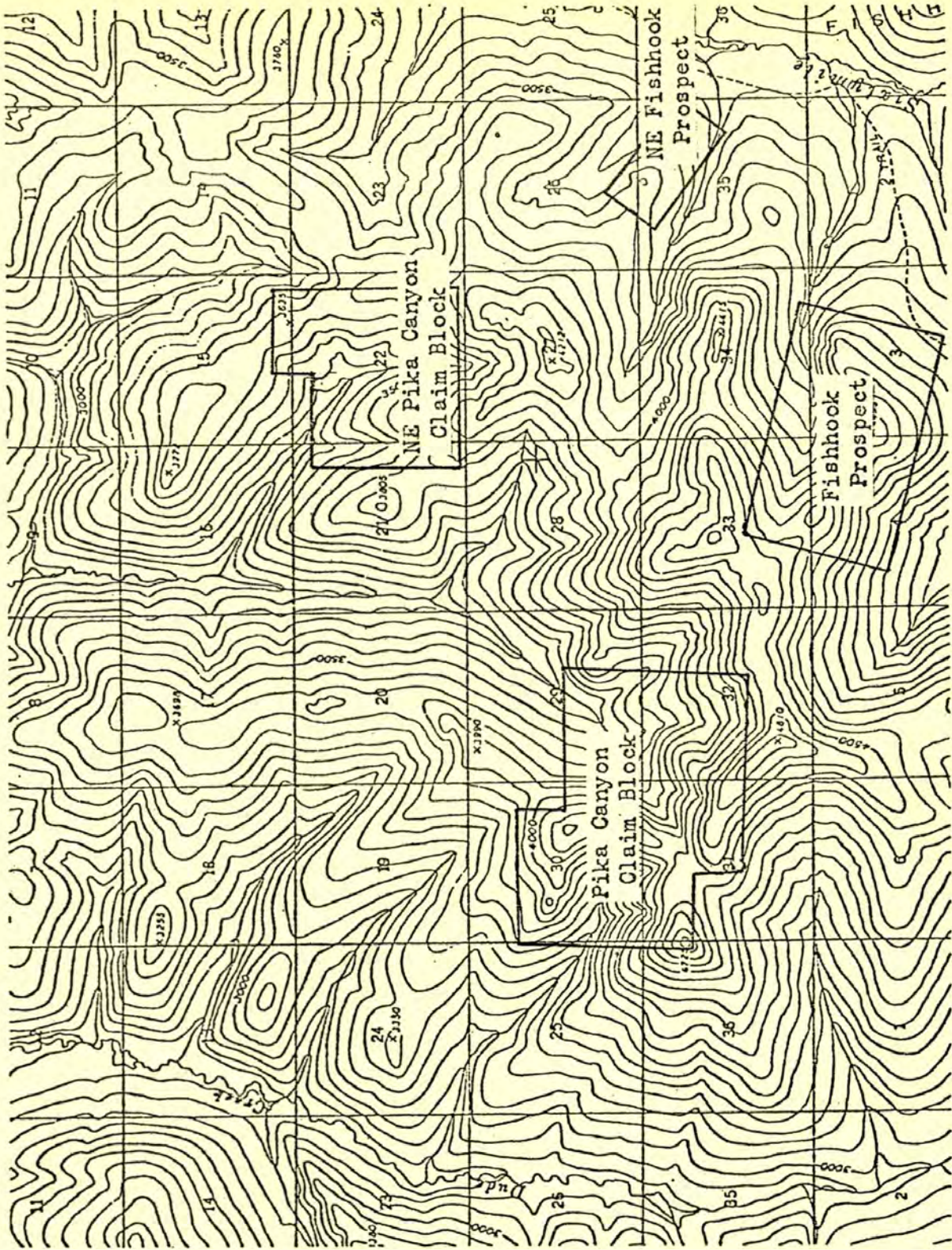


Fig. 26. Distribution of copper based on anomalous values from reconnaissance soil, rock-chip, and stream-sediment samples.



CONTOUR INTERVAL 100 FEET
 DATUM IS MEAN SEA LEVEL

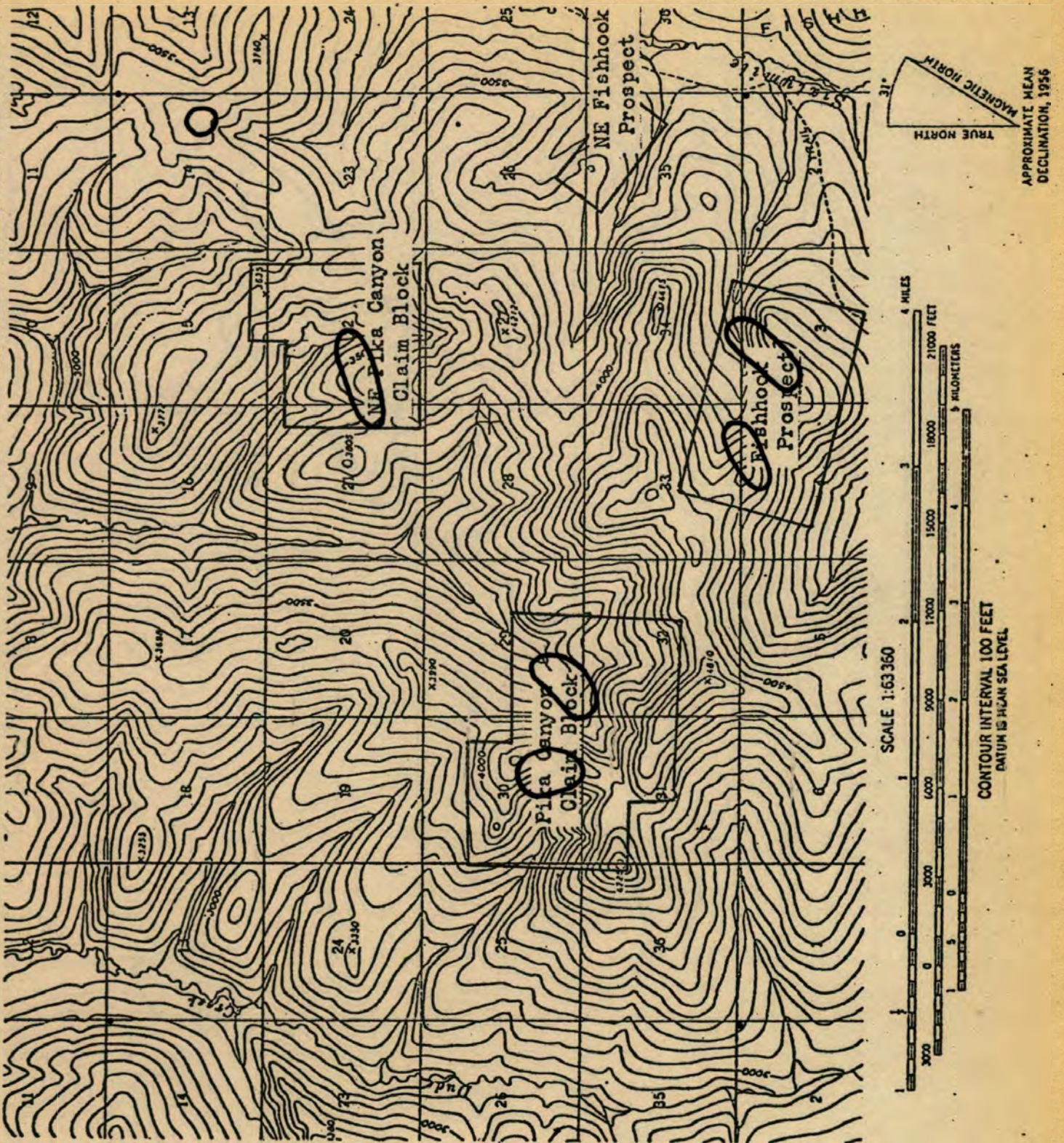
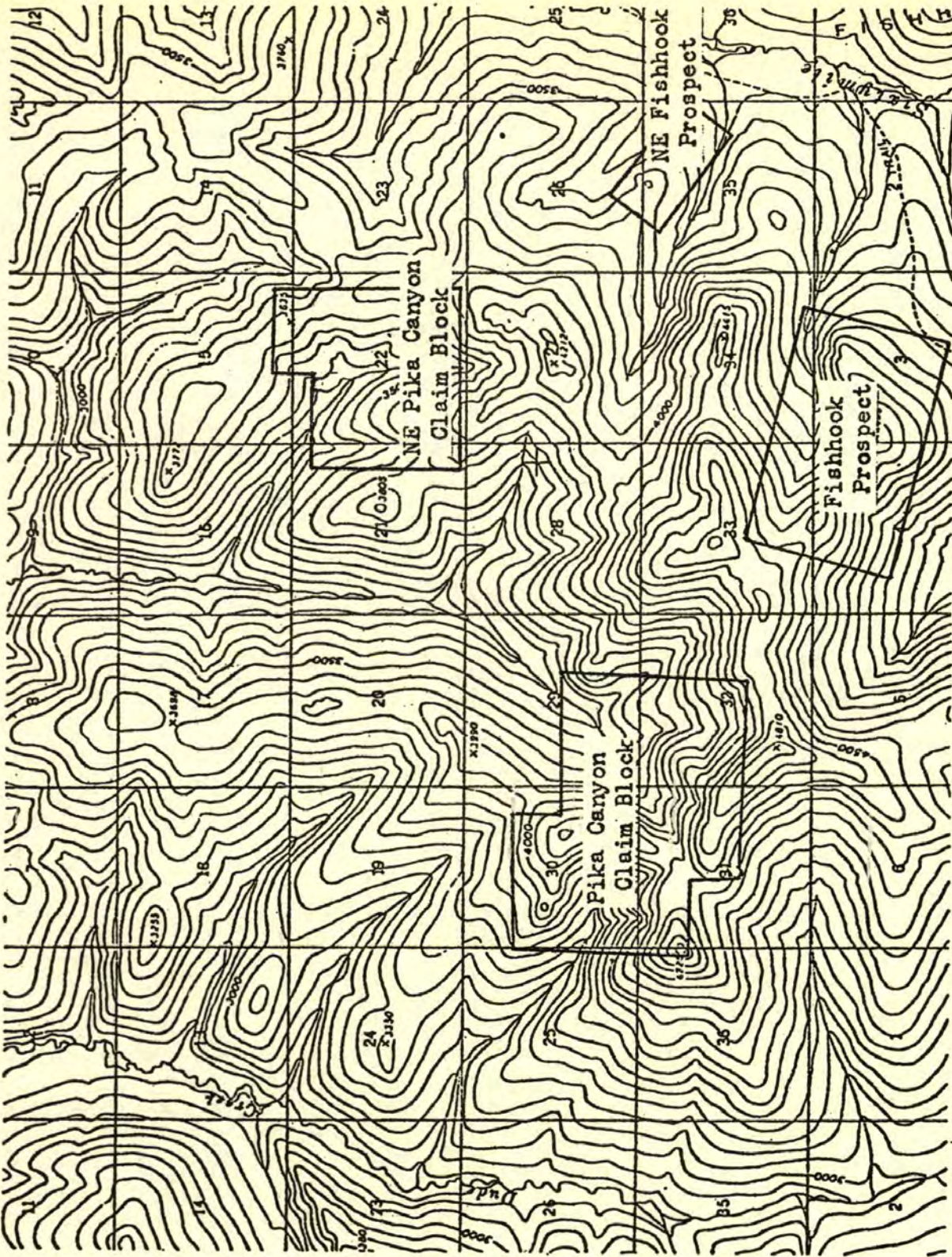
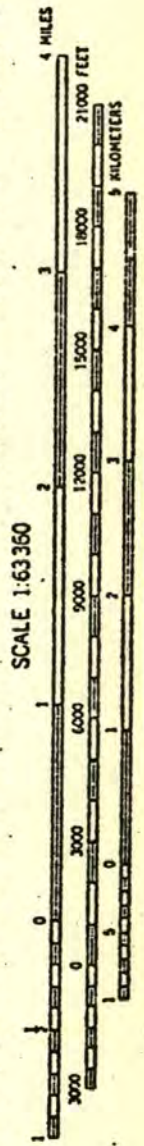


Fig. 27. Distribution of molybdenum based on anomalous values from reconnaissance soil, rock-chip, and stream-sediment samples.



APPROXIMATE MEAN DECLINATION, 1956



SCALE 1:63,360

CONTOUR INTERVAL 100 FEET
DATUM IS MICHIGAN SEA LEVEL

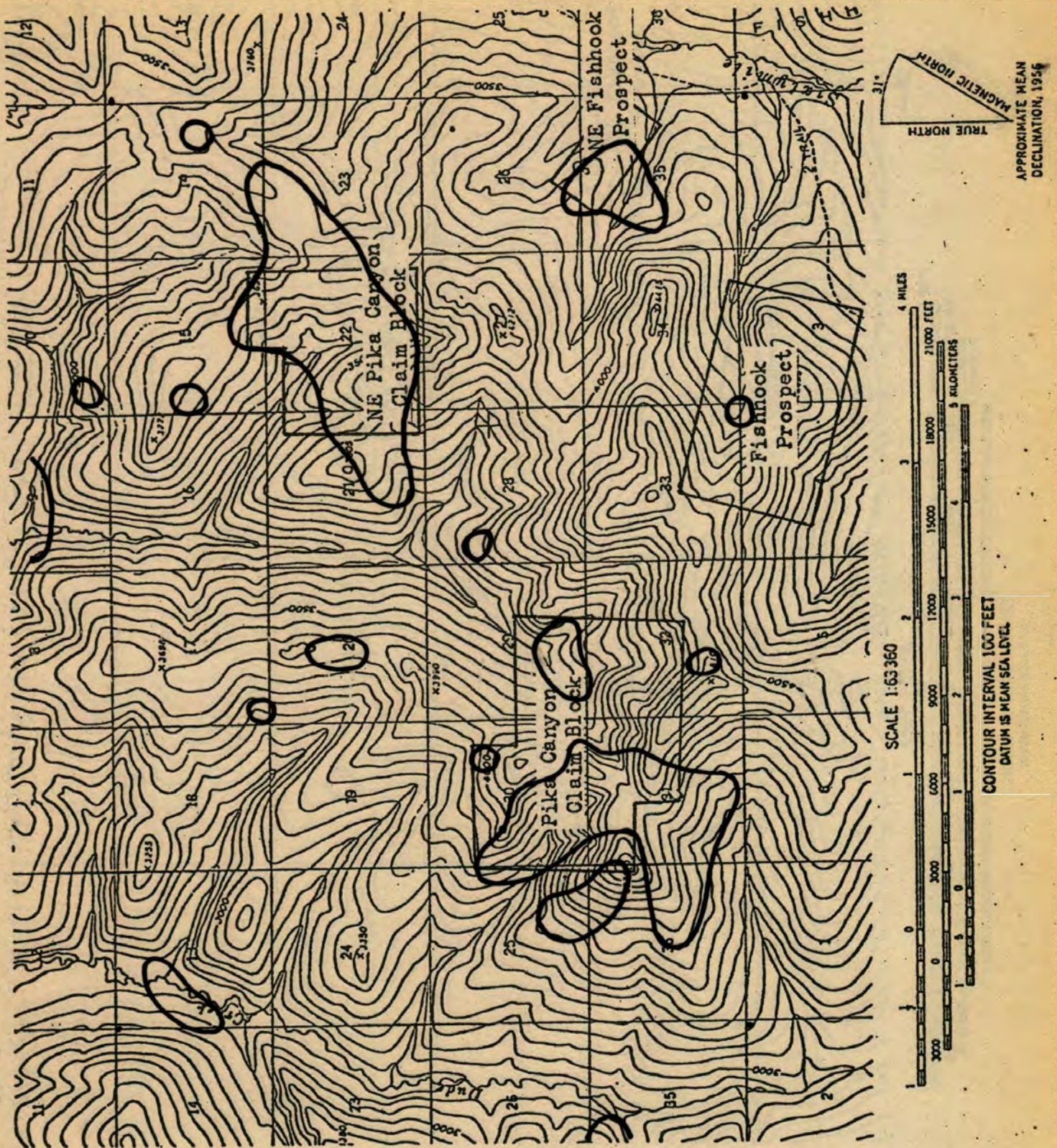
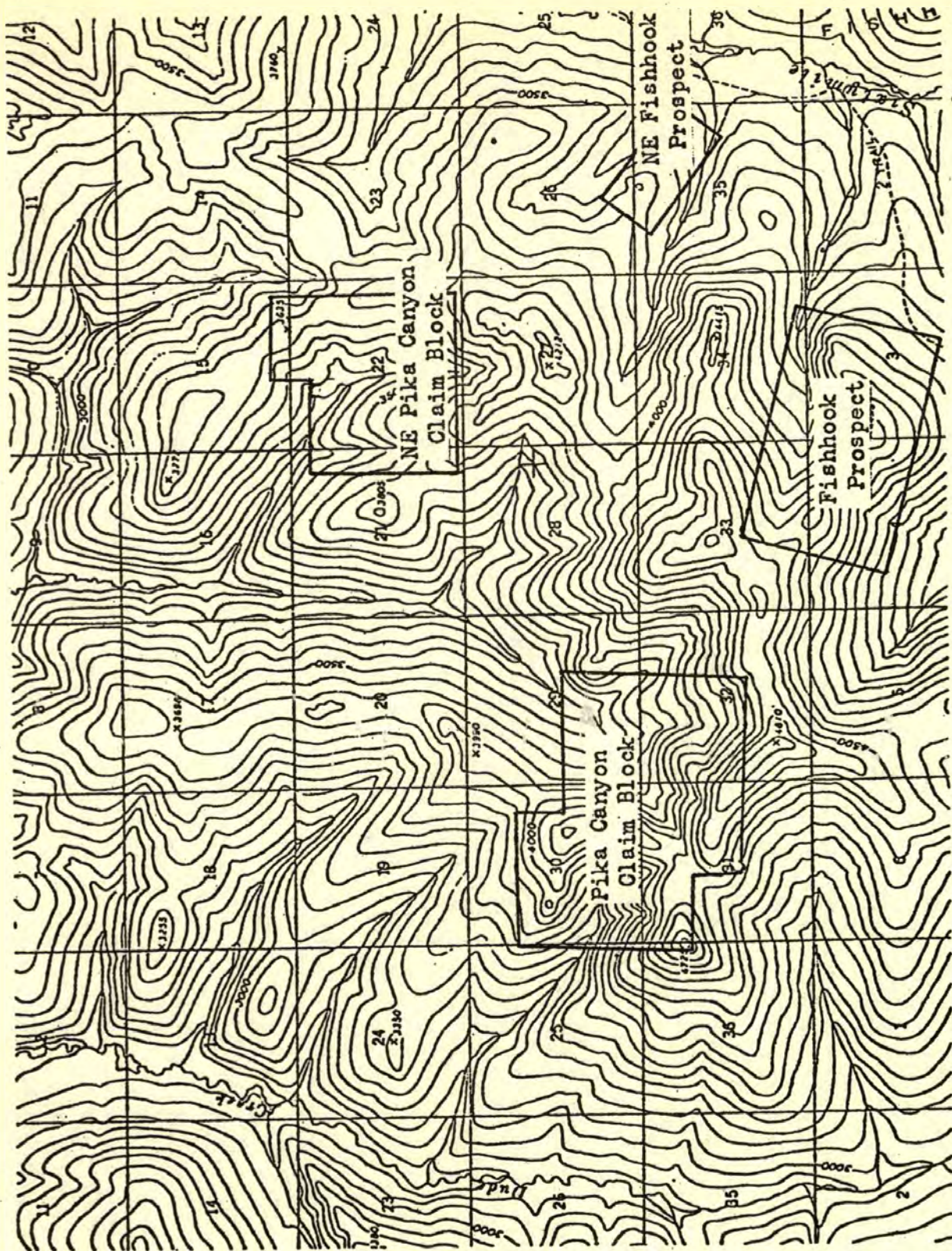
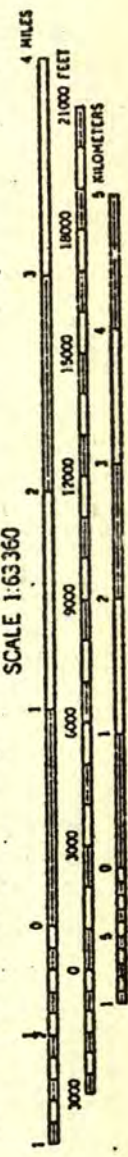


Fig. 28. Distribution of zinc based on anomalous values from reconnaissance soil, rock-chip, and stream-sediment samples.



APPROXIMATE MEAN DECLINATION, 1956



SCALE 1:63360

CONTOUR INTERVAL 100 FEET
DATUM IS MEAN SEA LEVEL

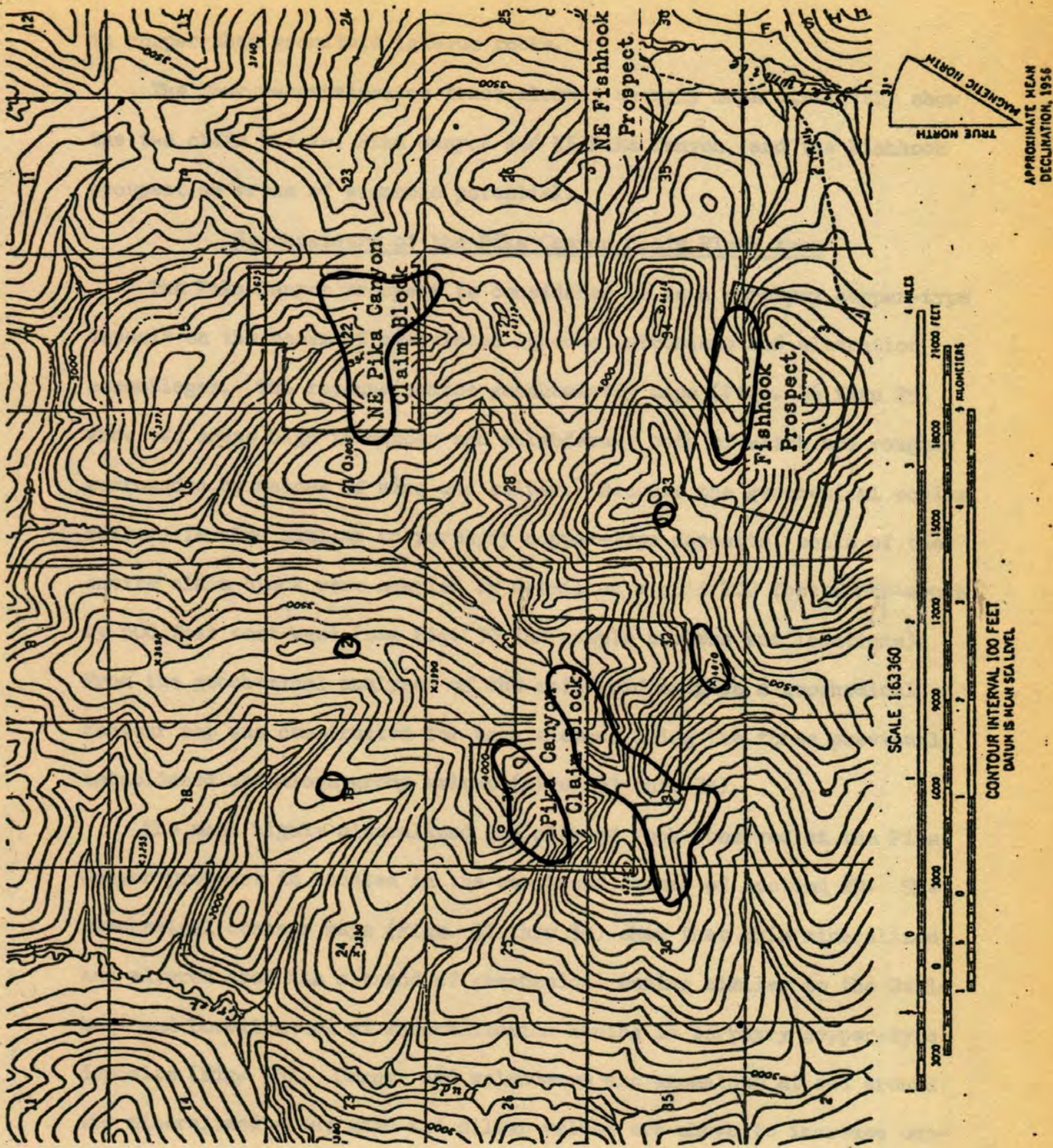
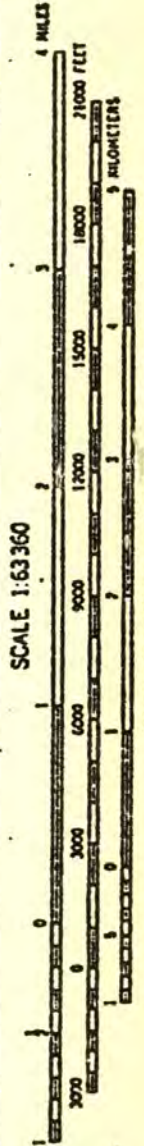
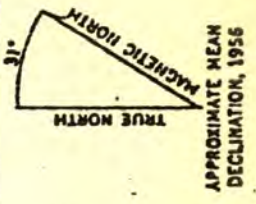
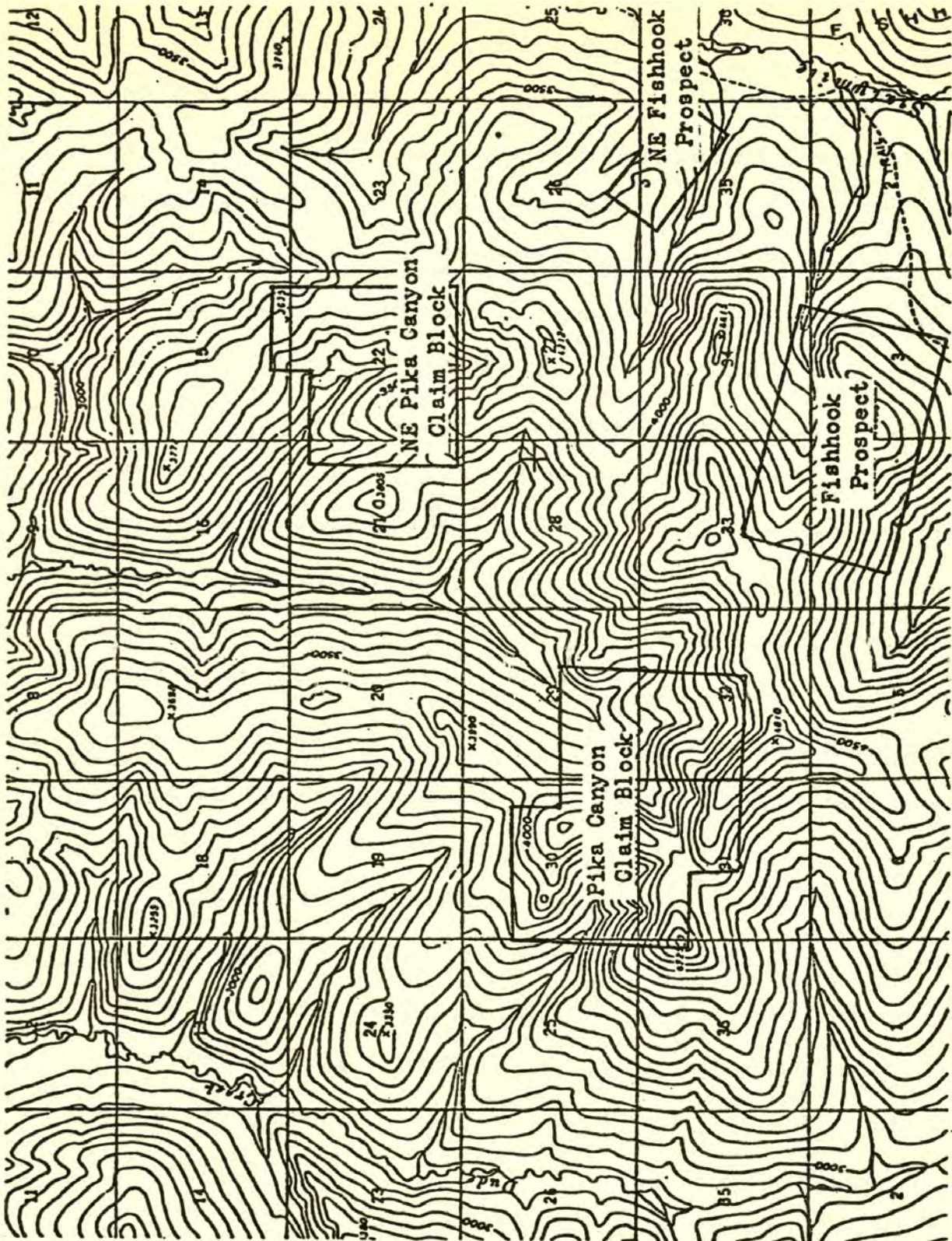


Fig. 29. Distribution of silver based on anomalous values from reconnaissance soil, rock-chip, and stream-sediment samples.



CONTOUR INTERVAL 100 FEET
DATUM IS MEAN SEA LEVEL

in copper than granitoid igneous rocks.

The four reconnaissance trace element anomaly maps distinctly show the two claim blocks, Pika Canyon and NE Pika Canyon, and the Fishhook prospect as areas of economic potential.

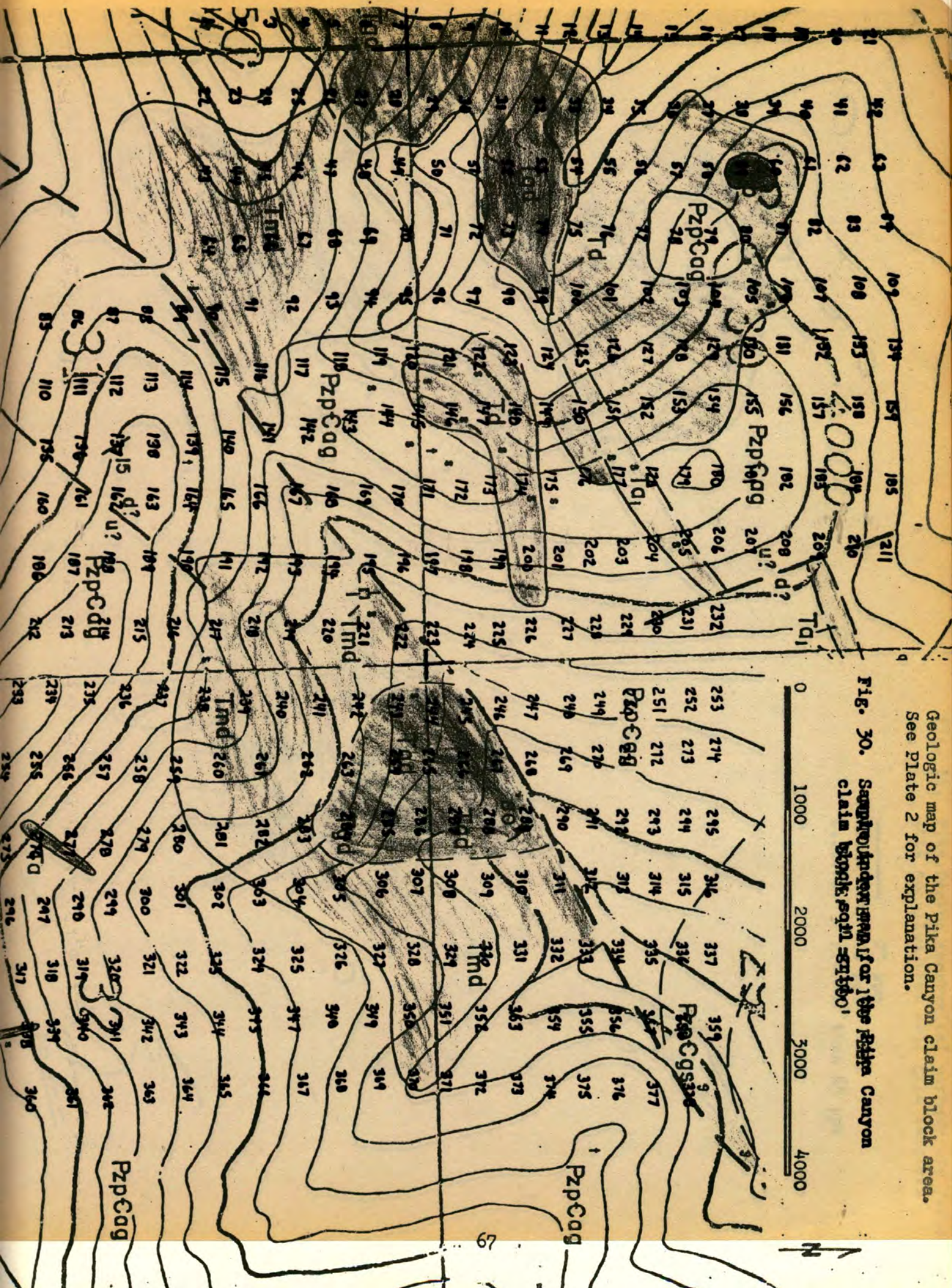
Geochemistry of the Pika Canyon Claim Block Area

The Pika Canyon prospect is considered to be a porphyry copper-type deposit on the basis of associated igneous intrusions and alteration assemblages. The reconnaissance geochemistry maps (Figs. 26 thru 29) show two areas high in copper and molybdenum, both of which are roughly surrounded by haloes of zinc and silver. Because the geochemical zoning pattern is also similar to porphyry copper-type deposits, soils of the entire claim block were sampled in detail on a grid 200 feet north-south by 500 feet east-west (see Fig. 30 for sample numbers and locations). From the geochemical analyses of the soil grid samples a geochemical contour map was constructed for each element using the three previously established anomalous group values (Figs. 31 thru 34).

The most highly mineralized and altered rock observed at the Pika Canyon prospect is located in the southwest corner of section 29. The geochemical contour maps (Figs. 31 thru 34) show that this mineralized and altered area has a trend of geochemical zoning similar to the Guilbert and Lowell model of mineralization zoning in porphyry copper-type deposits (Fig. 35). Copper and molybdenum are anomalous at and around the mineralized area; zinc and silver values are shown to increase outward. Another area of interest is in the central portion of section 30. At this location the geochemical anomaly is larger than that of the known mineralized area, and shows a similar geochemical zoning pattern. The anomaly is located on a south-facing slope which suggests that thawing of the permafrost would promote solifluction; thereby enlarging the secondary

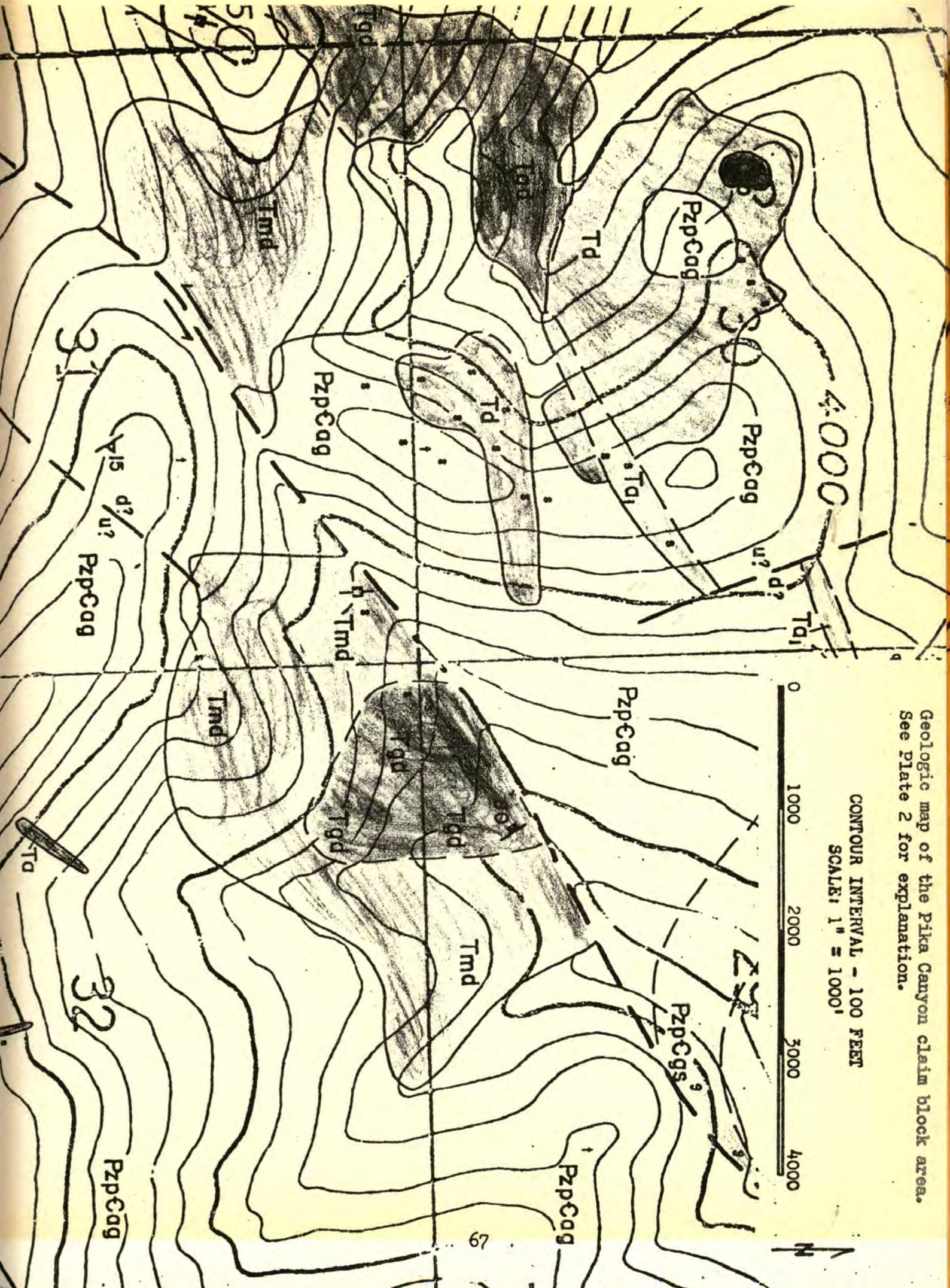
Geologic map of the Pika Canyon claim block area.
See Plate 2 for explanation.

Fig. 30. Sample locations for the Pika Canyon claim block area.



Geologic map of the Pika Canyon claim block area.
See Plate 2 for explanation.

CONTOUR INTERVAL - 100 FEET
SCALE: 1" = 1000'



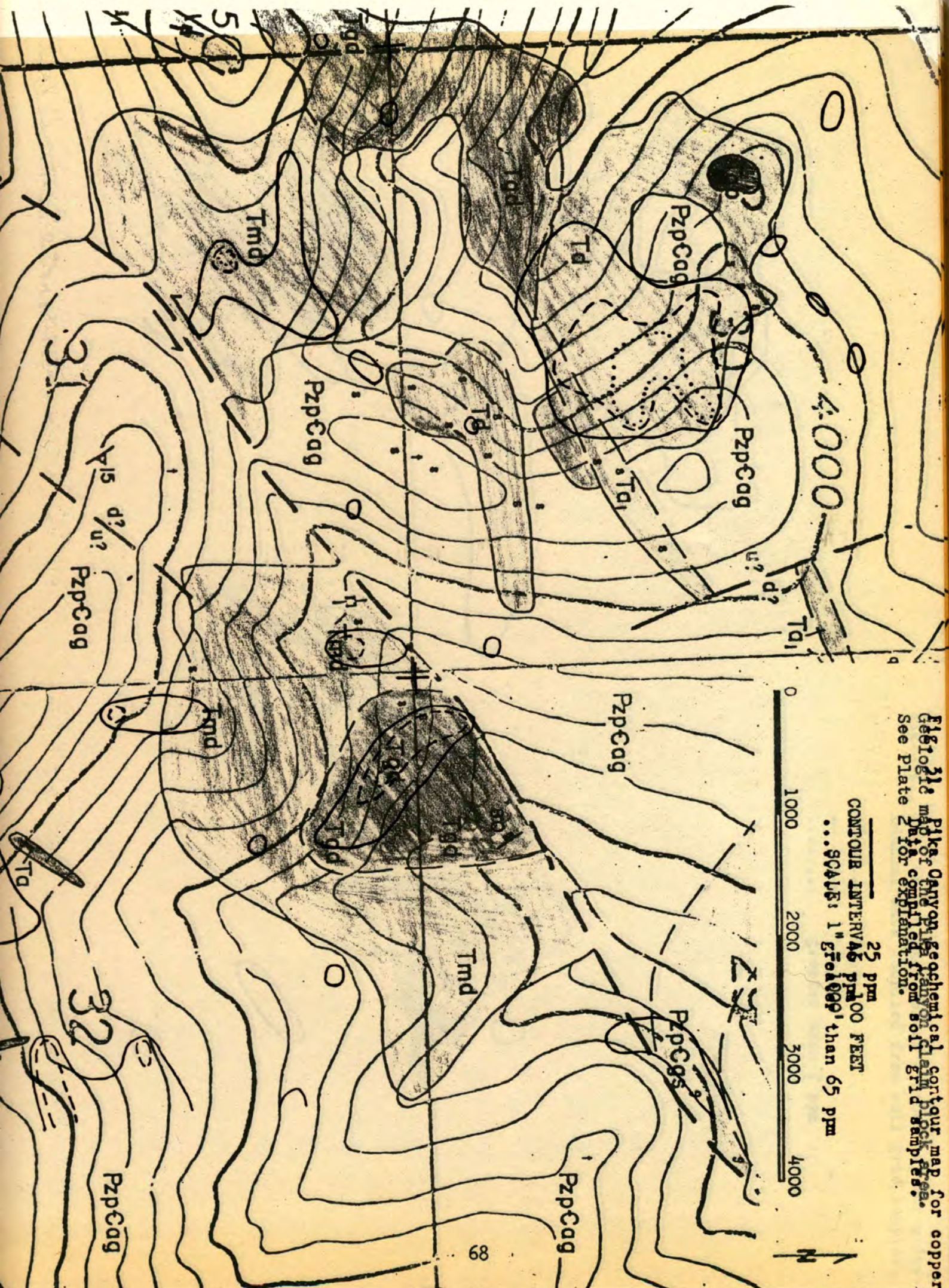
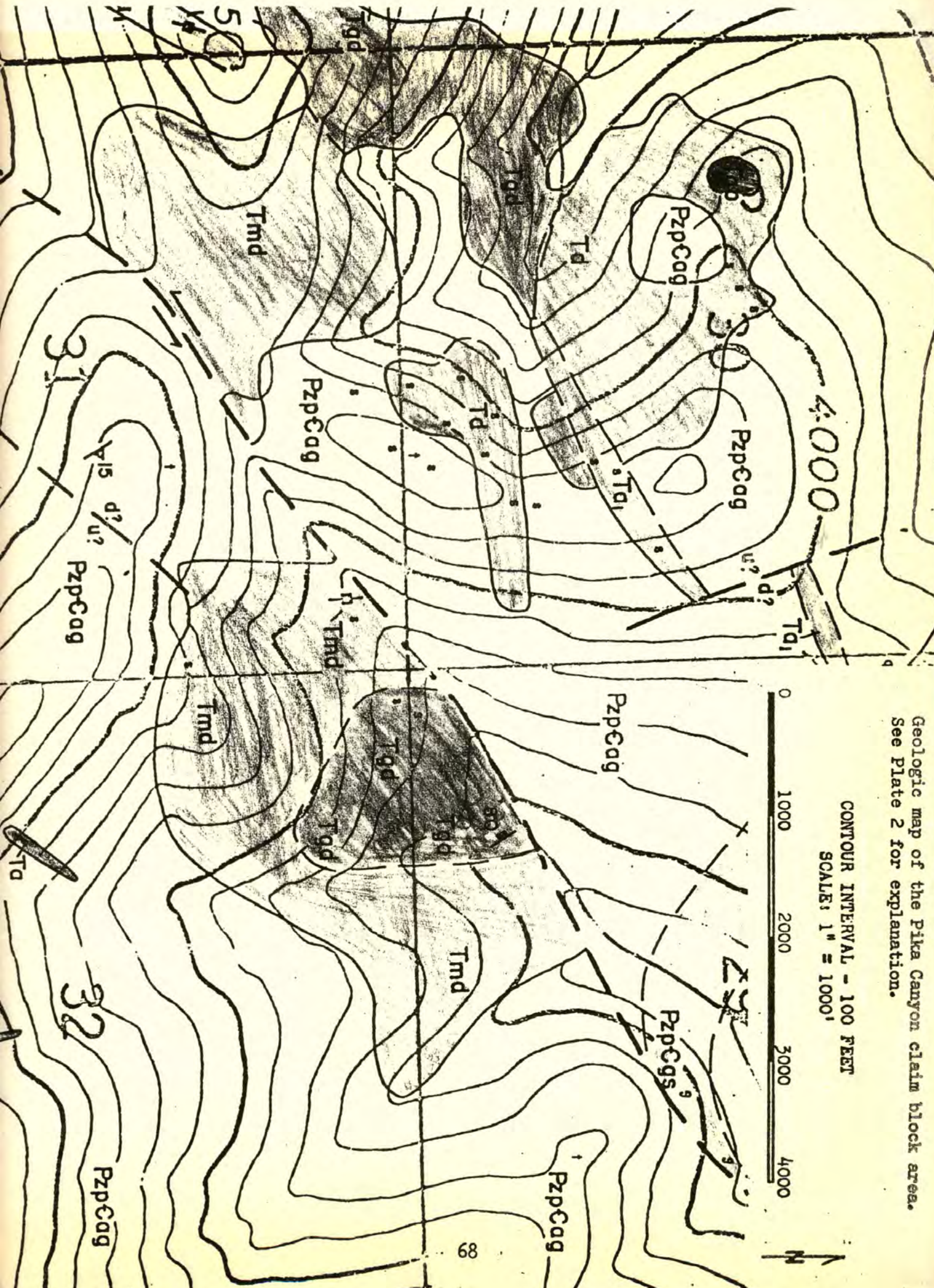
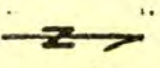
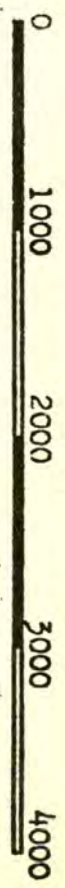


Fig. 31. Plate Canyon geochemical contour map for copper. Data compiled from soil grid samples. See Plate 2 for explanation.

25 ppm
 CONTOUR INTERVALS 100 FEET
 ...SCALE: 1" = 6000' (than 65 ppm)

Geologic map of the Pika Canyon claim block area.
See Plate 2 for explanation.

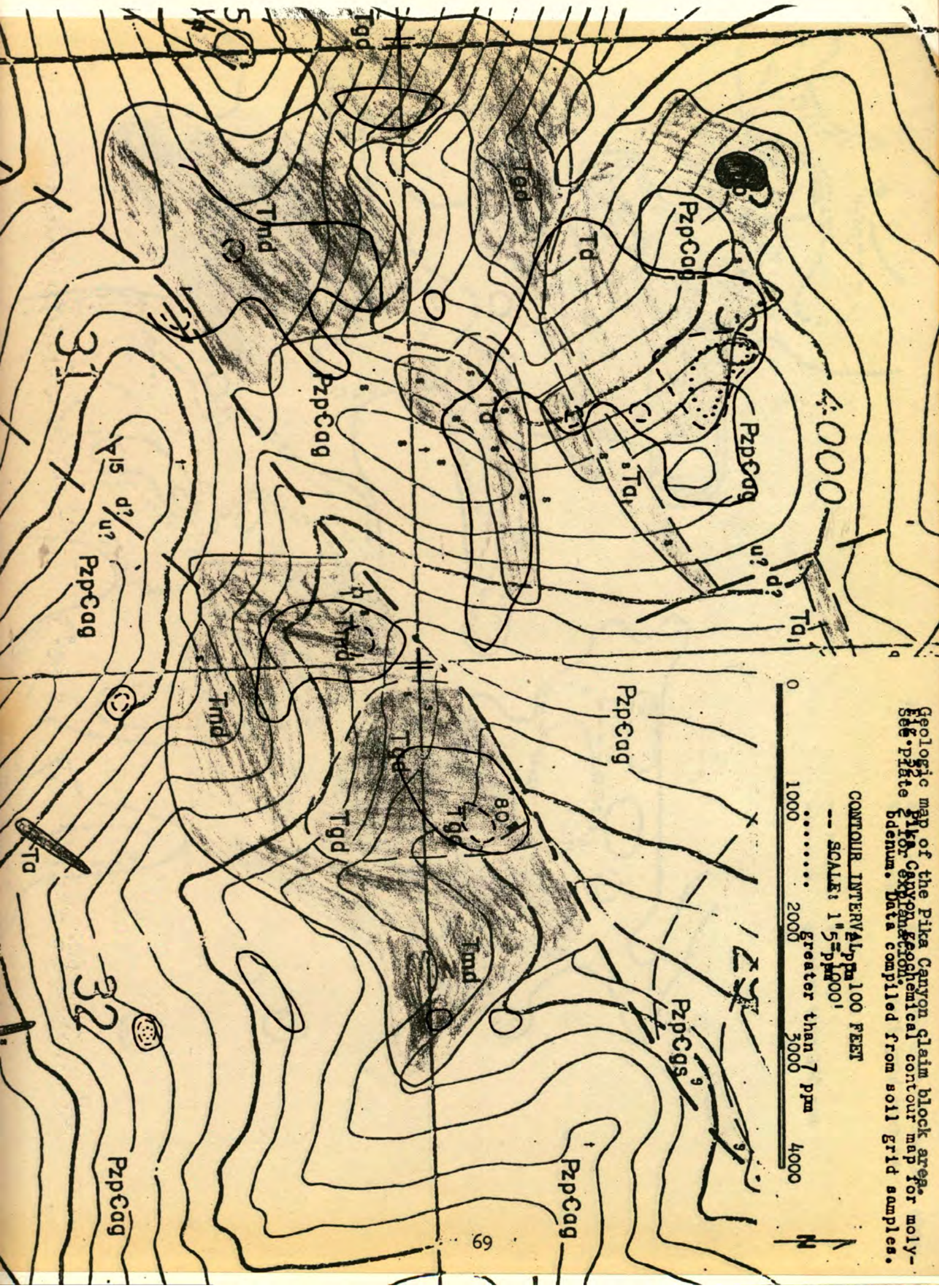
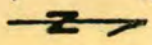
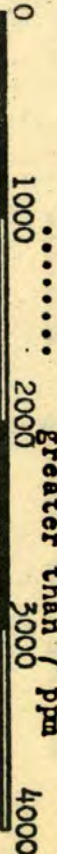
CONTOUR INTERVAL - 100 FEET
SCALE: 1" = 1000'



Geologic map of the Pika Canyon claim block area, Big Pine, California. See Plate 1 for Pika Canyon geologic map for molybdenum. Data compiled from soil grid samples.

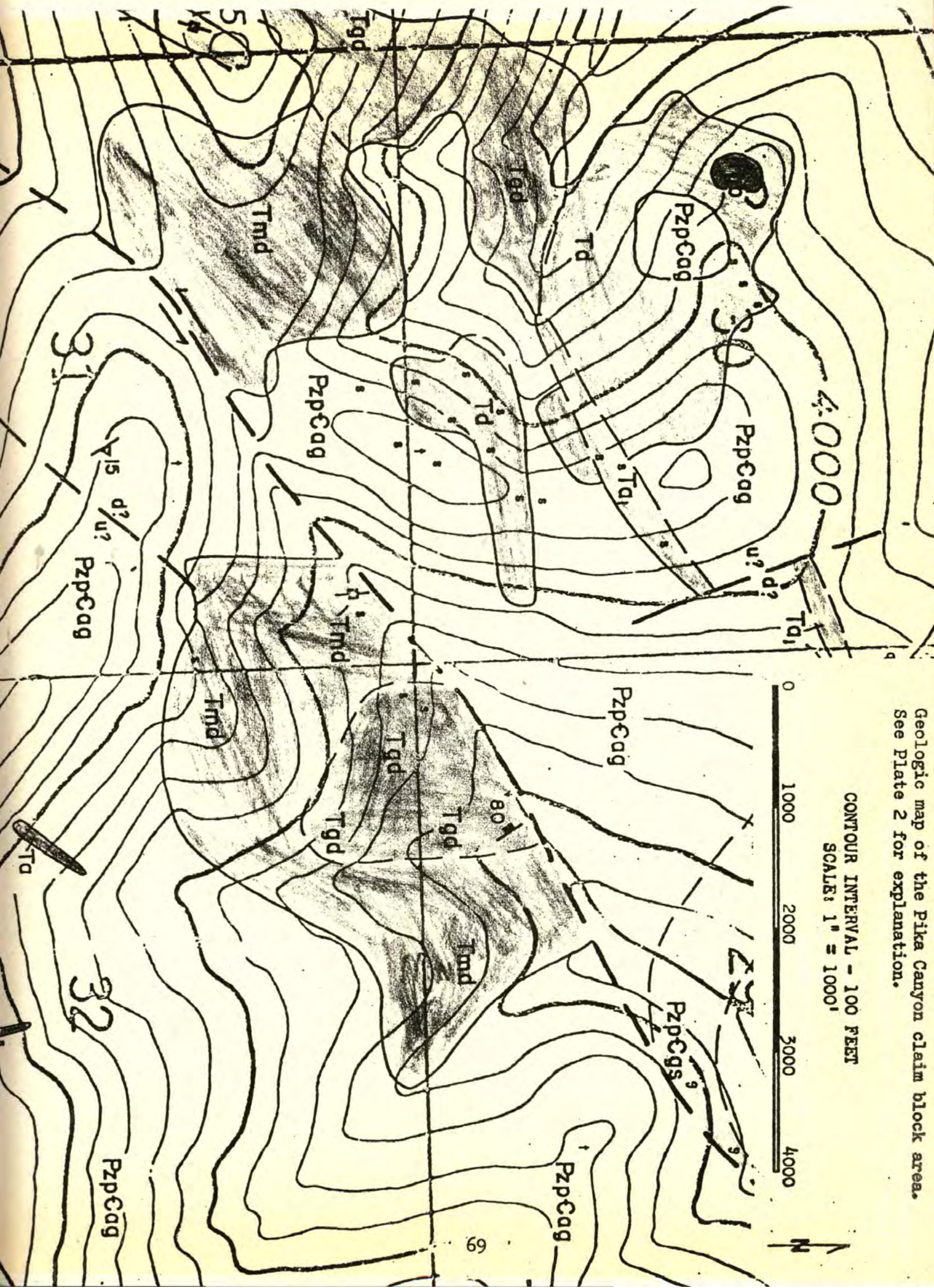
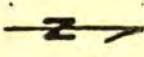
CONTOUR INTERVAL 100 FEET

SCALE: 1" = 500'



Geologic map of the Pika Canyon claim block area.
See Plate 2 for explanation.

CONTOUR INTERVAL - 100 FEET
SCALE: 1" = 1000'

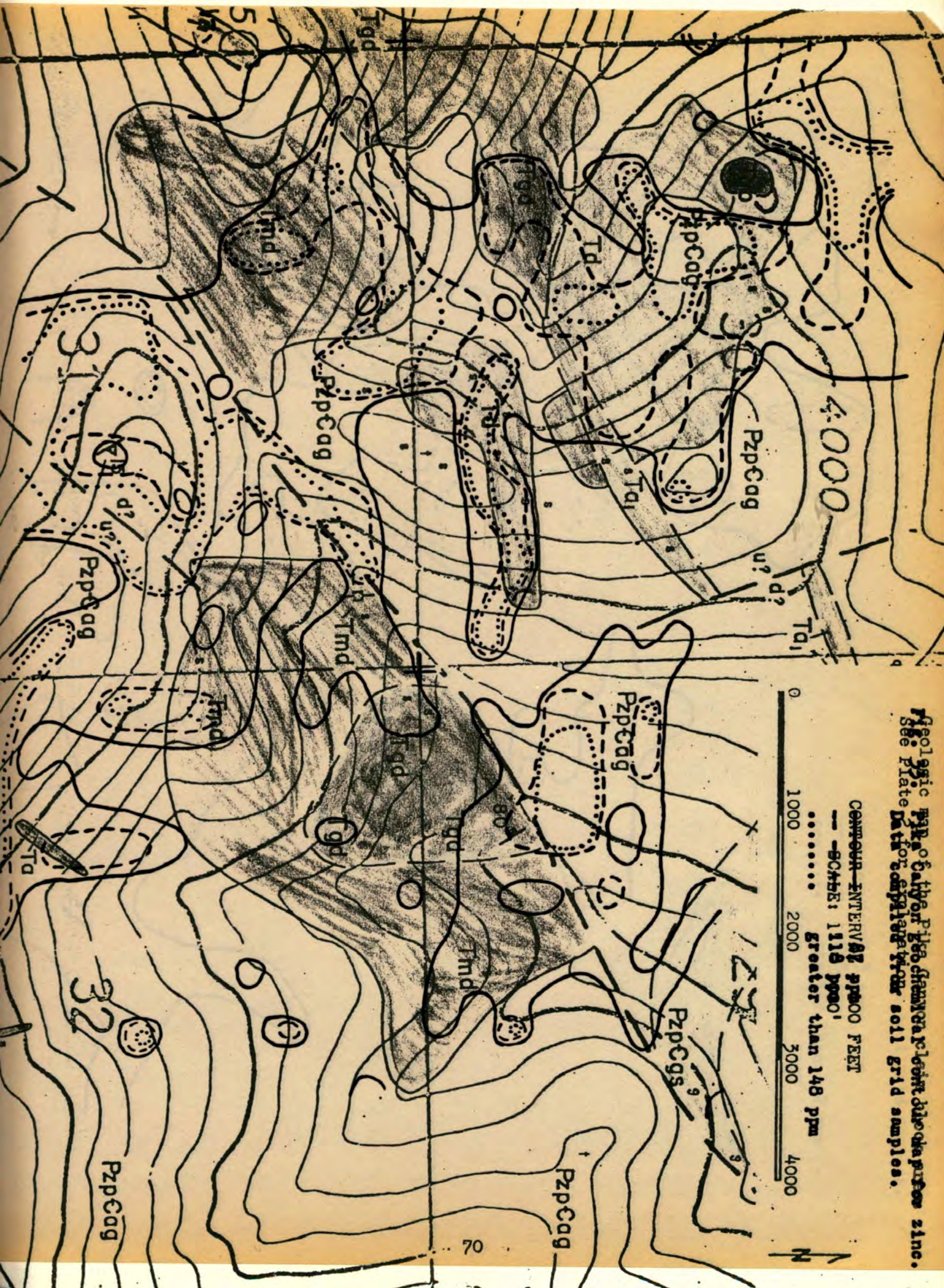
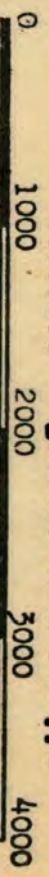


Geologic map of the Pilsbry Mountains, Clark County, Nevada, showing zinc concentrations in soil samples. See Plate 1 for complete map of soil samples.

CONTOUR INTERVAL 200 FEET

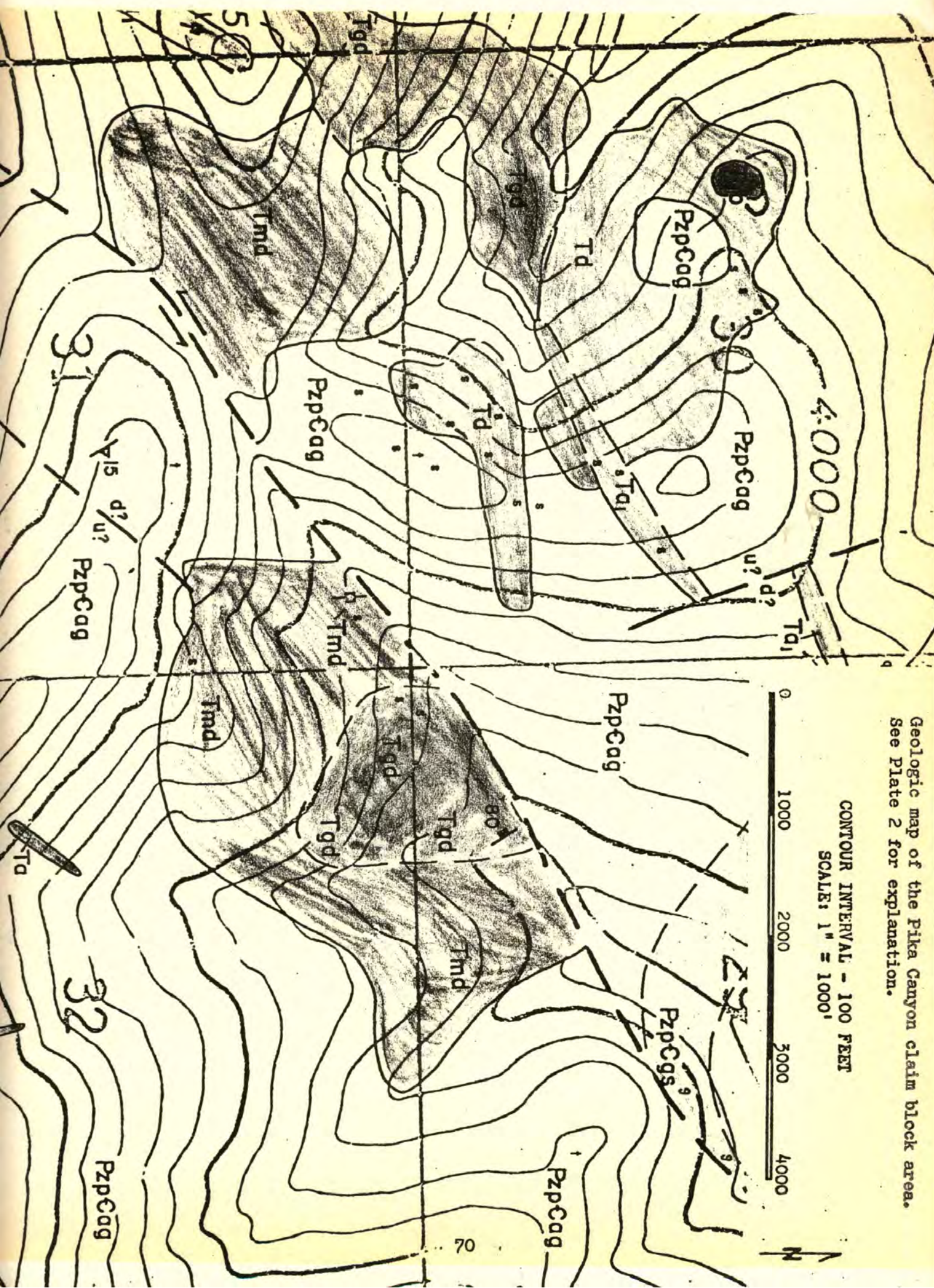
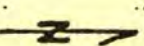
--- 9045: 1115 ppm

..... Greater than 148 ppm



Geologic map of the Pika Canyon claim block area.
See Plate 2 for explanation.

CONTOUR INTERVAL - 100 FEET
SCALE: 1" = 1000'

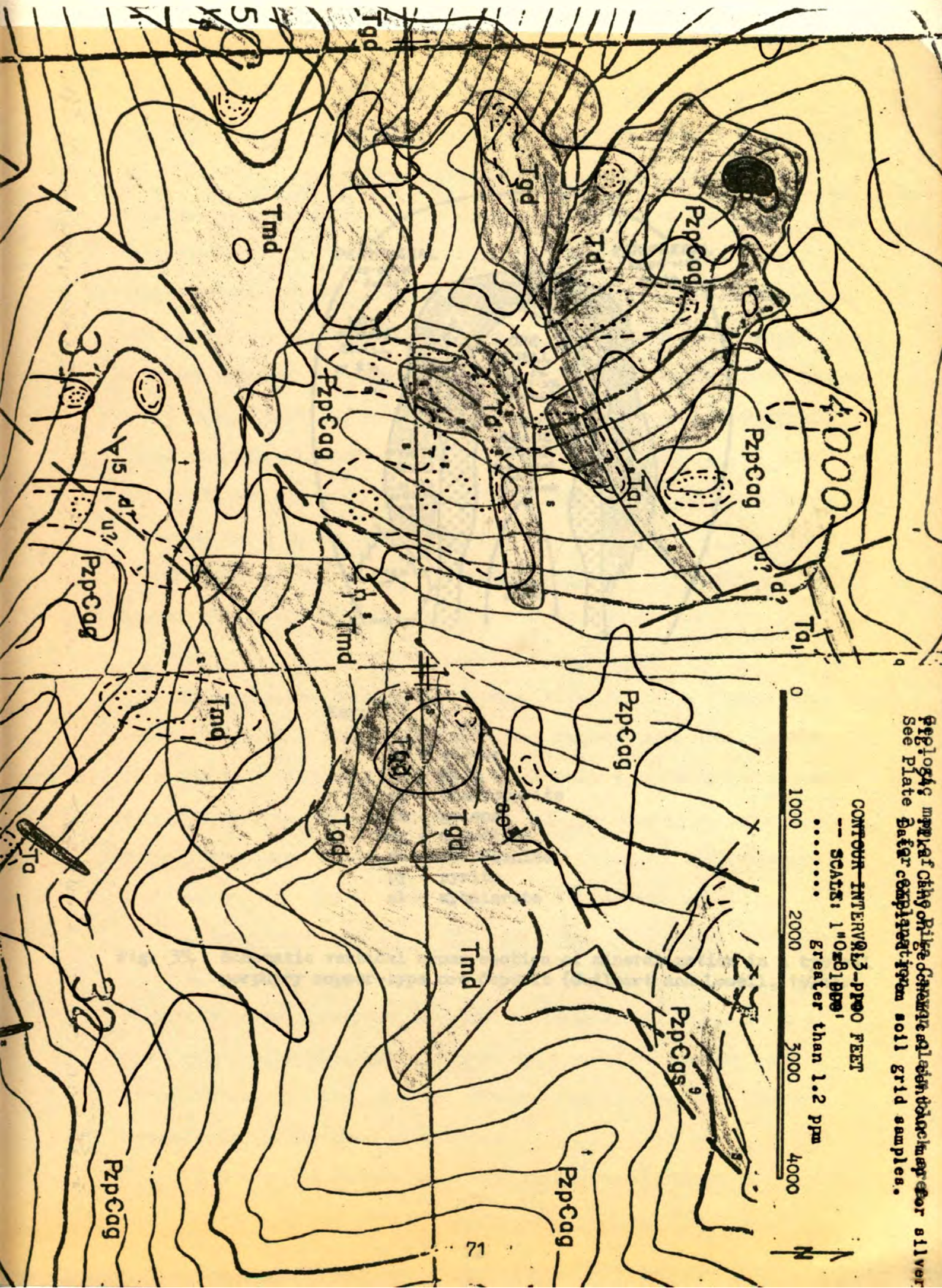


PzppCag map for City of Rio Grande. See Plate for explanation of silver See Plate for explanation of soil grid samples.

CONTOUR INTERVAL 0.5-1.00 FEET

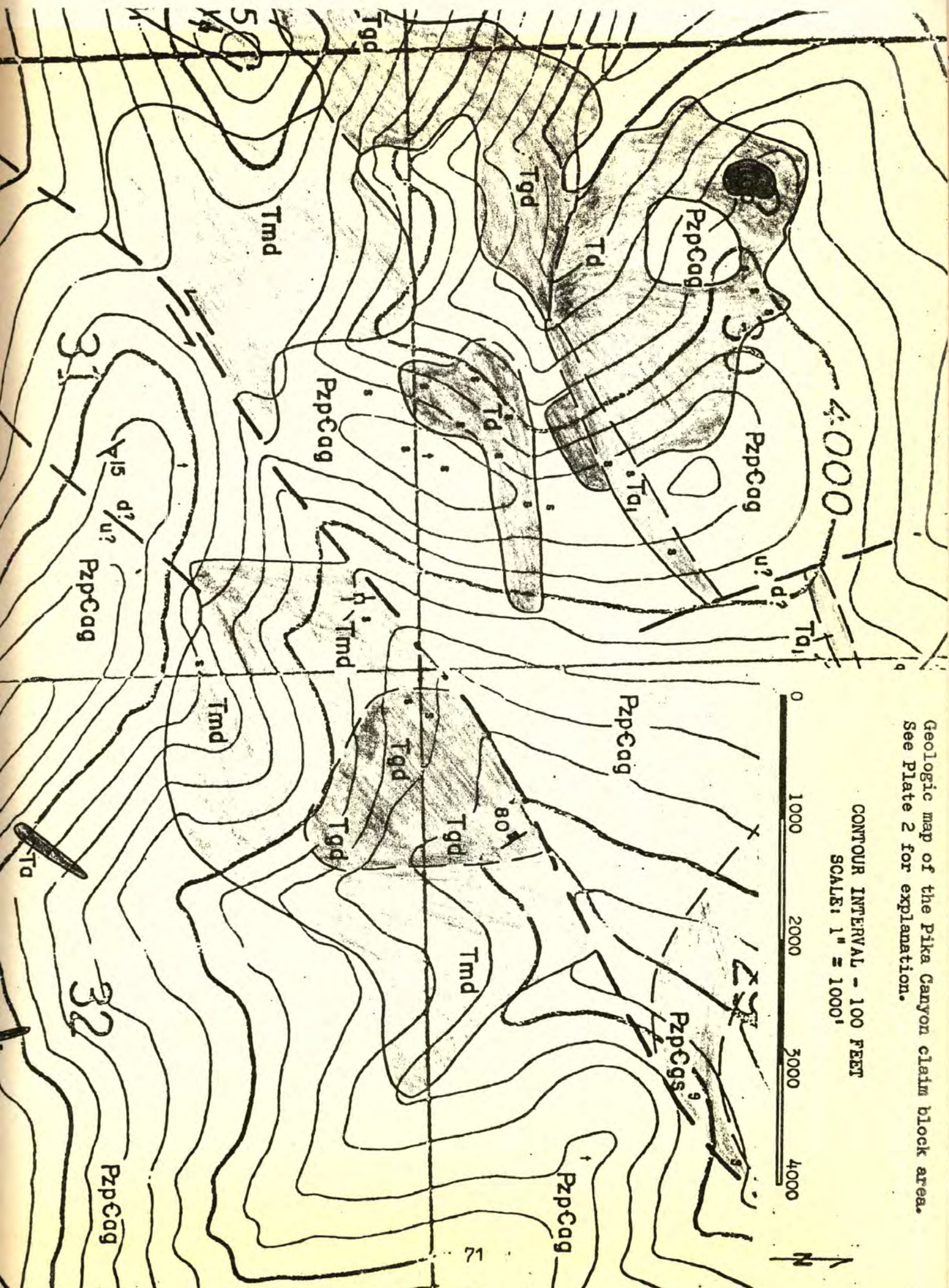
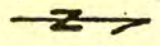
--- SCATS: 1" 0.81 ppm

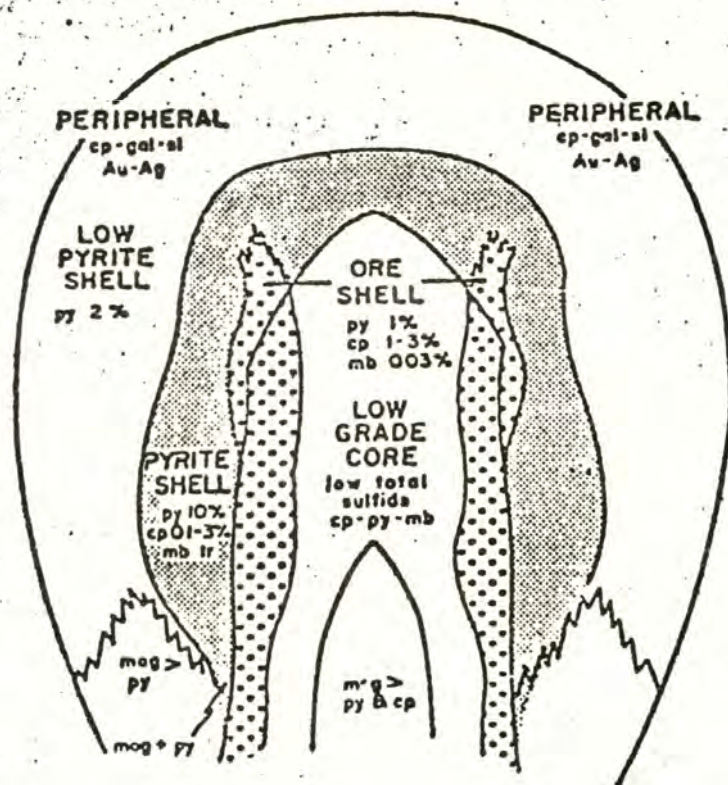
..... Greater than 1.2 ppm



Geologic map of the Pika Canyon claim block area.
See Plate 2 for explanation.

CONTOUR INTERVAL - 100 FEET
SCALE: 1" = 1000'





Key:

Ag - silver
 Au - gold
 cp - chalcopyrite
 gal - galena
 mag - magnetite
 mb - molybdenite
 py - pyrite
 sl - sphalerite

Fig. 35. Schematic vertical cross section of mineralization in a typical porphyry copper-type ore deposit (Guilbert and Lowell, 1974).

dispersion halo. However, Archer and Main (1971), in their research at the similar Casino deposit in the Yukon, found that copper and molybdenum in soils more or less coincide with underlying bedrock mineralization. Neither copper nor molybdenum is widely dispersed, even where solifluction is rapid. The limited amount of zinc and silver within the copper and molybdenum zones at both locations suggests that the secondary dispersion may in fact closely follow the primary dispersion in the underlying mineralized bedrock. Although traverses along the south-facing scree covered slope in section 30 did not reveal any mineralized or significantly altered material, this area should be given further consideration. The mineralization may possibly be associated with the north-south-trending lineament which passes through this area (see Fig. 9).

The geochemical contour maps also show a break in trend along the mapped fault, suggesting the fault is post-mineralization.

Geochemistry of the Fishhook Prospect Area

The reconnaissance geochemical maps (Figs. 26 thru 29) show that copper, molybdenum, and silver form poorly defined anomalies. However, it should be kept in mind that these trace element patterns are a composite of various types of samples, and that the sample density is erratic. Therefore, the zoning patterns of this prospect are not significant and only outline an area of geochemical interest.

Geochemistry of the NE Pika Canyon Claim Block Area

The reconnaissance geochemistry of the NE Pika Canyon prospect (Figs. 26 thru 29) shows a definite east-west to northeast-southwest trend of the elements molybdenum, zinc, silver, and copper; but copper, as mentioned before, is rather erratic. The geochemical anomaly is almost perpendicular to the trend of foliation.

In the previous section on Landsat imagery it was shown that two

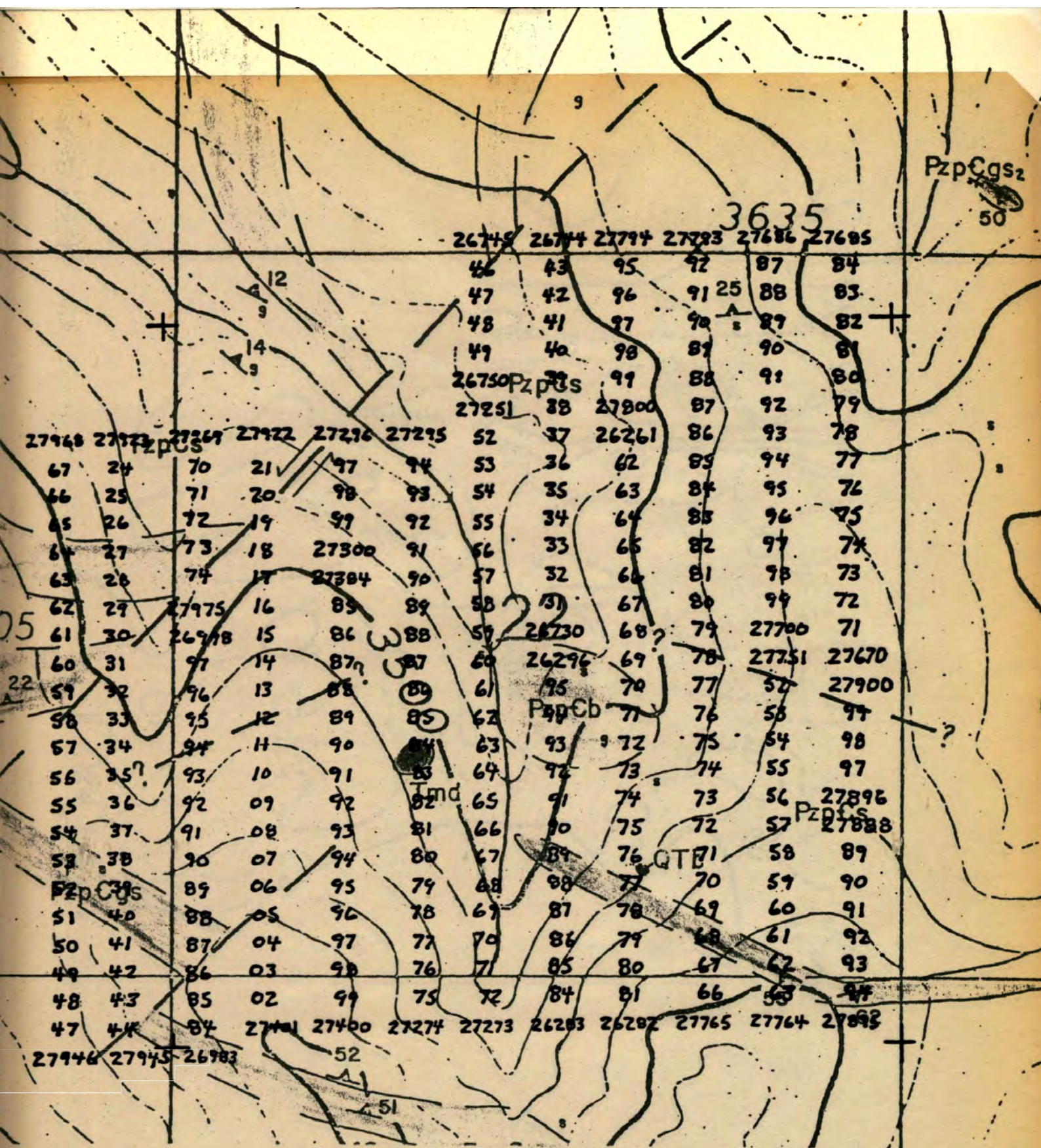
major lineaments and a mapped fault intersect in this general area (Fig. 9), which is the location of the reconnaissance geochemistry anomaly.

A detailed soil sample survey was conducted on the prospect with the same grid spacing as the Pika Canyon survey (for sample numbers and location see Fig. 36). Geochemical contour maps of each element (Figs. 37 thru 40) were constructed from the geochemical results of the soil grid samples by using the previously described method.

The general trend of the elements in the detailed survey is very similar to that observed on the reconnaissance geochemical maps. The geochemical contour maps show the distribution of elements to be rather erratic. The scatter could be reduced by increasing the parts per million values of the anomalous groups, but the same general trends would persist.

There is little evidence for geochemical zoning, but there is some indication of structural control. The detailed survey shows that the anomalous distribution of elements is mainly limited to the southeast side of the mapped fault, but note the small sample density on the northern side. Near the center of the claim block, there is a vaguely defined north-south break in the geochemical trends which is shown particularly well by the molybdenum and silver geochemical maps (Figs. 38 and 40). This trend is possibly the result of structural control along lineament F (see Fig. 9).

This geochemical anomaly could possibly be the result of mineralized fluids ascending along the proposed deep crustal lineaments. As these fluids ascended they may have been structurally controlled by the mapped fault. The geochemical trends suggest that fault gouge may have provided an impermeable boundary and contained the fluids along the southeast side. There the metals would have been deposited adjacent to the fault.



CONTOUR INTERVAL - 100 FEET

SCALE: 1" = 1000'

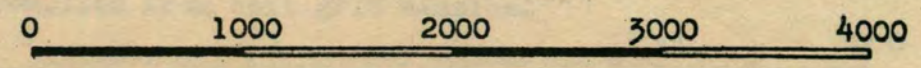
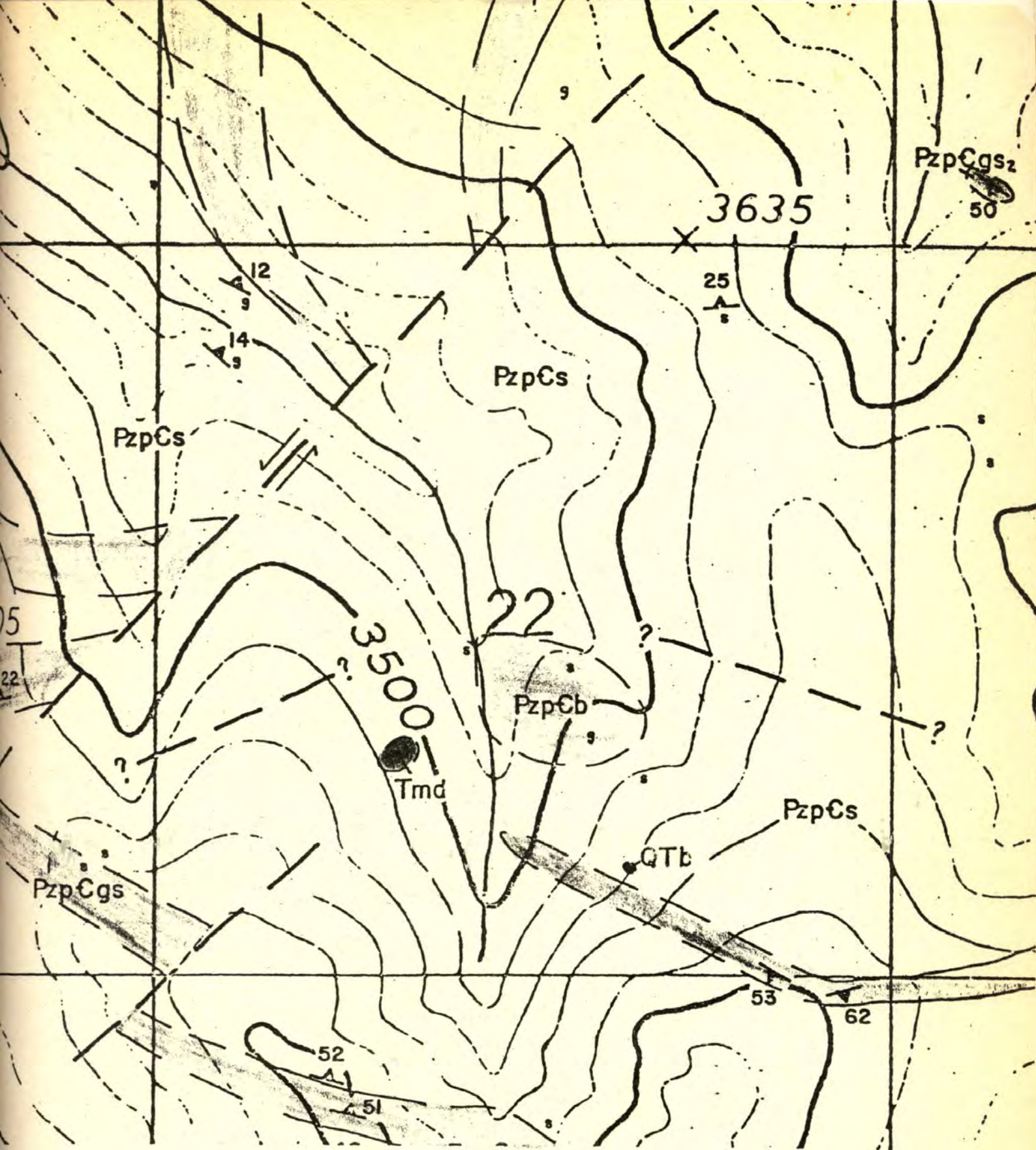


Fig. 36. Sample index map for the NE Pika Canyon claim block soil grid.
 Geologic map of the NE Pika Canyon claim block area. See Plate 2 for explanation.



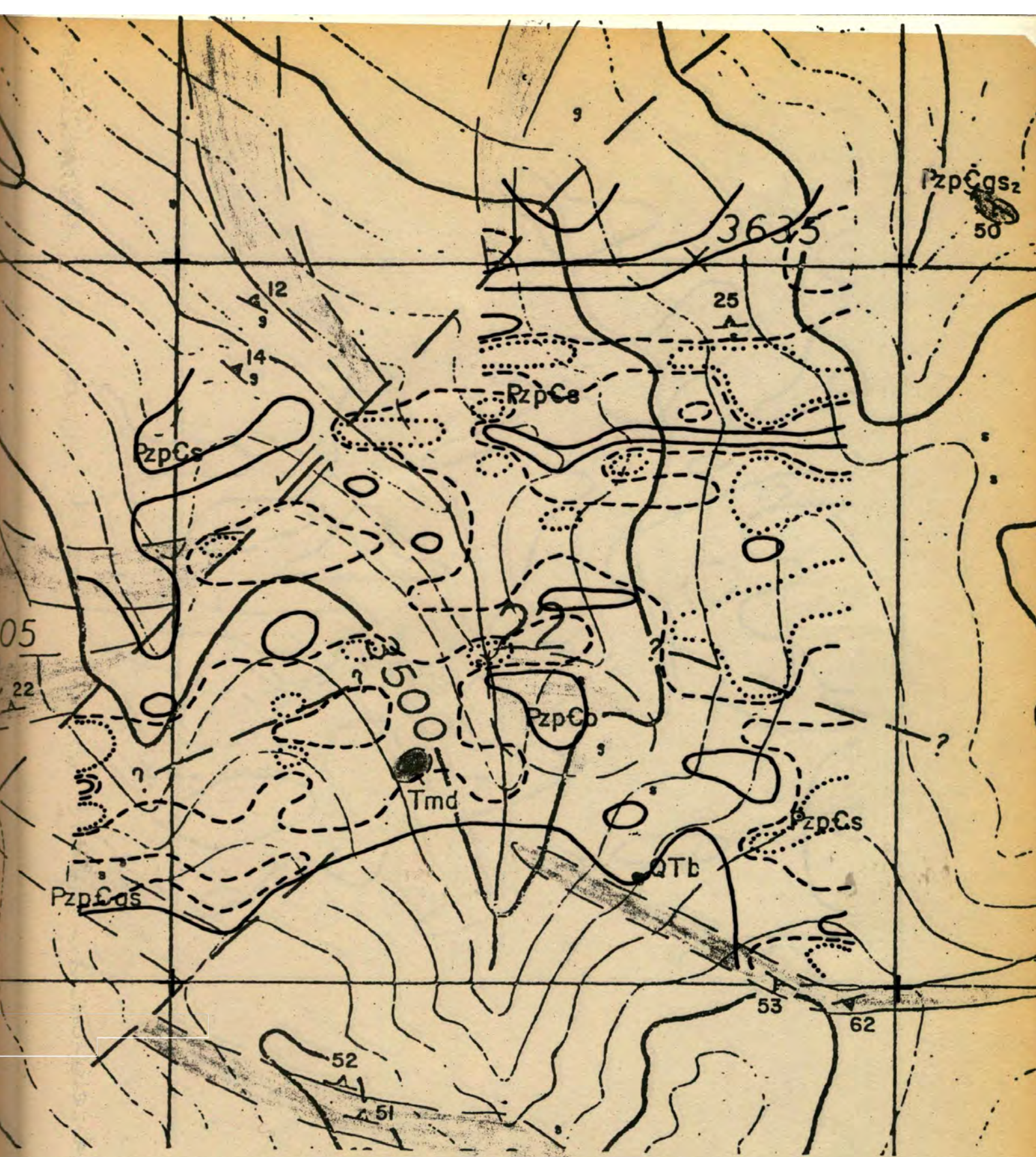
CONTOUR INTERVAL - 100 FEET

SCALE: 1" = 1000'

0 1000 2000 3000 4000

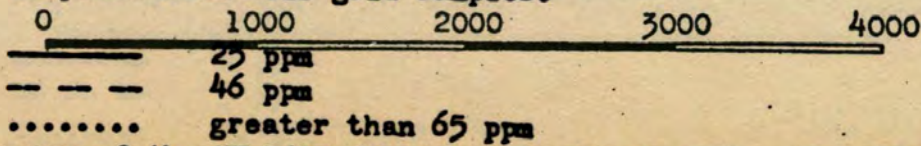


Geologic map of the NE Pika Canyon claim block area. See Plate 2 for explanation.

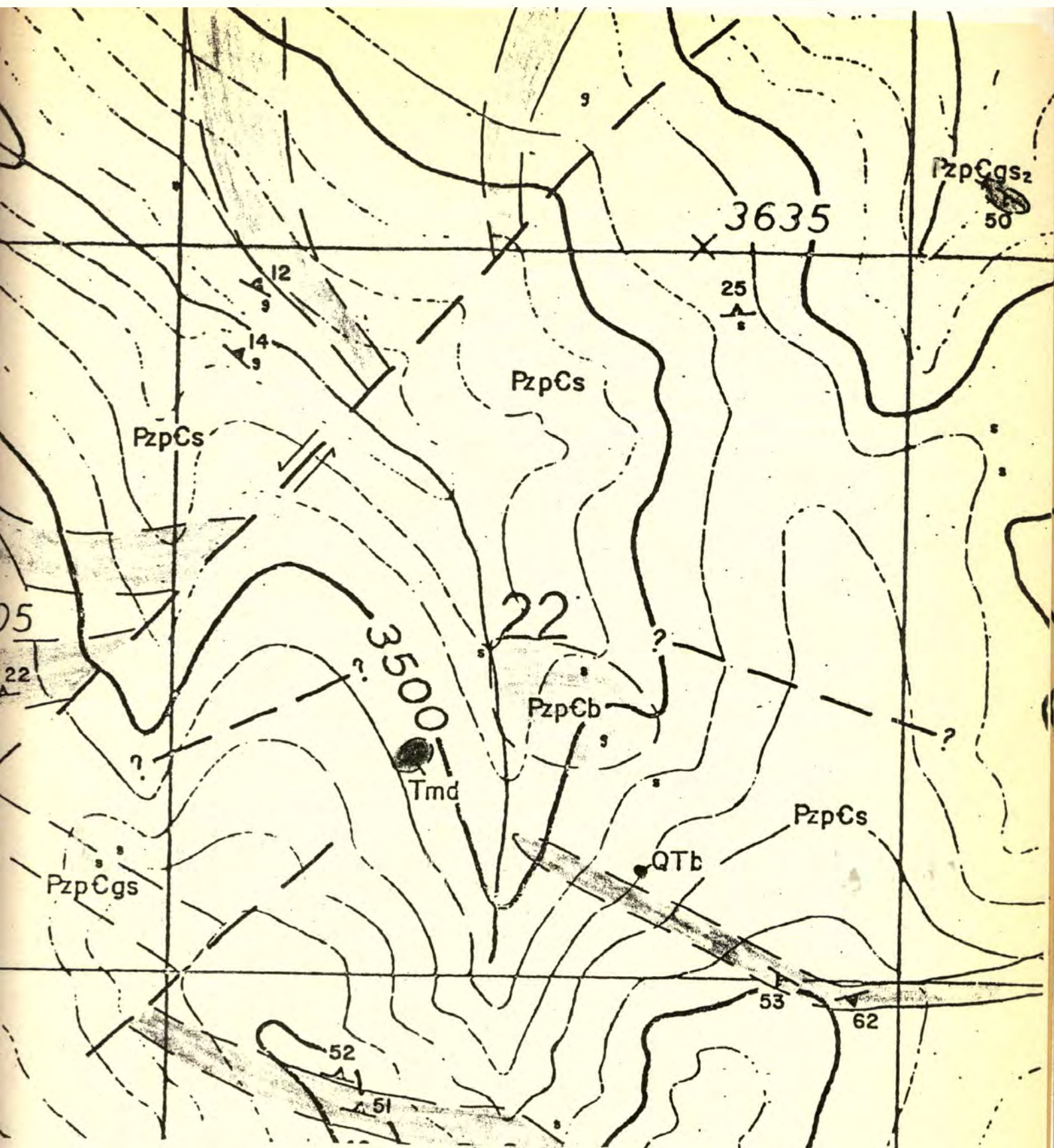


CONTOUR INTERVAL - 100 FEET

Fig. 37. NE Pika Canyon geochemical contour map for copper. Data compiled from soil grid samples.

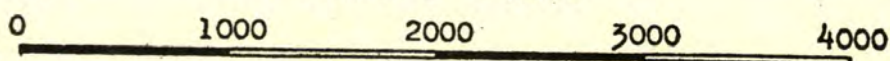


Geologic map of the NE Pika Canyon claim block area. See Plate 2 for explanation.

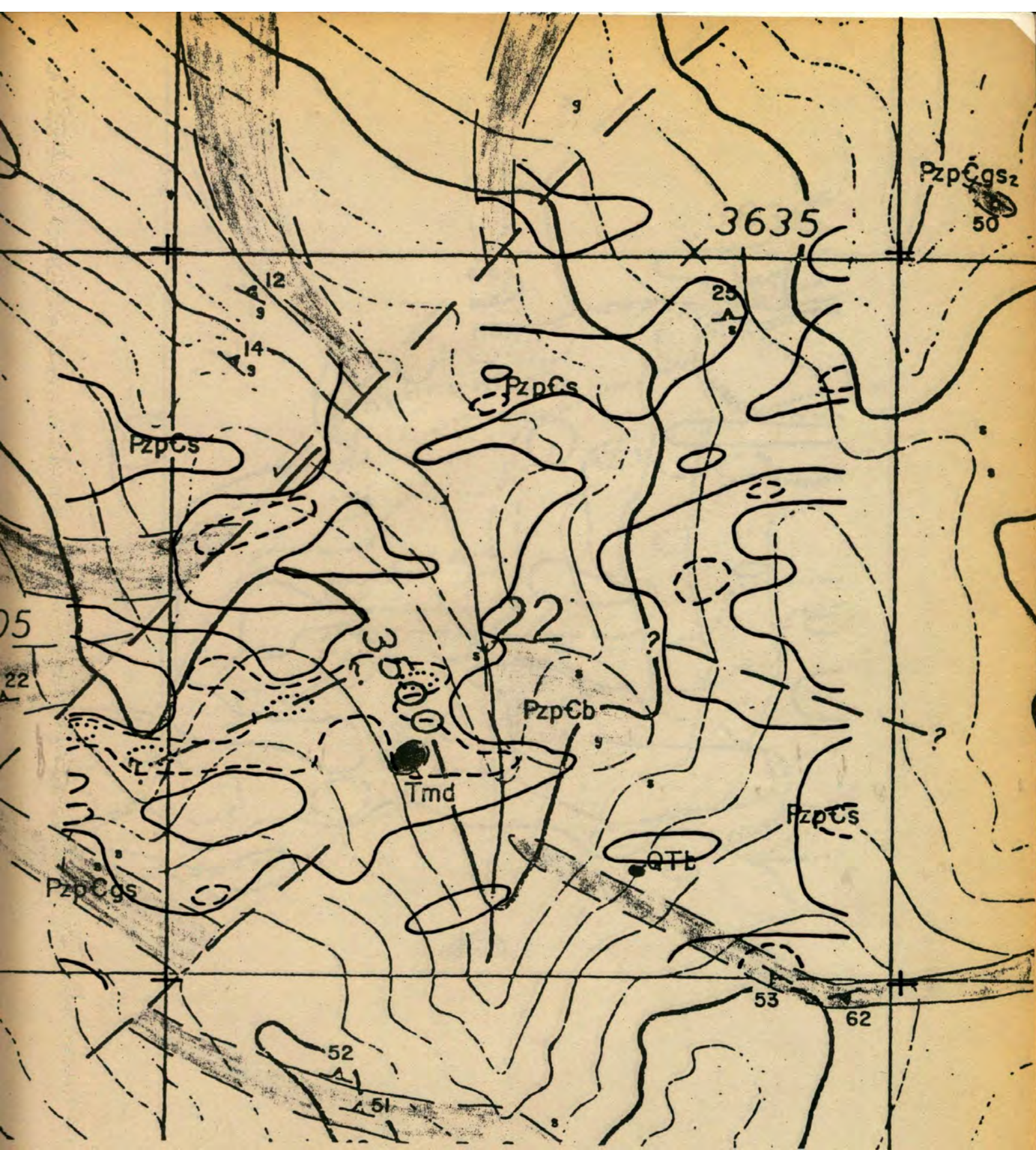


CONTOUR INTERVAL - 100 FEET

SCALE: 1" = 1000'

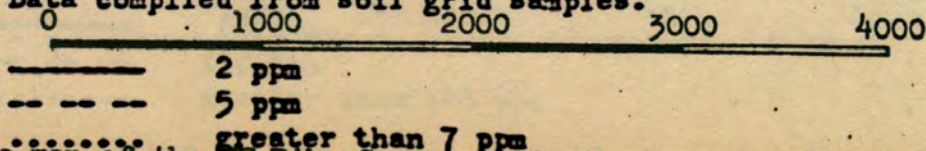


Geologic map of the NE Pika Canyon claim block area. See Plate 2 for explanation.

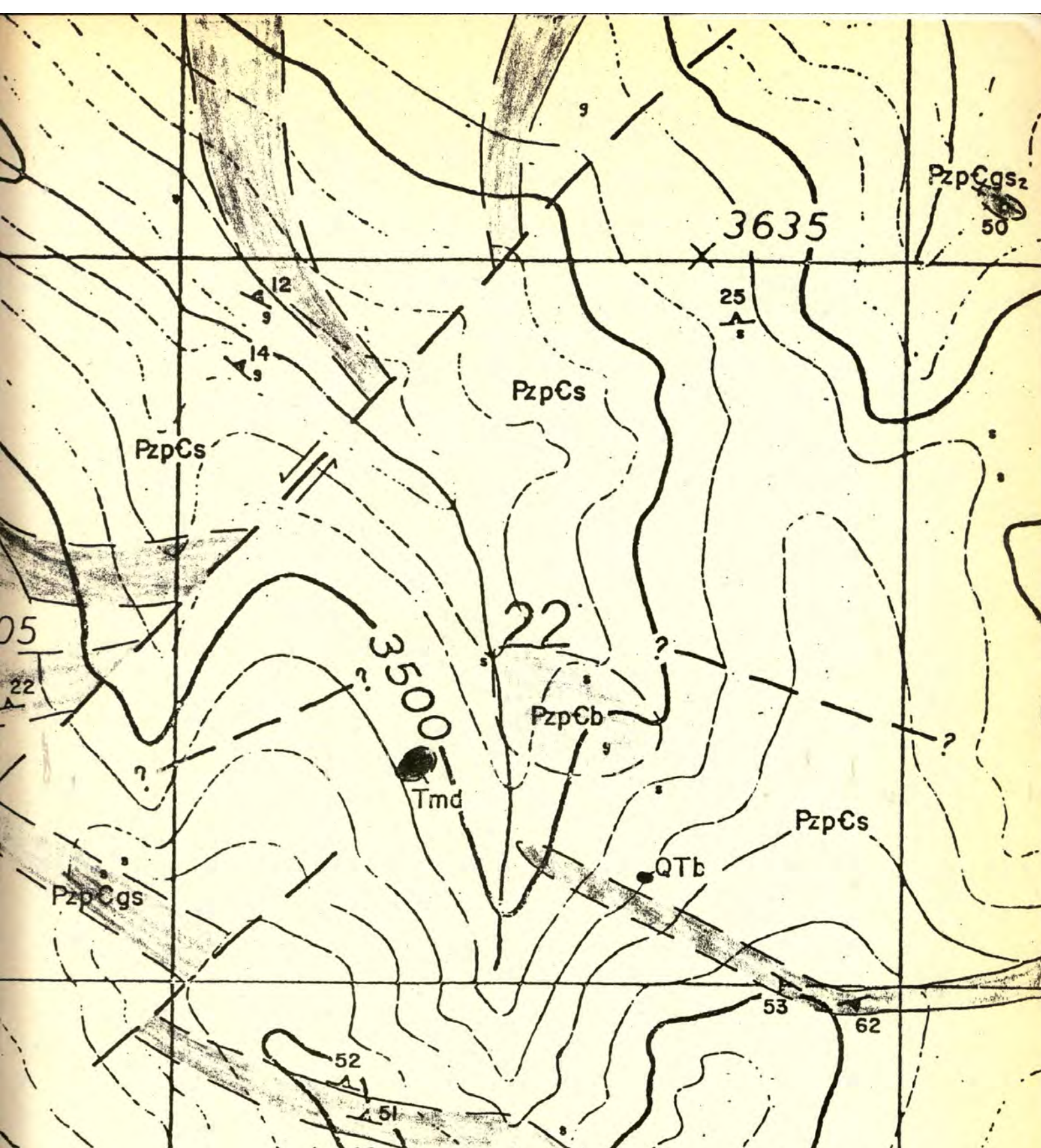


CONTOUR INTERVAL - 100 FEET

Fig. 38. NE Pika Canyon geochronological contour map for molybdenum. Data compiled from soil grid samples.

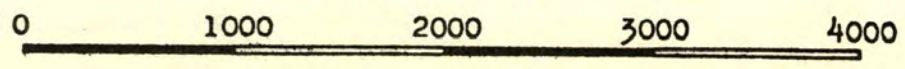


Geologic map of the NE Pika Canyon claim block area. See Plate 2 for explanation.



CONTOUR INTERVAL - 100 FEET

SCALE: 1" = 1000'



Geologic map of the NE Pika Canyon claim block area. See Plate 2 for explanation.

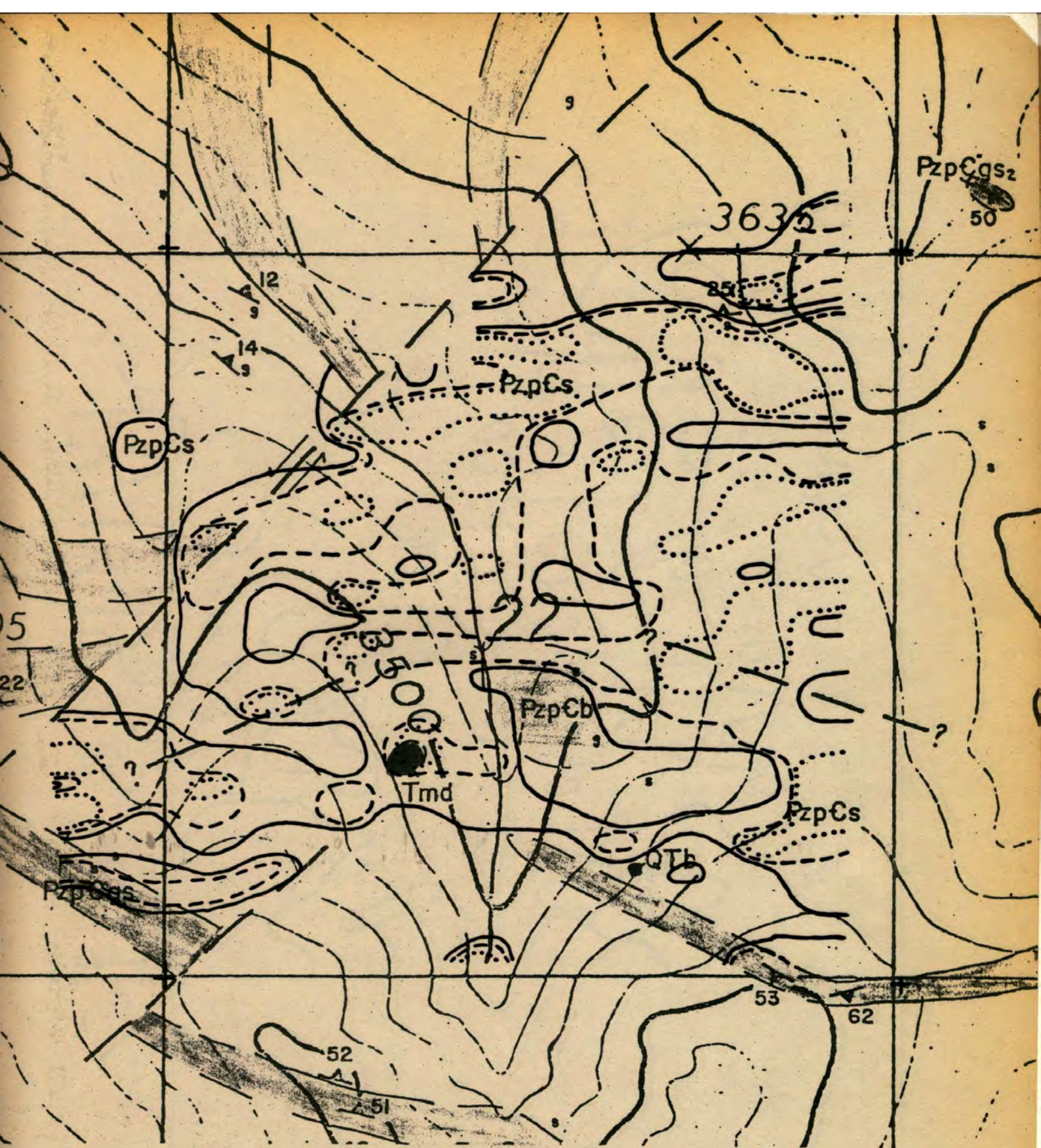
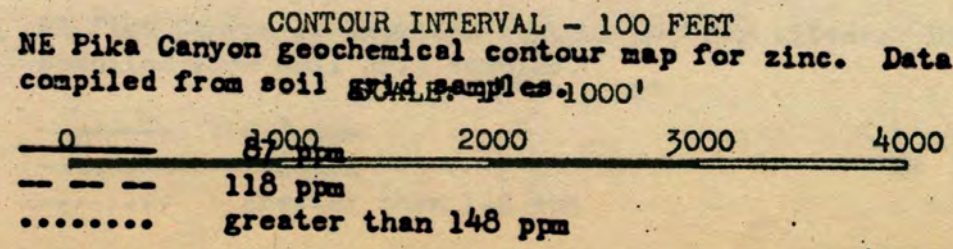
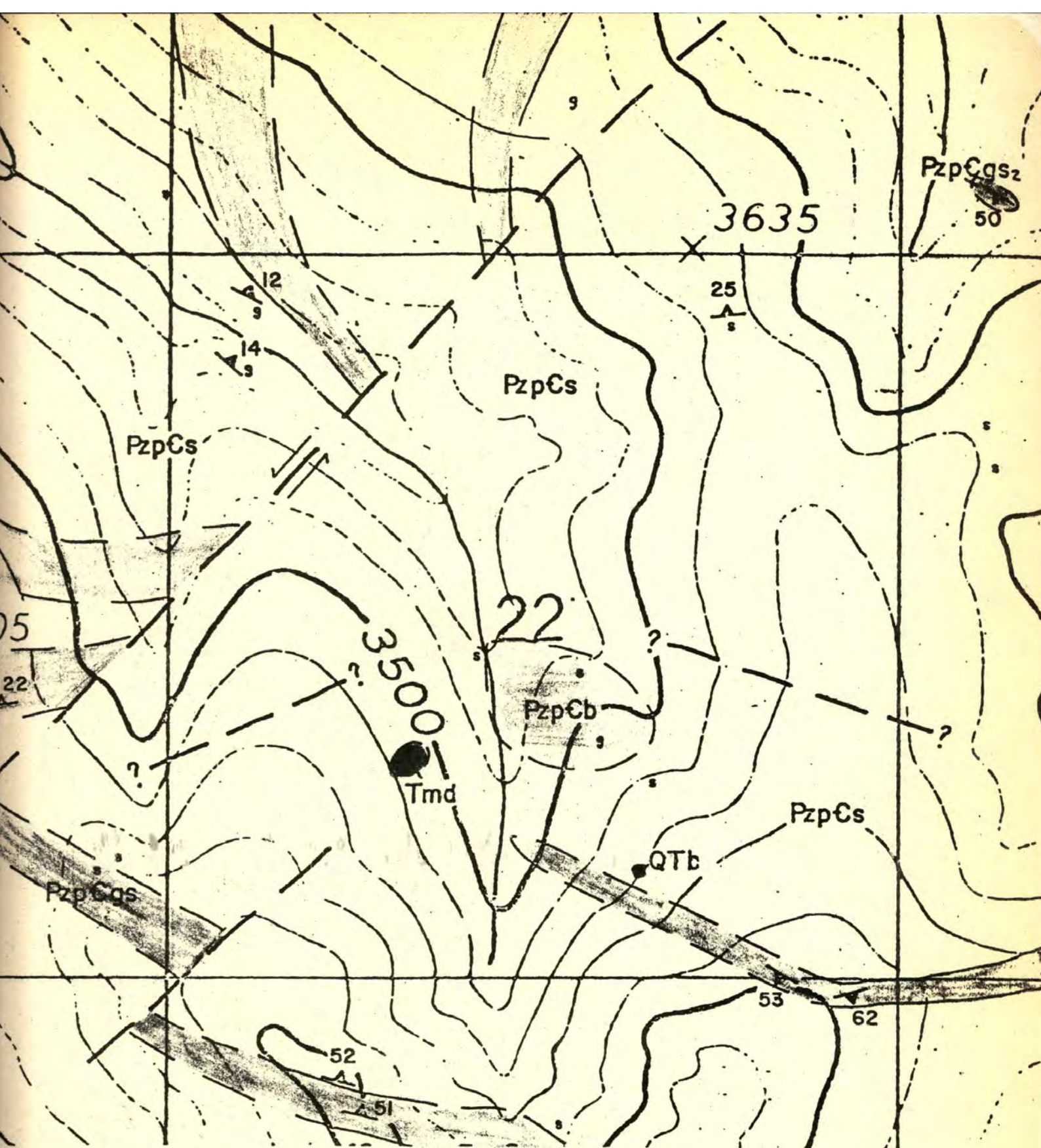


Fig. 39. NE Pika Canyon geochemical contour map for zinc. Data compiled from soil grid samples. 1000'

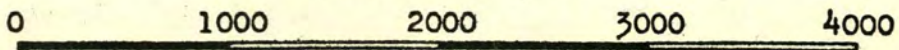


Geologic map of the NE Pika Canyon claim block area. See Plate 2 for explanation.



CONTOUR INTERVAL - 100 FEET

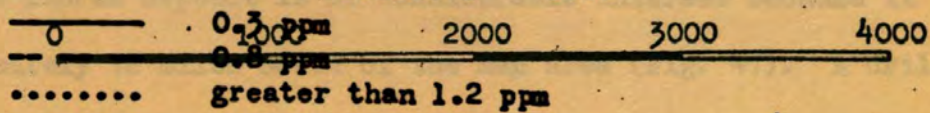
SCALE: 1" = 1000'



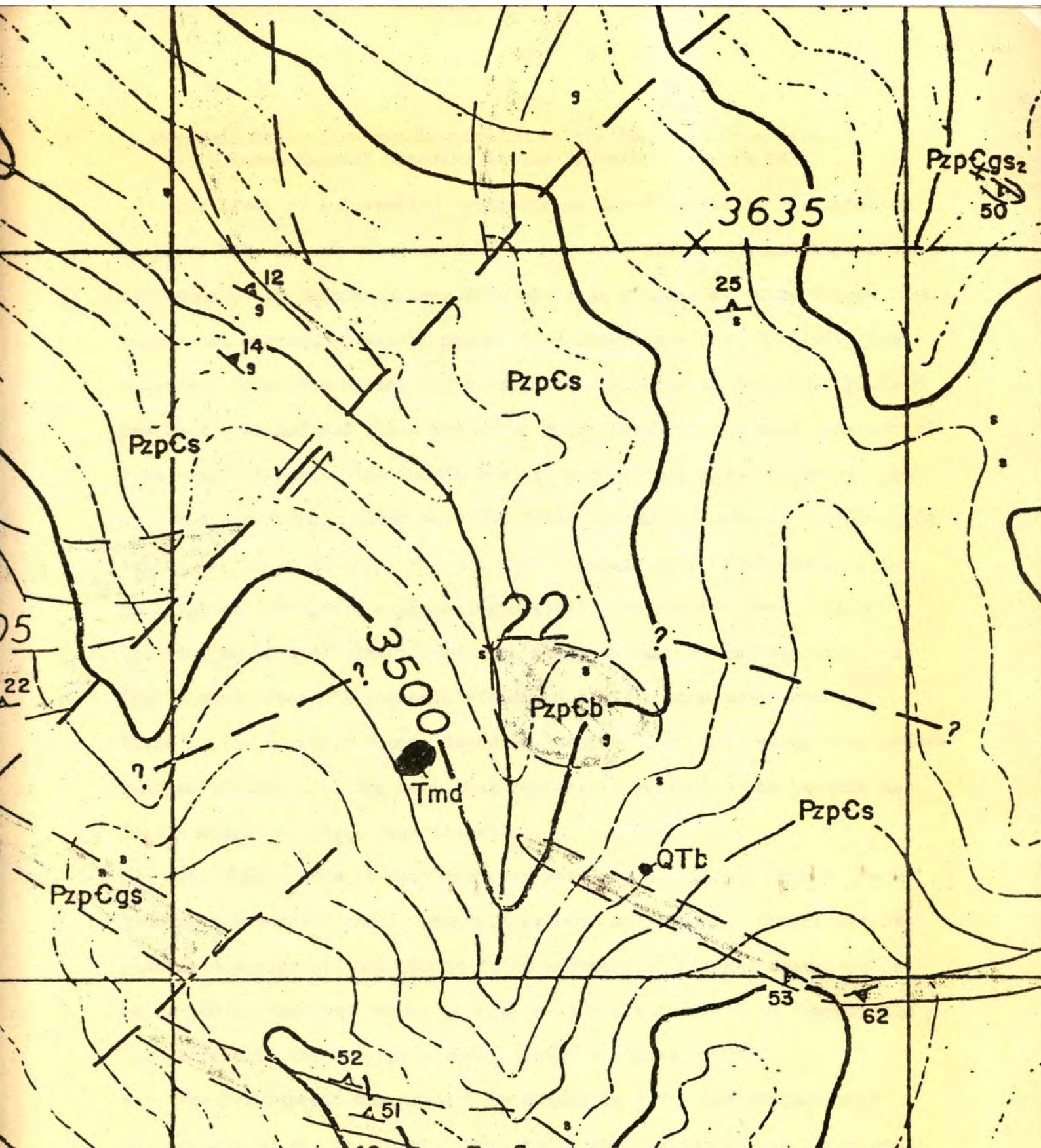
Geologic map of the NE Pika Canyon claim block area. See Plate 2 for explanation.



Fig. 40. NE Pika Canyon ^{CONTOUR INTERVAL 100 FEET} geochemical contour map for silver. Data compiled from soil grid samples. SCALE: 1" = 1000'

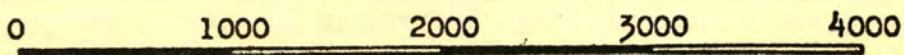


Geologic map of the NE Pika Canyon claim block area. See Plate 2 for explanation.



CONTOUR INTERVAL - 100 FEET

SCALE: 1" = 1000'



Geologic map of the NE Pika Canyon claim block area. See Plate 2 for explanation.

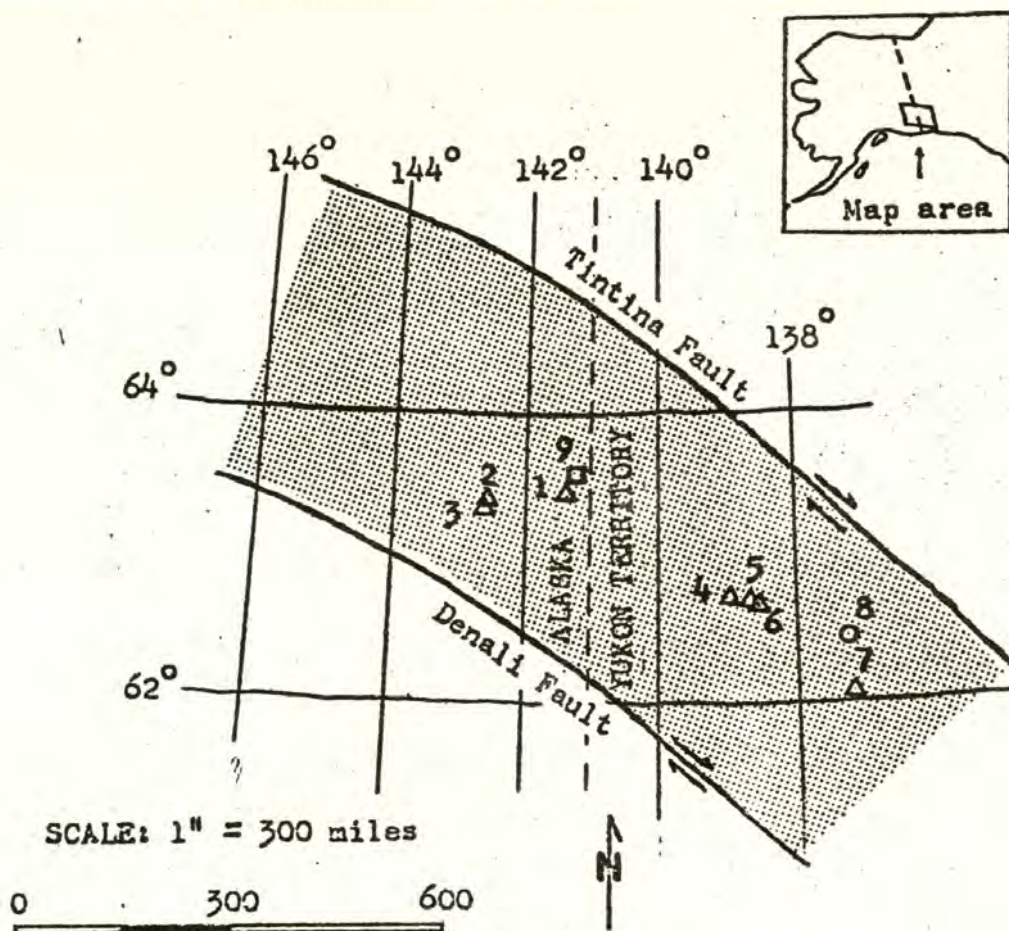
Economic Evaluation and Comparison of the Map Area Prospects with Known Mineral Deposits in the Interior Porphyry Belt

The level of information available on the deposits in the interior porphyry belt is extremely variable. Some are raw prospects whose classification could change as more data are made available. Others have been mapped and sampled in detail and most of these have been drilled. The names and locations of the major deposits are shown on Fig. 41. Table 3 has been compiled and lists the seven major porphyry deposits, one stratiform copper deposit, the thesis area prospects, and gives a general geologic and mineralogic description of these deposits. None of the deposits listed are in production, nor are they scheduled for development in the near future. However, exploration activity has demonstrated that substantial volumes of mineralized rock exist in many of the deposits and that a more favorable economic situation could change their status. Three of the porphyry copper deposits, Casino, Tok, and Taurus have undergone sufficient drilling such that reasonable estimates can be made as to the extent of their mineralization.

The Casino deposit contains over one hundred million tons of rock grading 0.4 percent copper and 0.03 percent molybdenum. Chalcocite replacing chalcopyrite and pyrite forms a supergene blanket described as being 100 to 300 feet thick. Copper grades are improved by approximately 100 percent in the supergene zone (Archer and Main, 1971).

The Tok deposit was drilled by ASARCO in 1971, and subsequently dropped due to the low grade; minor secondary chalcocite was found coating pyrite in many of the cores (Hedderly-Smith, 1975).

The Taurus deposit is of considerable interest because it is located approximately 12 miles south of the map area (Fig. 41). A drilling program in 1975, by Resource Associates of Alaska encountered appreciable



EXPLANATION



Interior Porphyry Belt



Porphyry Copper-type Deposits

- | | |
|------------|------------------|
| 1 - Taurus | 5 - Co |
| 2 - Dennis | 6 - Cockfield |
| 3 - Tok | 7 - Mount Nansen |
| 4 - Casino | |



Stratiform Copper Deposit

- 8 - Minto



Thesis Prospects

- 9 - Pika Canyon, NE Pika Canyon, and Fishhook

Fig. 41. Location of major mineral deposits and thesis area within the interior porphyry belt.

Table 3. General description of mineral deposits within the interior porphyry belt (modified after Hollister, V.F., Anzalons, S.A., and Reichter, D.H., 1974).

NAME	QUADRANGLE OR MAP AREA	LOCATION		TYPE	PLUTON AGE	HOST ROCK	ALTERATION ZONING SEQUENCE FROM CENTER	STRUCTURES	REFERENCES
		LAT	LONG						
PORPHYRY COPPER-TYPE DEPOSITS									
Taurus	Tanacross	63°29'	141°20'	Qtz monzonite porphyry	Cretaceous-Tertiary	Paleozoic or older, meta-morphics	Pot-phy-arg-prop	Stockwork	
Dennis	Tanacross	63°23'	142°27'	Qtz monzonite porphyry	Cretaceous-Tertiary	Paleozoic or older, meta-morphics	Pot-phy-arg-prop	Stockwork	
Tok	Tanacross	63°20'	142°30'	Rhyolite porphyry	Cretaceous-Tertiary	Paleozoic or older, meta-morphics	Phy-arg		
Casino	Snag	62°44'	138°50'	Qtz feldspar porphyry	Cretaceous-(70 m.y.)	Permian? Granodiorite		Breccia	Tempelmann-Kluit, 1973
Co	Snag	62°40'	138°50'	Qtz monzonite porphyry	Cretaceous-Tertiary	Permian? Granodiorite	Pot-arg-prop		Tempelmann-Kluit, 1973
Cockfield	Snag	62°39'	138°28'	Qtz monzonite	Cretaceous-Tertiary	Cretaceous-Tertiary volcanics			Tempelmann-Kluit, 1973
Mount Hansen	Carmacks	62°03'	137°09'	Rhyolite porphyry	Cretaceous-Tertiary	Paleozoic or older meta-morphics			Saager and Bianco, 1971
Pika Canyon	Tanacross	63°50'	141°25'	Granodiorite	Cretaceous-Tertiary	Paleozoic or older meta-morphics	Pot-phy-prop		Gill, 1977
Fishhook	Tanacross	63°50'	141°20'	Granodiorite	Cretaceous-Tertiary	Paleozoic or older meta-morphics	Phy-prop		Gill, 1977
STRATIFORM COPPER DEPOSIT									
Minto	Carmacks	62°50'	137°10'			Gneissic Biotite granodiorite			Gleeson and Brummer, 1976
STRUCTURALLY CONTROLLED DEPOSIT ?									
NE Pika Canyon	Tanacross	63°52'	141°20'			Paleozoic or older meta-morphics		Faults and lineaments?	Gill, 1977

secondary chalcocite even at the bottom of 900 foot holes, but did not delineate an actual blanket of supergene material. One diamond drill hole averaged 0.35 percent copper and 0.04 percent molybdenum over 878 feet, and five other holes have intercepted mineralization of 0.1 percent copper or better (Hedderly-Smith, 1975).

At the present stage of exploration the economic potential of the map area prospects can not be determined, and under the current economic conditions a deposit in Alaska will have to have large tonnage and high-grade ore to prove economic. A porphyry copper-type deposit would have to have a tonnage of 100 million tons or more, and the grade of protore would have to be at least 0.6 percent copper and 0.04 percent molybdenum with supergene enrichment to improve the copper grade 100 percent over protore grade. But, if several low tonnage and high-grade ore deposits were in close proximity to each other, they may become economically feasible. The map area prospects may fall into this category.

SUMMARY AND CONCLUSIONS

The study area is located in the northeast corner of the Tanacross quadrangle, Alaska, and is within a complex Precambrian and (or) Paleozoic metamorphic terrain that has been intruded by numerous late Cretaceous to early Tertiary igneous stocks and dikes of various compositions. The metamorphic terrain is bordered by two major right lateral strike-slip faults; the Tintina fault to the north and the Denali fault to the south. This block of terrain has been defined as the interior porphyry belt and contains numerous occurrences of porphyry copper-type deposits. This area was not glaciated during Pleistocene time. The lack of glaciation suggests that large zones of supergene enrichment may be present at the porphyry copper deposits.

Lithologies within the map area consist predominately of metamorphic rock units including; 1) greenschist, 2) mica schist, and 3) Pelly Gneiss. The term greenschist does not imply metamorphic grade, but has been used in both field mapping and petrographic analysis to group schists containing greater than 5 percent mafic minerals. The metamorphic grade of the greenschist and mica schist units is transitional from greenschist to amphibolite facies.

The igneous intrusive rocks range in composition from granodiorite to gabbro. The igneous extrusive rocks are mainly andesitic in composition. Also, three isolated occurrences of alkaline basalt were noted, which may be Quaternary in age.

From the general structural pattern it appears that the Pelly Gneiss intruded the mica schist and greenschist units prior to metamorphism, possibly as a large granitic stock. The Pelly Gneiss has now been faulted and intruded by much younger igneous rocks. The greenschist and mica

schist units were not mapped in detail due to limited outcrop exposure, but field evidence suggests structural complexity.

A northeast-trending left lateral strike-slip fault passes through the map area and intersects both Pika Canyon and NE Pika Canyon claim blocks. Field evidence, geochemistry, and magnetics suggest the fault is younger than the Mesozoic-Tertiary intrusives. Numerous other north-northeast-trending faults were mapped, but their displacements could not be determined.

A report prepared by Albert and Steele (1976) has shown six major lineaments passing through the study area. The lineaments are thought to be related to deep crustal fractures and the occurrence of alkaline basalt in the general proximity of several lineaments supports this hypothesis.

An aeromagnetic map of the Tanacross quadrangle was prepared by Griscom (1976); showing a large magnetic high in the southern-half and a large magnetic low in the northern-half of the study area. The magnetic high represents igneous rock and the size suggests a large pluton that is only partly unroofed. The magnetic low has been interpreted to represent metamorphic rocks of uniform and weak magnetization.

A ground magnetic survey was conducted on the Pika Canyon and NE Pika Canyon claim blocks to aid in preparing the geologic map. The igneous rocks in general show a greater magnetization than the metamorphic rocks. Therefore, the magnetic maps have helped to define contacts between igneous and metamorphic rocks in areas of limited outcrop exposure.

Reconnaissance alteration mapping has delineated five alteration types: potassic, phyllic, propylitic, silicification, and carbonatization. The alteration phases are in general confined to the Pika Canyon claim

block and Fishhook prospect areas, with the exception of carbonatization.

Alteration assemblages at both areas show zonation similar to typical porphyry copper-type deposits of the southwestern United States, (i.e., the Guilbert and Lowell model - a potassic core with phyllic, argillic and propylitic alteration assemblages progressing outward).

At the Pika Canyon area potassic, phyllic, and propylitic alteration are present, but no potassic alteration was noted at the Fishhook prospect. At both areas the alteration phases do not form concentric zones as expected from the Guilbert and Lowell model, but instead, irregular patches in roughly concentric patterns. One possible explanation for the patchy zoning patterns is that hydrothermal fluids were restricted by metamorphic rocks of low permeability and that there was a lack of structural deformation prior to and during intrusive emplacement, which would have provided avenues for fluid migration. A second theory is that the alteration systems are just beginning to be unroofed by erosion and that the system will become more pervasive and well-defined with depth.

At Pika Canyon the host rock is the Pelly Gneiss. There is limited structural deformation and silicification, and field evidence suggests that the intrusive complex is just beginning to be exposed by erosion. Therefore the patchy alteration zoning patterns at Pika Canyon are probably related to both proposed theories.

At the Fishhook prospect phyllic alteration is generally associated with the intrusive rock and the immediate surrounding host rock (Pelly Gneiss). Silicification, however, is pervasive and probably associated with post-intrusive faults and lineaments. If this is true, then the same theories for the patchy alteration zones would also apply at this prospect.

Numerous isolated occurrences of silicification are present throughout the map area and are generally spatially associated with mapped faults.

Carbonatization was noted at one location in the northeast corner of the map area, and is associated with extrusive rock of andesitic composition.

Reconnaissance geochemistry is represented by soil, rock-chip, and stream-sediment samples. All samples were analyzed for the elements copper, molybdenum, zinc, and silver. Anomalous values of each element were plotted on a map to show anomaly patterns. The anomalous element distributions have shown three areas of geochemical interest. They are Pika Canyon and NE Pika Canyon claim blocks and the Fishhook prospects. Soils of both claim blocks were sampled in detail but only reconnaissance geochemical data is available for the Fishhook prospect. Because of the limited number of samples collected at the Fishhook prospect no definite geochemical trends can be delineated.

At the Pika Canyon claim block the geochemical soil survey has shown two areas with secondary dispersion patterns which are characteristic of primary mineral zoning in typical porphyry copper-type deposits of the southwestern United States.

Exploration at known deposits within the unglaciated interior porphyry belt has shown that residual soils generally represent the geochemistry of the immediately underlying bedrock; and that solifluction even on south-facing slopes does not readily affect the secondary dispersion patterns. This suggests that secondary dispersion zoning at the Pika Canyon prospect may in fact reflect primary dispersion of the underlying bedrock.

The NE Pika Canyon soil geochemistry is erratic and definite zoning patterns are questionable. Both reconnaissance and detailed geochemistry show the same general trends, which indicate that the geochemistry is structurally controlled by the mapped faults and lineaments.

The current economic conditions in Alaska necessitate a deposit to have large tonnage and high-grade ore to prove economic. However, if several low tonnage and high-grade ore deposits were in close proximity they may become economically feasible. This may be the case at the study area prospects, but at the present stage of exploration the economic potential can not be determined.

REFERENCES

- Albert, N. R. D., and Steele, W. C., 1976, Interpretation of Landsat imagery of the Tanacross quadrangle, Alaska: U. S. Geol. Survey Open-File Rept. 76-850, 27 p.
- Archer, A. R., and Main, C. A., 1971, Casino, Yukon - A geochemical discovery of an unglaciated Arizona-type porphyry: *Geochem. Expl. CIM*, spec. vol. 11, p. 67-77.
- Boyle, R. W., 1970, Regularities in wall-rock alteration phenomena associated with epigenetic deposits: *Internat. Union Geol. Sci.*, vol. A, no. 2, p. 233-260.
- Brooks, A. H., 1900, A reconnaissance in the Tanana and White River basins, Alaska, in 1898: U. S. Geol. Survey Ann. Rept. 20, p. 425-494.
- Cockfield, W. E., 1921, Sixtymile and Ladue Rivers area, Yukon: Canada Geol. Survey Mem. 123, 60 p.
- Coope, J. A., 1966, Geochemical prospecting in the Dawson Range: *Mining Cong. Jour.*, vol. 52, no. 5, p. 257-310.
- Eardly, A. J., 1962, *Structural Geology Of North America* (2nd ed.): New York, Harper and Row, Publishers, 743 p.
- Foster, H. L., Forbes, R. B., and Ragan, D. M., 1966, Granulite and peridotite inclusions from Prindle Volcano Yukon-Tanana Upland, Alaska: U. S. Geol. Survey Prof. Paper 550-B, p. B115-B119.
- _____, 1969, Reconnaissance geology of the Eagle A-1 and A-2 quadrangles, Alaska: U. S. Geol. Survey Bull., vol. 1271-G, p. G1-G30.
- _____, 1970, Reconnaissance geologic map of the Tanacross quadrangle, Alaska: U. S. Geol. Survey, Misc. Geol. Invest. Map I-593.
- _____, and Keith, T. E. C., 1974, Ultramafic rocks of the Eagle quadrangle, east-central Alaska: *Jour. Research U. S. Geol. Survey*, vol. 2, no. 6, p. 657-669.
- _____, Albert, N. R. D., Barnes, D. F., Curtin, G. C., Griscom, A., Singer, D. A., and Smith, J. G., 1976, The Alaskan mineral resource assessment program: background information to accompany folio of geologic and mineral resource maps of the Tanacross quadrangle, Alaska: *Geol. Survey Circ.* 734, p. 1-23.
- Freeland, G. L., and Dietz, R. S., 1973, Rotation history of Alaskan tectonic blocks: *Tectonophysics*, vol. 18, no. 2, p. 379-389.
- Gleeson, C. F., and Brummer, J. J., 1976, Reconnaissance stream-sediment geochemistry applied to exploration for porphyry Cu-Mo deposits in southwestern Yukon Territory: *CIM Bull.*, 69, no. 769, p. 91-102.
- Griscom, A., 1976, Aeromagnetic map and interpretation of the Tanacross quadrangle, Alaska: U. S. Geol. Survey Map MF-767-A.

- Guilbert, J. M., and Lowell, D. J., 1974, Variations in zoning patterns in porphyry ore deposits: CIM Bull., vol. 67, no. 744, p. 99-109.
- Hedderly-Smith, D., 1975, Final Report Tanacross Project: Cities Service Minerals Corporation, Anchorage, Alaska, 49 p.
- Hollister, V. F., Anzalone, S. A., and Reichter, D. H., 1974, Porphyry copper belts of southern Alaska and contiguous Yukon Territory: CIM annual meeting in Montreal, 27 p.
- Horsnail, R. F., and Fox, P. E., 1974, Geochemical exploration in permafrost terrains with particular reference to the Yukon Territory: CIM Transactions, vol. 77, p. 22-26.
- Lathram, E. H., 1974, New Alaskan mineral exploration rationale: U. S. Geol. Survey Circ. 700, p. 34-35.
- _____, Tailleux, I. L., Patton, W. W., Jr., and Fischer, W. A., 1973, Preliminary geologic application of ERTS imagery in Alaska: U. S. Natl. Aeronautics and Space Adm., Spec. pub. Sp-327, vol. I, sec. A, p. 257-264.
- Levinson, E. A., 1974, Introduction To Exploration Geochemistry: Applied Publishing Ltd., Maywood, Illinois, 614 p.
- Lowell, J. D., 1974, Regional characteristics of porphyry copper deposits of the southwest: Econ. Geol., vol. 69, no. 5, p. 601-617.
- _____, and Guilbert, J. M., 1970, Lateral and vertical alteration-mineralization zoning in porphyry ore deposits: Econ. Geol., vol. 65, no. 10, p. 373-408.
- Mertie, J. B., 1937, The Yukon-Tanana region Alaska: U. S. Geol. Survey Bull. 872, 276 p.
- O'Leary, D. W., Friedman, J. D., and Pohn, H. A., 1976, Lineament, linear, lineation: some proposed new standards for old terms: Geol. Soc. America Bull., vol. 87, no. 10, p. 1463-1469.
- Sangster, D. F., 1973, Precambrian volcanogenic massive sulfide deposits in Canada: a review: Geol. Survey of Canada, Paper 72-22, 44 p.
- Sillitoe, R. H., 1972, Relation of metal provinces in western America to subduction of oceanic lithosphere: Geol. Soc. America Bull., vol. 83, no. 3, p. 813-818.
- St. Amand, P., 1957, Geological and geophysical synthesis of the tectonics of portions of British Columbia, the Yukon Territory, and Alaska: Geol. Soc. America Bull., vol. 68, no. 10, p. 1343-1370.
- Taylor, H. P., 1974, The application of oxygen and hydrogen isotope studies to problems of hydrothermal alteration and ore deposition: Econ. Geol., vol. 69, no. 6, p. 843-883.

White, D. E., 1974, Diverse origins of hydrothermal ore fluids: Econ. Geol., vol. 69, no. 6, p. 954-973.

APPENDIX A

Mineral Assemblages Observed in Thin Section

Key:

M - major minerals

a - accessory minerals

' - alteration minerals

* - primary and (or) secondary quartz

APPENDIX A

MINERAL ASSEMBLAGES OBSERVED IN GREENSCHIST UNIT

Sample	Plagioclase	K-feldspar	Quartz	Hornblende	Actinolite	Anthophyllite	Biotite	Chlorite	Muscovite	Sericite	Cordierite	Antigorite	Talc	Magnesite	Calcite	Epidote	Garnet	Tourmaline	Opagues
0	M		M					M							a	M			a
1	M		a	M				a								M			a
2	M		a	M				a								a			a
3	a		a	M						M					a	M			a
11	M		M				a	M	a	a									a
13	M			M						a						M			a
31	M		M	M				M	a							M			a
43	M		a	M				M								M			a
49	M				M		M	a		a						M			a
54	M		M				M	a	M								a		a
56	M		M				M	a	M								M		a
59	a		M					a	M								M		a
74	M		M				a	a	M	a						a			a
78	M			M				M		a						a			a
79	M		M				M	a	M	a							a		a
146	M		a	M				M		a					a				a
153	a		M				a	a	M								M	a	a
161	M		M				a	M	M								M		a
162	M		M				a	M	M								M		a
165	M		a	M				a							a	M			a
171	M		M	M			M										M		a

APPENDIX A (contd.)

MINERAL ASSEMBLAGES OBSERVED IN GREENSCHIST UNIT

Sample	Plagioclase	K-feldspar	Quartz	Hornblende	Actinolite	Anthophyllite	Biotite	Chlorite	Muscovite	Sericite	Cordierite	Antigorite	Talc	Magnesite	Calcite	Epidote	Garnet	Tourmaline	Opques
177	M		M				M		M	a							a		a
178	a		M				M	a	M	M							a		a
195			M				a		M								M		a

MINERAL ASSEMBLAGES OBSERVED IN GREENSCHIST UNIT 1

123	a		M				M	M									a		a
126	a		M					a		M							a		a
211	a		M				M	a		M							a		M
212			M				a	a		M									M
217	a		M				M	a		M							a		a
219	a		M				a	a		a							a		a
222	a		M				M										a		a

MINERAL ASSEMBLAGES OBSERVED IN GREENSCHIST UNIT 2

25							M					M	M						
46							M							M	M				
67	M						M	M				a							a
67a											a	M	M	M					

MINERAL ASSEMBLAGES OBSERVED IN MICA SCHIST UNIT

4	M		M				a	a	M								a		a
---	---	--	---	--	--	--	---	---	---	--	--	--	--	--	--	--	---	--	---

APPENDIX A (contd.)

MINERAL ASSEMBLAGES OBSERVED IN MICA SCHIST UNIT

Sample	Plagioclase	K-feldspar	Quartz	Hornblende	Actinolite	Anthophyllite	Biotite	Chlorite	Muscovite	Sericite	Cordierite	Antigorite	Talc	Magnesite	Calcite	Epidote	Garnet	Tourmaline	Opagues
5	M		M						M										a
10	M		M						M	a									a
12	M		M						M	a					a				a
14	M		M				a		M						a		a		a
18	M		M						M										a
19	M		M						a	a									a
23	M		M						M										a
24	M		M						M										a
26	M		M				a		M										a
45	M		M				a		M							a			a
47	M		a				a	a		a					a	a			a
48	M		M						M	a									a
50	M		M						M	a									a
58	M		M					a	M	a									a
68	M		M				a	a	M	a									a
71	M		M				a		M	a									a
72	M		M				a		M	a									a
73	M		M						M										a
81	M		M						M										a
84	M		M				a	a	M							a	a		a
86			M																a

APPENDIX A (contd.)

MINERAL ASSEMBLAGES OBSERVED IN MICA SCHIST UNIT

Sample	Plagioclase	K-feldspar	Quartz	Hornblende	Actinolite	Anthophyllite	Biotite	Chlorite	Muscovite	Sericite	Cordierite	Antigorite	Talc	Magnesite	Calcite	Epidote	Garnet	Tourmaline	Opques	Pyroxene
87	M	M							M											p
90	M	M							M	a										p
93	M	M						a	M	a					a					a
95	M	M							M											a
105	M	M								a										a
106	M	M					a			a							p			a
120	M	M					a		M	a							a			a
147	M	M					a		M	a										a
150	M	M					a		M											a
172	M	M						a	M	a										a
206	M	M					a								M					a
223	M	M							M	a										a

MINERAL ASSEMBLAGES OBSERVED IN MARBLE UNIT

70		a													M					
166															M					

MINERAL ASSEMBLAGES OBSERVED IN SKARN-LIKE ROCK

108	M	M													M	a	a			a
205															M		a			M

APPENDIX A (contd.)

MINERAL ASSEMBLAGES OBSERVED IN META-QUARTZDIORITE

Sample	Plagioclase	K-feldspar	Quartz	Hornblende	Actinolite	Anthophyllite	Biotite	Chlorite	Muscovite	Sericite	Cordierite	Antigorite	Talc	Magnesite	Calcite	Epidote	Garnet	Tourmaline	Opakes
22	M	a	M	M			a	a		M					a	a			a
104	M	a	M	M			a	a								a	a		a

MINERAL ASSEMBLAGES OBSERVED IN PELLY GNEISS

7	a	M	M				M		a	a									a
36	a	M	M						a	a									a
37	a	M	M						a	a									a
39		M	M				a	a		a									a
41		M	M				a		a	a									a
55	M	M					M		a										a
57	a	M	M						M	a									a
60	M	M	M						a	a									a
61	a	M	M				a			a									a
64	a	M	M				a		a								a		a
77	a	M							M	a									a
96		M	M				M	a	a	a									a
100		M	M*							M'									a
111	a	M	M						M	a									a
113	a	M	M				M	a	a	a									a
114	a	M	M*				a			a									a
115		M	M*						a	M'									a

APPENDIX A (contd.)

MINERAL ASSEMBLAGES OBSERVED IN PELLY GNEISS

Sample	Plagioclase	K-feldspar	Quartz	Hornblende	Actinolite	Anthophyllite	Biotite	Chlorite	Muscovite	Sericite	Cordierite	Antigorite	Talc	Magnesite	Calcite	Epidote	Garnet	Tourmaline	Opques
116		M	M*				a	a'	a	a'									a
118		M	M*							M'									a
119		M	M*							M'									a
121	a	M	M*				a	a'		M'									a
124	a	M	M							a									a
127		M	M*				a	a'		M'									a
128	a	M	M						M	a									a
129		M	M						M	a								a	a
130	a	M	M						M	a								a	a
131	a	M	M						M	a								a	a
133	a	M	M				a			a								a	a
134		M	M				M	a		a									a
135	a	M	M				a			a								a	a
136	a	M	M				a	a		a									a
137		M	M						a	a									a
138	a	M	M				a	a		a									a
139		M	M				a	a	M	a									a
140	a	M	M				M	a	a	a									a
141		M	M						M	a									a
144	a	M	M							a									a
151	a	M	M						a	a								a	a

APPENDIX A (contd.)

MINERAL ASSEMBLAGES OBSERVED IN PELY GNEISS

Sample	Plagioclase	K-feldspar	Quartz	Hornblende	Actinolite	Anthophyllite	Biotite	Chlorite	Muscovite	Sericite	Cordierite	Antigorite	Talc	Magnesite	Calcite	Epidote	Garnet	Tourmaline	Opques
152	a	M	M				a	a	a	a									a
154	a	M	M						a	a									a
157		M	M						a	a									a
158		M	M					a	a	a									a
159		M	M				a	a	a	a									a
160		M	M						M	a									a
163		M	M						M	a								a	a
175	a	M	M					a	M	a									a
176	a	M	M				a	a	M	a									a
179	a	M	M				a		a	a							a		a
180	a	M	a	a			M	a	a	a						a			a
183	a	M	M						M	a									a
185	a	M	M*						a	M'									a
189		M	M*						M	a									a
192		M	M*						a	M'									a
193		M	M						M	a									a
196	a	M	M*							M'									a
207		M	M*							M'									a
209		M	M*							M'									a
220a		M	M*						a	M'									a
221	a	M	M				a	a	M	a									a

APPENDIX A (contd.)

MINERAL ASSEMBLAGES OBSERVED IN PELY GNEISS

Sample	Plagioclase	K-feldspar	Quartz	Hornblende	Actinolite	Anthophyllite	Biotite	Chlorite	Muscovite	Sericite	Cordierite	Antigorite	Talc	Magnesite	Calcite	Epidote	Garnet	Tourmaline	Opques
225		M	M*						a	M'									p
228		M	M*						a	M'									p

APPENDIX A (contd.)

MINERAL ASSEMBLAGES OBSERVED IN DIORITE

Sample	Plagioclase	K-feldspar	Quartz	Hornblende	Pyroxene	Biotite	Muscovite	Chlorite	Olivine	Apatite	Rutile	Tourmaline	Epidote	Sericite	Calcite	Opagues
186	M	a	a*	M				a'						M'	a'	a
187	M	a	a*	M		M		a'						M'		a
188	M	a	a		M	a		a'								a
190	M		a*					a'					a'	M'	a'	a
226	M		a*	M	a			a'					a'	M'		a
227	M	a	a*	a				a'					a'	a'		a
227a	M		a*	M	a									M'		a

MINERAL ASSEMBLAGES OBSERVED IN MONZODIORITE, MONZONITE

21	M	M	a	a		a		a'					a'	M'	a'	a
42	M	M	a		M	a		a'					a'	a'		a
103	M	a	a	a		a		a'						a'		a
125	M	M	M		a	a		a'					a'	M'	a'	a
143	M	M	M	a		M		a'								a
145	M	M	a			M		a'								a
181	M	M	M	M		a		a'					a'	a'		a
198	M	M	M		a	M		a'						a'		a
199	M	a	M	a		a		a'					a'	a'		a
200	M	a	M	a		a								a'		a
203	M	M	M		a	a										a
216	M	a	M*											M'		a
218	M	a	M	a				a'						M'	a'	a

APPENDIX A (contd.)

MINERAL ASSEMBLAGES OBSERVED IN GRANODIORITE

Sample	Plagioclase	K-feldspar	Quartz	Hornblende	Pyroxene	Biotite	Muscovite	Chlorite	Olivine	Apatite	Rutile	Tourmaline	Epidote	Sericite	Calcite	Opakes
40	M	M	M	a	a	M		a'					a'	a'	a'	a
117	M	M	M*				a							M'		a
122	M	M	M*			a		a'					a'	M'		a
201	a	M*	M*					a'				a'	a'	M'	a'	a
202	M	M	M			M		a'						a'		a
204	M	M	M	a		a		a'						a'		a
208	M	M	M			a		a'		a	a			M'		a

MINERAL ASSEMBLAGES OBSERVED IN GABBRO

184	M				M	a								a'		a
191	M				M	a										a

MINERAL ASSEMBLAGES OBSERVED IN ANDESITE

28	a		a*											M'	a'	a
28a	a		M*												M'	a
98	a		a*										a'	M'		a
101	a	a	M*									a'	a'	M'	a'	a
142	M		M*											M'		a
213	M	a	a*					a'						M'	a'	a
220	M	a	a*											M'		a

APPENDIX A (contd.)

MINERAL ASSEMBLAGES OBSERVED IN HORNBLENDE ANDESITE

Sample	Plagioclase	K-feldspar	Quartz	Hornblende	Pyroxene	Biotite	Muscovite	Chlorite	Olivine	Apatite	Rutile	Tourmaline	Epidote	Sericite	Calcite	Opagues
35	M		a*	M				a'						M'		a
62	M		a*	a				a'					a'	a'	a'	a
63	M	a	a	a				a'					a'		a'	a
101b	M		a*	a				a'					a'	a'	a'	a
173	a		a*	M				a'						M'	a'	a
174	M		a*	a				a'					a'	M'		a
210	M	a	a*	a										M'		a

MINERAL ASSEMBLAGES OBSERVED IN PYROXENE ANDESITE

27	a	a			a				a						a'	a
27a	a	a			a				a						a'	a
29	M	a			a									M'	a'	a

MINERAL ASSEMBLAGE OBSERVED IN PYROXENE-HORNBLLENDE ANDESITE PORPHYRY

30	M			M	a										a'	a
----	---	--	--	---	---	--	--	--	--	--	--	--	--	--	----	---

MINERAL ASSEMBLAGES OBSERVED IN BASALT

33	a				M				a							a
51	a				M				a						a'	a

APPENDIX B

Raw Geochemical and Magnetic Data

Key:

Cu - copper in ppm

Mo - molybdenum in ppm

Zn - zinc in ppm

Ag - silver in ppm

MAG - magnetic values in gammas

ID - sample number

Code - type of sample:

RS - reconnaissance soil

RR - reconnaissance rock-chip

RW - reconnaissance stream-sediment

PS - Pika Canyon claim block soil grid

NS - NE Pika Canyon claim block soil grid

APPENDIX B

Raw Geochemical and Magnetic Data

Cu (ppm)	Mo (ppm)	Zn (ppm)	Ag (ppm)	MAG (gammas)	ID	Code
39.0	2.0	135.0	.80	390.0	26261	NS
40.0	2.0	96.0	.30	390.0	26262	NS
18.0	1.0	92.0	.40	430.0	26263	NS
112.0	1.0	820.0	.00	420.0	26264	NS
38.0	1.0	140.0	.70	410.0	26265	NS
54.0	1.0	120.0	.00	440.0	26266	NS
40.0	2.0	120.0	.70	440.0	26267	NS
46.0	2.0	125.0	.10	450.0	26268	NS
10.0	1.0	18.0	.40	420.0	26269	NS
40.0	1.0	90.0	.70	450.0	26270	NS
36.0	1.0	120.0	.40	430.0	26271	NS
32.0	1.0	130.0	.20	440.0	26272	NS
40.0	1.0	98.0	.30	430.0	26273	NS
30.0	1.0	97.0	.20	440.0	26274	NS
30.0	1.0	80.0	.60	430.0	26275	NS
34.0	1.0	82.0	.40	450.0	26276	NS
16.0	1.0	28.0	.30	450.0	26277	NS
40.0	2.0	125.0	.20	470.0	26278	NS
28.0	1.0	74.0	.20	470.0	26279	NS
21.0	1.0	48.0	.30	450.0	26280	NS
14.0	1.0	47.0	.30	ND	26281	NS
10.0	1.0	32.0	.20	380.0	26282	NS
8.0	1.0	19.0	.10	470.0	26283	NS
18.0	1.0	30.0	.10	450.0	26284	NS
12.0	1.0	42.0	.80	450.0	26285	NS
10.0	1.0	35.0	.50	450.0	26286	NS
24.0	1.0	58.0	.10	470.0	26287	NS
26.0	1.0	105.0	.30	490.0	26288	NS
31.0	1.0	58.0	.10	530.0	26289	NS
34.0	2.0	73.0	.40	320.0	26290	NS
23.0	1.0	62.0	.30	330.0	26291	NS
21.0	1.0	55.0	.30	410.0	26292	NS
14.0	1.0	28.0	.40	430.0	26293	NS
50.0	1.0	130.0	.50	430.0	26294	NS
48.0	1.0	100.0	.00	420.0	26295	NS
20.0	1.0	45.0	.30	410.0	26296	NS
40.0	1.0	64.0	.10	430.0	26730	NS
50.0	1.0	90.0	.60	420.0	26731	NS
70.0	1.0	70.0	.10	420.0	26732	NS
34.0	4.0	98.0	.40	410.0	26733	NS
18.0	1.0	78.0	.50	380.0	26734	NS
32.0	1.0	64.0	.50	410.0	26735	NS
40.0	1.0	165.0	.70	400.0	26736	NS
50.0	2.0	130.0	.80	420.0	26737	NS
82.0	2.0	180.0	.10	390.0	26738	NS

APPENDIX B (contd.)

Raw Geochemical and Magnetic Data

Cu (ppm)	Mo (ppm)	Zn (ppm)	Ag (ppm)	MAG (gammas)	ID	Code
30.0	1.0	83.0	.10	410.0	26739	NS
34.0	1.0	86.0	.10	390.0	26740	NS
16.0	1.0	55.0	.10	390.0	26741	NS
32.0	4.0	75.0	.20	380.0	26742	NS
20.0	2.0	62.0	.10	430.0	26743	NS
16.0	1.0	50.0	.10	400.0	26744	NS
24.0	1.0	52.0	.20	ND	26983	NS
24.0	1.0	70.0	.10	620.0	26984	NS
35.0	1.0	83.0	.10	ND	26985	NS
63.0	5.0	130.0	.20	ND	26986	NS
40.0	4.0	82.0	.10	ND	26987	NS
44.0	1.0	100.0	.20	ND	26988	NS
48.0	1.0	125.0	.20	ND	26989	NS
60.0	1.0	165.0	.90	ND	26990	NS
52.0	5.0	110.0	.10	ND	26991	NS
54.0	4.0	82.0	.80	ND	26992	NS
50.0	3.0	78.0	.40	ND	26993	NS
48.0	6.0	95.0	.00	ND	26994	NS
38.0	2.0	100.0	.30	ND	26995	NS
40.0	1.0	92.0	.80	ND	26996	NS
40.0	2.0	120.0	.10	ND	26997	NS
64.0	3.0	130.0	.40	540.0	26998	NS
32.0	2.0	57.0	.10	390.0	27245	NS
34.0	1.0	55.0	.10	390.0	27246	NS
48.0	1.0	86.0	.10	390.0	27247	NS
22.0	1.0	62.0	.10	380.0	27248	NS
38.0	1.0	120.0	.10	400.0	27249	NS
18.0	1.0	32.0	.50	390.0	27250	NS
72.0	4.0	190.0	.20	390.0	27251	NS
42.0	1.0	88.0	.30	400.0	27252	NS
88.0	5.0	250.0	.40	440.0	27253	NS
22.0	1.0	130.0	.20	400.0	27254	NS
96.0	4.0	165.0	.00	390.0	27255	NS
64.0	2.0	190.0	.60	410.0	27256	NS
48.0	2.0	120.0	.80	380.0	27257	NS
50.0	2.0	125.0	.40	390.0	27258	NS
52.0	3.0	180.0	.70	430.0	27259	NS
60.0	2.0	120.0	.50	440.0	27260	NS
30.0	1.0	105.0	.30	450.0	27261	NS
80.0	2.0	120.0	.40	420.0	27262	NS
16.0	1.0	70.0	.20	400.0	27263	NS
44.0	1.0	105.0	.70	450.0	27264	NS
38.0	1.0	100.0	.80	470.0	27265	NS
64.0	6.0	130.0	.50	460.0	27266	NS
50.0	2.0	110.0	.50	480.0	27267	NS
32.0	1.0	100.0	.40	460.0	27268	NS

APPENDIX B (contd.)

Raw Geochemical and Magnetic Data

Cu (ppm)	Mo (ppm)	Zn (ppm)	Ag (ppm)	MAG (gammas)	ID	Code
20.0	1.0	84.0	.20	490.0	27269	NS
14.0	1.0	47.0	.40	430.0	27270	NS
12.0	2.0	64.0	.60	430.0	27271	NS
10.0	1.0	35.0	.40	460.0	27272	NS
23.0	1.0	188.0	.60	490.0	27273	NS
16.0	1.0	75.0	.30	560.0	27274	NS
18.0	2.0	75.0	.30	600.0	27275	NS
20.0	1.0	58.0	.20	600.0	27276	NS
14.0	1.0	37.0	.40	630.0	27277	NS
10.0	1.0	55.0	.60	630.0	27278	NS
26.0	2.0	55.0	.50	620.0	27279	NS
40.0	2.0	100.0	.70	580.0	27280	NS
60.0	7.0	160.0	.60	590.0	27281	NS
54.0	5.0	150.0	.50	770.0	27282	NS
48.0	3.0	100.0	.30	560.0	27283	NS
46.0	8.0	110.0	.50	540.0	27284	NS
42.0	3.0	138.0	.80	540.0	27285	NS
34.0	3.0	88.0	.20	510.0	27286	NS
52.0	4.0	130.0	.80	550.0	27287	NS
26.0	1.0	78.0	.10	510.0	27288	NS
18.0	2.0	110.0	.20	510.0	27289	NS
42.0	2.0	105.0	.40	500.0	27290	NS
43.0	3.0	130.0	.70	460.0	27291	NS
50.0	1.0	140.0	.40	500.0	27292	NS
66.0	2.0	160.0	.40	530.0	27293	NS
58.0	2.0	160.0	.50	500.0	27294	NS
30.0	3.0	68.0	.40	510.0	27295	NS
43.0	3.0	100.0	.20	480.0	27296	NS
32.0	3.0	100.0	.10	530.0	27297	NS
68.0	4.0	195.0	.40	500.0	27298	NS
44.0	4.0	80.0	.30	540.0	27299	NS
22.0	2.0	118.0	.50	520.0	27300	NS
40.0	1.0	160.0	.30	520.0	27384	NS
60.0	1.0	143.0	.40	500.0	27385	NS
38.0	1.0	100.0	.30	500.0	27386	NS
41.0	3.0	150.0	.20	510.0	27387	NS
30.0	1.0	62.0	.40	540.0	27388	NS
78.0	2.0	270.0	.00	570.0	27389	NS
58.0	5.0	130.0	.60	600.0	27390	NS
44.0	6.0	115.0	.20	570.0	27391	NS
43.0	4.0	78.0	.30	640.0	27392	NS
52.0	3.0	85.0	.20	660.0	27393	NS
50.0	4.0	120.0	.20	600.0	27394	NS
52.0	2.0	130.0	.60	600.0	27395	NS
36.0	2.0	78.0	.10	610.0	27396	NS
20.0	2.0	70.0	.30	640.0	27397	NS

APPENDIX B (contd.)

Raw Geochemical and Magnetic Data

Cu (ppm)	Mo (ppm)	Zn (ppm)	Ag (ppm)	MAG (gammas)	ID	Code
12.0	1.0	48.0	.30	560.0	27398	NS
10.0	1.0	32.0	.20	590.0	27399	NS
15.0	1.0	48.0	.40	610.0	27400	NS
88.0	1.0	200.0	.60	390.0	27670	NS
68.0	1.0	130.0	.20	370.0	27671	NS
46.0	1.0	125.0	.10	400.0	27672	NS
50.0	1.0	120.0	.10	300.0	27673	NS
210.0	3.0	700.0	.70	60.0	27674	NS
34.0	1.0	110.0	.10	-1500.0	27675	NS
22.0	1.0	58.0	.20	580.0	27676	NS
40.0	1.0	140.0	.70	460.0	27677	NS
74.0	6.0	200.0	.30	430.0	27678	NS
54.0	2.0	120.0	.30	420.0	27679	NS
48.0	2.0	130.0	.20	410.0	27680	NS
32.0	1.0	90.0	.40	410.0	27681	NS
56.0	3.0	140.0	.70	370.0	27682	NS
48.0	2.0	92.0	.60	380.0	27683	NS
50.0	1.0	128.0	.00	370.0	27684	NS
30.0	1.0	78.0	.20	380.0	27685	NS
20.0	1.0	74.0	.10	390.0	27686	NS
8.0	1.0	25.0	.20	380.0	27687	NS
26.0	1.0	72.0	.10	380.0	27688	NS
36.0	1.0	110.0	.40	380.0	27689	NS
38.0	1.0	220.0	.10	400.0	27690	NS
32.0	1.0	78.0	.50	420.0	27691	NS
88.0	1.0	195.0	.40	360.0	27692	NS
86.0	1.0	190.0	.40	400.0	27693	NS
112.0	4.0	205.0	.60	380.0	27694	NS
14.0	1.0	28.0	.40	370.0	27695	NS
96.0	1.0	140.0	.30	370.0	27696	NS
124.0	5.0	330.0	.30	380.0	27697	NS
72.0	1.0	200.0	.40	380.0	27698	NS
44.0	1.0	120.0	.50	380.0	27699	NS
46.0	4.0	110.0	.60	420.0	27700	NS
84.0	1.0	170.0	.60	400.0	27751	NS
70.0	1.0	195.0	.60	410.0	27752	NS
70.0	2.0	200.0	.90	390.0	27753	NS
76.0	4.0	135.0	.30	390.0	27754	NS
40.0	2.0	130.0	.20	400.0	27755	NS
50.0	1.0	130.0	.40	400.0	27756	NS
13.0	1.0	22.0	.10	390.0	27757	NS
18.0	1.0	24.0	.80	420.0	27758	NS
40.0	1.0	88.0	.50	400.0	27759	NS
72.0	1.0	150.0	.70	400.0	27760	NS
26.0	1.0	78.0	.10	400.0	27761	NS
26.0	1.0	65.0	.10	380.0	27762	NS

APPENDIX B (contd.)

Raw Geochemical and Magnetic Data

Cu (ppm)	Mo (ppm)	Zn (ppm)	Ag (ppm)	MAG (gammas)	ID	Code
36.0	1.0	70.0	.20	440.0	27763	NS
58.0	6.0	125.0	.10	440.0	27764	NS
16.0	2.0	55.0	.40	460.0	27765	NS
12.0	1.0	44.0	.10	450.0	27766	NS
16.0	1.0	33.0	.30	450.0	27767	NS
22.0	1.0	98.0	.20	490.0	27768	NS
24.0	2.0	78.0	.20	510.0	27769	NS
28.0	1.0	95.0	.20	450.0	27770	NS
28.0	1.0	72.0	.40	400.0	27771	NS
16.0	1.0	30.0	.20	380.0	27772	NS
44.0	1.0	88.0	.20	430.0	27773	NS
34.0	1.0	125.0	.10	430.0	27774	NS
62.0	2.0	215.0	.20	410.0	27775	NS
46.0	3.0	150.0	.50	420.0	27776	NS
70.0	4.0	140.0	.30	450.0	27777	NS
52.0	6.0	148.0	.70	450.0	27778	NS
60.0	7.0	130.0	.80	400.0	27779	NS
50.0	3.0	160.0	.20	420.0	27780	NS
48.0	4.0	120.0	.40	410.0	27781	NS
40.0	1.0	120.0	.40	410.0	27782	NS
52.0	3.0	100.0	.10	410.0	27783	NS
10.0	1.0	23.0	.20	410.0	27784	NS
50.0	1.0	110.0	.30	400.0	27785	NS
45.0	1.0	100.0	.50	380.0	27786	NS
70.0	4.0	185.0	.70	360.0	27787	NS
44.0	4.0	170.0	.40	380.0	27788	NS
24.0	2.0	52.0	.10	360.0	27789	NS
28.0	1.0	110.0	.20	420.0	27790	NS
16.0	1.0	38.0	.40	400.0	27791	NS
26.0	1.0	60.0	.10	390.0	27792	NS
25.0	1.0	68.0	.20	410.0	27793	NS
32.0	1.0	72.0	.20	400.0	27794	NS
26.0	2.0	65.0	.20	400.0	27795	NS
26.0	1.0	65.0	.10	410.0	27796	NS
20.0	1.0	56.0	.40	370.0	27797	NS
27.0	1.0	73.0	.30	410.0	27798	NS
44.0	1.0	120.0	.40	410.0	27799	NS
50.0	2.0	140.0	.20	390.0	27800	NS
50.0	2.0	250.0	.50	410.0	27888	NS
74.0	4.0	290.0	.30	420.0	27889	NS
82.0	6.0	160.0	.50	430.0	27890	NS
60.0	4.0	118.0	.60	400.0	27891	NS
46.0	2.0	93.0	.40	380.0	27892	NS
36.0	2.0	100.0	.30	420.0	27893	NS
20.0	1.0	55.0	.20	400.0	27894	NS
45.0	2.0	87.0	.20	420.0	27895	NS

APPENDIX B (contd.)

Raw Geochemical and Magnetic Data

Cu (ppm)	Mo (ppm)	Zn (ppm)	Ag (ppm)	MAG (gammas)	ID	Code
58.0	1.0	130.0	.40	400.0	27896	NS
44.0	2.0	100.0	.50	410.0	27897	NS
33.0	1.0	100.0	.30	420.0	27898	NS
42.0	1.0	140.0	.40	390.0	27899	NS
58.0	1.0	90.0	.30	400.0	27900	NS
12.0	1.0	35.0	.20	650.0	27901	NS
21.0	1.0	61.0	.40	550.0	27902	NS
16.0	1.0	49.0	.20	530.0	27903	NS
54.0	1.0	140.0	.20	540.0	27904	NS
34.0	2.0	70.0	.20	560.0	27905	NS
46.0	1.0	90.0	.20	540.0	27906	NS
42.0	1.0	105.0	.40	510.0	27907	NS
66.0	6.0	100.0	.10	520.0	27908	NS
36.0	5.0	43.0	.20	500.0	27909	NS
80.0	8.0	200.0	.70	520.0	27910	NS
50.0	1.0	110.0	.50	490.0	27911	NS
14.0	1.0	25.0	.20	500.0	27912	NS
12.0	1.0	25.0	.10	490.0	27913	NS
34.0	2.0	80.0	.60	490.0	27914	NS
50.0	1.0	94.0	.30	510.0	27915	NS
62.0	2.0	120.0	.40	510.0	27916	NS
52.0	6.0	140.0	.60	520.0	27917	NS
26.0	1.0	110.0	.30	500.0	27918	NS
28.0	1.0	72.0	.20	520.0	27919	NS
22.0	1.0	70.0	.20	550.0	27920	NS
22.0	1.0	70.0	.20	520.0	27921	NS
32.0	1.0	50.0	.20	510.0	27922	NS
18.0	1.0	78.0	.30	580.0	27923	NS
14.0	1.0	47.0	.20	580.0	27924	NS
34.0	1.0	100.0	.30	570.0	27925	NS
28.0	2.0	110.0	.30	570.0	27926	NS
20.0	1.0	47.0	.10	550.0	27927	NS
41.0	1.0	50.0	.20	530.0	27928	NS
34.0	1.0	62.0	.30	520.0	27929	NS
24.0	1.0	62.0	.40	530.0	27930	NS
24.0	1.0	65.0	.40	ND	27931	NS
24.0	1.0	80.0	.10	ND	27932	NS
21.0	4.0	85.0	.20	ND	27933	NS
25.0	1.0	62.0	.10	ND	27934	NS
20.0	1.0	60.0	.40	ND	27935	NS
50.0	1.0	120.0	.60	ND	27936	NS
60.0	8.0	125.0	.70	ND	27937	NS
60.0	3.0	145.0	.30	ND	27938	NS
27.0	1.0	58.0	.40	ND	27939	NS
40.0	2.0	80.0	.40	ND	27940	NS
52.0	4.0	105.0	.50	ND	27941	NS

APPENDIX B (contd.)

Raw Geochemical and Magnetic Data

Cu (ppm)	Mo (ppm)	Zn (ppm)	Ag (ppm)	MAG (gammas)	ID	Code
44.0	3.0	120.0	.20	ND	27942	NS
22.0	1.0	52.0	.20	ND	27943	NS
16.0	1.0	52.0	.30	620.0	27944	NS
23.0	2.0	80.0	.20	ND	27945	NS
22.0	1.0	55.0	.20	ND	27946	NS
14.0	1.0	55.0	.40	620.0	27947	NS
16.0	1.0	47.0	.30	650.0	27948	NS
46.0	1.0	72.0	.40	650.0	27949	NS
52.0	1.0	125.0	.20	680.0	27950	NS
41.0	1.0	84.0	.20	680.0	27951	NS
92.0	5.0	235.0	.50	640.0	27952	NS
10.0	1.0	32.0	.40	680.0	27953	NS
134.0	9.0	460.0	.50	630.0	27954	NS
72.0	6.0	140.0	.30	630.0	27955	NS
32.0	1.0	68.0	.30	600.0	27956	NS
40.0	1.0	70.0	.60	620.0	27957	NS
25.0	1.0	41.0	.70	620.0	27958	NS
30.0	2.0	57.0	.20	630.0	27959	NS
26.0	1.0	52.0	.30	630.0	27960	NS
22.0	1.0	54.0	.10	560.0	27961	NS
14.0	1.0	55.0	.50	660.0	27962	NS
17.0	1.0	48.0	.10	620.0	27963	NS
16.0	3.0	50.0	.30	630.0	27964	NS
15.0	4.0	50.0	.20	590.0	27965	NS
17.0	2.0	42.0	.10	610.0	27966	NS
12.0	3.0	42.0	.20	600.0	27967	NS
19.0	1.0	56.0	.10	540.0	27968	NS
28.0	1.0	57.0	.20	520.0	27969	NS
36.0	1.0	60.0	.10	560.0	27970	NS
27.0	1.0	65.0	.20	560.0	27971	NS
14.0	2.0	32.0	.10	560.0	27972	NS
30.0	1.0	62.0	.10	550.0	27973	NS
28.0	3.0	88.0	.20	540.0	27974	NS
76.0	6.0	180.0	.10	530.0	27975	NS
24.0	1.0	144.0	.10	-970.0	0001	PS
22.0	1.0	108.0	.10	-860.0	0002	PS
22.0	1.0	114.0	.10	-860.0	0003	PS
28.0	1.0	90.0	.10	1225.0	0004	PS
36.0	1.0	112.0	.10	10.0	0005	PS
22.0	1.0	80.0	.10	-920.0	0006	PS
24.0	1.0	70.0	.10	-920.0	0007	PS
14.0	1.0	24.0	.10	-830.0	0008	PS
18.0	1.0	98.0	.10	-700.0	0009	PS
14.0	1.0	86.0	.10	-1075.0	0010	PS
10.0	1.0	20.0	.10	-1100.0	0011	PS
12.0	1.0	42.0	.10	-1150.0	0012	PS

APPENDIX B (contd.)

Raw Geochemical and Magnetic Data

Cu (ppm)	Mo (ppm)	Zn (ppm)	Ag (ppm)	MAG (gammas)	ID	Code
8.0	1.0	24.0	.10	-1400.0	0013	PS
10.0	1.0	32.0	.10	-1300.0	0014	PS
18.0	1.0	72.0	.10	-1300.0	0015	PS
16.0	1.0	134.0	.10	-1300.0	0016	PS
12.0	1.0	78.0	.10	-1300.0	0017	PS
26.0	1.0	108.0	.50	-1300.0	0018	PS
20.0	1.0	120.0	.10	-1300.0	0019	PS
22.0	1.0	114.0	.10	-1325.0	0020	PS
10.0	1.0	38.0	.10	-1350.0	0021	PS
20.0	1.0	102.0	.20	890.0	0022	PS
22.0	1.0	102.0	.00	-580.0	0023	PS
16.0	1.0	76.0	.10	280.0	0024	PS
20.0	1.0	46.0	.20	-20.0	0025	PS
24.0	1.0	90.0	.10	-810.0	0026	PS
20.0	2.0	140.0	.50	-470.0	0027	PS
26.0	3.0	84.0	.10	-330.0	0028	PS
14.0	2.0	74.0	.10	-990.0	0029	PS
14.0	1.0	56.0	.10	-980.0	0030	PS
8.0	1.0	52.0	.80	-900.0	0031	PS
10.0	1.0	48.0	.10	-1100.0	0032	PS
8.0	1.0	36.0	.10	120.0	0033	PS
18.0	1.0	72.0	.10	-1200.0	0034	PS
20.0	1.0	78.0	.10	-1125.0	0035	PS
16.0	1.0	60.0	.10	-790.0	0036	PS
16.0	1.0	96.0	.10	-1325.0	0037	PS
10.0	1.0	30.0	.10	-1025.0	0038	PS
16.0	1.0	360.0	.20	-1050.0	0039	PS
14.0	1.0	290.0	.20	-1300.0	0040	PS
28.0	1.0	80.0	.10	-1300.0	0041	PS
8.0	1.0	14.0	.10	-1325.0	0042	PS
18.0	2.0	80.0	.20	580.0	0043	PS
18.0	1.0	84.0	.10	700.0	0044	PS
16.0	1.0	80.0	.10	950.0	0045	PS
30.0	1.0	106.0	.20	-500.0	0046	PS
18.0	1.0	350.0	.30	-160.0	0047	PS
20.0	1.0	122.0	.60	-1250.0	0048	PS
20.0	1.0	100.0	.40	-1100.0	0049	PS
12.0	1.0	68.0	.10	-1600.0	0050	PS
16.0	1.0	76.0	.10	-1375.0	0051	PS
12.0	1.0	134.0	.20	ND	0052	PS
24.0	1.0	148.0	.30	-740.0	0053	PS
18.0	1.0	78.0	.40	-1325.0	0054	PS
20.0	1.0	106.0	.10	-590.0	0055	PS
26.0	1.0	168.0	.60	-40.0	0056	PS
16.0	1.0	60.0	.10	-180.0	0057	PS
16.0	1.0	52.0	.10	920.0	0058	PS

APPENDIX B (contd.)

Raw Geochemical and Magnetic Data

Cu (ppm)	Mo (ppm)	Zn (ppm)	Ag (ppm)	MAG (gammas)	ID	Code
12.0	1.0	46.0	.10	850.0	0059	PS
20.0	1.0	42.0	.10	340.0	0060	PS
18.0	1.0	64.0	.10	-1700.0	0061	PS
14.0	1.0	290.0	.10	-1400.0	0062	PS
16.0	1.0	370.0	.50	-1375.0	0063	PS
22.0	3.0	92.0	.10	-760.0	0064	PS
130.0	5.0	154.0	.30	280.0	0065	PS
20.0	3.0	158.0	.10	110.0	0066	PS
28.0	2.0	166.0	.40	300.0	0067	PS
16.0	2.0	92.0	.10	470.0	0068	PS
20.0	2.0	114.0	.20	370.0	0069	PS
20.0	1.0	146.0	.20	-1225.0	0070	PS
16.0	1.0	92.0	.20	-1350.0	0071	PS
10.0	1.0	102.0	.20	-800.0	0072	PS
18.0	1.0	142.0	.10	130.0	0073	PS
22.0	1.0	110.0	.50	-1100.0	0074	PS
28.0	2.0	140.0	.80	-310.0	0075	PS
26.0	2.0	106.0	.30	-370.0	0076	PS
16.0	1.0	80.0	.10	-600.0	0077	PS
20.0	1.0	160.0	.40	-580.0	0078	PS
20.0	1.0	159.0	.10	-660.0	0079	PS
24.0	1.0	350.0	.70	-1225.0	0080	PS
26.0	1.0	130.0	.20	-1375.0	0081	PS
16.0	1.0	118.0	.30	-1375.0	0082	PS
14.0	1.0	174.0	.20	-1375.0	0083	PS
14.0	1.0	70.0	.30	-1400.0	0084	PS
14.0	1.0	128.0	.10	-1175.0	0085	PS
20.0	1.0	180.0	.10	-1150.0	0086	PS
18.0	1.0	158.0	.10	-1125.0	0087	PS
20.0	1.0	196.0	.10	-1050.0	0088	PS
8.0	5.0	104.0	.10	-770.0	0089	PS
40.0	2.0	100.0	.10	-390.0	0090	PS
22.0	1.0	98.0	.10	900.0	0091	PS
36.0	2.0	116.0	.50	250.0	0092	PS
26.0	1.0	88.0	.20	820.0	0093	PS
20.0	2.0	86.0	.10	500.0	0094	PS
30.0	1.0	230.0	.30	-960.0	0095	PS
32.0	2.0	430.0	.30	-1550.0	0096	PS
14.0	1.0	146.0	.40	-1550.0	0097	PS
6.0	1.0	34.0	.10	-1175.0	0098	PS
36.0	3.0	134.0	.60	-380.0	0099	PS
38.0	2.0	350.0	.40	-210.0	0100	PS
46.0	2.0	186.0	.50	280.0	0101	PS
42.0	3.0	128.0	.90	-1050.0	0102	PS
38.0	2.0	180.0	.30	-1225.0	0103	PS
62.0	3.0	112.0	.30	-410.0	0104	PS

APPENDIX B (contd.)

Raw Geochemical and Magnetic Data

Cu (ppm)	Mo (ppm)	Zn (ppm)	Ag (ppm)	MAG (gammas)	ID	Code
40.0	2.0	106.0	.20	-1125.0	0105	PS
20.0	1.0	110.0	.40	-1225.0	0106	PS
20.0	2.0	150.0	.80	-1300.0	0107	PS
24.0	1.0	146.0	.20	-1375.0	0108	PS
20.0	2.0	106.0	.20	-1375.0	0109	PS
20.0	1.0	180.0	.50	-1175.0	0110	PS
20.0	1.0	210.0	.20	-1125.0	0111	PS
18.0	1.0	130.0	.10	-1050.0	0112	PS
18.0	1.0	170.0	.20	-1050.0	0113	PS
20.0	1.0	120.0	.20	-940.0	0114	PS
14.0	1.0	78.0	.10	-590.0	0115	PS
12.0	1.0	118.0	.70	300.0	0116	PS
14.0	1.0	102.0	.20	-1150.0	0117	PS
24.0	2.0	200.0	.10	-1200.0	0118	PS
28.0	1.0	360.0	.00	-1300.0	0119	PS
16.0	1.0	340.0	.80	-1125.0	0120	PS
20.0	1.0	146.0	.80	-1200.0	0121	PS
16.0	1.0	102.0	.40	-860.0	0122	PS
24.0	2.0	190.0	.50	-840.0	0123	PS
16.0	2.0	102.0	.60	-1350.0	0124	PS
62.0	4.0	110.0	.50	-200.0	0125	PS
60.0	3.0	134.0	.10	580.0	0126	PS
80.0	4.0	118.0	.30	430.0	0127	PS
102.0	6.0	110.0	.20	270.0	0128	PS
56.0	8.0	126.0	.10	-90.0	0129	PS
34.0	9.0	130.0	.50	-1300.0	0130	PS
24.0	1.0	74.0	.10	-1300.0	0131	PS
20.0	1.0	90.0	.20	-1300.0	0132	PS
26.0	1.0	104.0	.10	-1325.0	0133	PS
24.0	1.0	94.0	.20	-1350.0	0134	PS
22.0	1.0	174.0	.20	-1175.0	0135	PS
22.0	1.0	90.0	.10	-1100.0	0136	PS
18.0	1.0	80.0	.10	-1075.0	0137	PS
20.0	1.0	96.0	.10	-1050.0	0138	PS
18.0	1.0	128.0	.10	-1025.0	0139	PS
18.0	1.0	194.0	.20	-1050.0	0140	PS
12.0	1.0	186.0	.20	-660.0	0141	PS
16.0	1.0	116.0	.30	-1100.0	0142	PS
20.0	1.0	102.0	.50	-1100.0	0143	PS
22.0	1.0	64.0	.20	-1100.0	0144	PS
20.0	1.0	58.0	.20	-1050.0	0145	PS
18.0	2.0	86.0	.10	760.0	0146	PS
40.0	3.0	250.0	.30	940.0	0147	PS
18.0	1.0	50.0	.00	-280.0	0148	PS
18.0	1.0	106.0	.70	-1380.0	0149	PS
26.0	5.0	114.0	.10	-1300.0	0150	PS

APPENDIX B (contd.)

Raw Geochemical and Magnetic Data

Cu (ppm)	Mo (ppm)	Zn (ppm)	Ag (ppm)	MAG (gammas)	ID	Code
28.0	1.0	134.0	.20	-570.0	0151	PS
126.0	7.0	130.0	.20	-150.0	0152	PS
34.0	4.0	116.0	.20	-600.0	0153	PS
78.0	12.0	122.0	.30	-990.0	0154	PS
24.0	1.0	74.0	.40	-1200.0	0155	PS
22.0	1.0	50.0	.20	-1350.0	0156	PS
16.0	1.0	62.0	.20	-1325.0	0157	PS
14.0	1.0	60.0	.80	-1350.0	0158	PS
12.0	1.0	50.0	.20	-1325.0	0159	PS
14.0	1.0	126.0	.10	-1175.0	0160	PS
20.0	1.0	310.0	.70	-1100.0	0161	PS
22.0	1.0	220.0	.10	-1000.0	0162	PS
26.0	1.0	450.0	.60	-710.0	0163	PS
12.0	1.0	74.0	.20	-940.0	0164	PS
16.0	1.0	172.0	.40	-1000.0	0165	PS
10.0	1.0	24.0	.10	-1075.0	0166	PS
22.0	1.0	186.0	.70	-1075.0	0167	PS
16.0	1.0	210.0	.80	-1250.0	0168	PS
38.0	1.0	118.0	.00	-1200.0	0169	PS
32.0	1.0	70.0	.00	-1150.0	0170	PS
22.0	1.0	84.0	.60	-1050.0	0171	PS
24.0	1.0	62.0	.00	-960.0	0172	PS
18.0	4.0	160.0	.00	-770.0	0173	PS
30.0	3.0	128.0	.20	-270.0	0174	PS
22.0	1.0	70.0	.10	-1000.0	0175	PS
22.0	1.0	54.0	.20	-1150.0	0176	PS
14.0	1.0	68.0	.20	-1300.0	0177	PS
18.0	1.0	50.0	.10	-1600.0	0178	PS
22.0	2.0	150.0	.70	-1200.0	0179	PS
24.0	2.0	121.0	.10	-1350.0	0180	PS
14.0	2.0	80.0	.40	-1300.0	0181	PS
10.0	1.0	44.0	.30	-1300.0	0182	PS
14.0	1.0	38.0	.30	-1300.0	0183	PS
22.0	1.0	86.0	.30	-1300.0	0184	PS
16.0	1.0	72.0	.10	-1300.0	0185	PS
16.0	1.0	72.0	.10	-1125.0	0186	PS
20.0	1.0	68.0	.10	-1100.0	0187	PS
18.0	1.0	48.0	.10	-1050.0	0188	PS
22.0	1.0	230.0	.80	-850.0	0189	PS
16.0	1.0	190.0	.10	150.0	0190	PS
14.0	1.0	88.0	.20	170.0	0191	PS
12.0	1.0	116.0	.10	-160.0	0192	PS
18.0	1.0	94.0	.10	-350.0	0193	PS
16.0	1.0	72.0	.10	-400.0	0194	PS
20.0	1.0	188.0	.70	-410.0	0195	PS
2.0	1.0	12.0	.20	-1250.0	0196	PS

APPENDIX B (contd.)

Raw Geochemical and Magnetic Data

Cu (ppm)	Mo (ppm)	Zn (ppm)	Ag (ppm)	MAG (gammas)	ID	Code
2.0	1.0	10.0	.20	-1175.0	0197	PS
18.0	1.0	54.0	.40	-1125.0	0198	PS
14.0	3.0	98.0	.00	200.0	0199	PS
24.0	2.0	152.0	.40	-720.0	0200	PS
12.0	1.0	52.0	.10	-1000.0	0201	PS
16.0	1.0	60.0	.10	-1200.0	0202	PS
16.0	1.0	70.0	.20	-1250.0	0203	PS
24.0	1.0	86.0	.10	-1275.0	0204	PS
16.0	1.0	86.0	.10	-1350.0	0205	PS
16.0	1.0	54.0	.10	-1300.0	0206	PS
14.0	1.0	60.0	.10	-1300.0	0207	PS
22.0	1.0	52.0	.50	-1300.0	0208	PS
22.0	1.0	72.0	.20	-1300.0	0209	PS
14.0	1.0	34.0	.10	-1300.0	0210	PS
12.0	1.0	36.0	.10	-1300.0	0211	PS
24.0	1.0	82.0	.10	-1100.0	0212	PS
20.0	1.0	154.0	.60	-1050.0	0213	PS
20.0	1.0	108.0	.20	-960.0	0214	PS
18.0	1.0	112.0	.30	-880.0	0215	PS
18.0	1.0	116.0	.50	-790.0	0216	PS
22.0	1.0	74.0	.50	-260.0	0217	PS
22.0	1.0	114.0	.30	-780.0	0218	PS
24.0	3.0	78.0	.10	-760.0	0219	PS
30.0	4.0	96.0	.10	-810.0	0220	PS
46.0	8.0	104.0	.10	-1025.0	0221	PS
26.0	2.0	100.0	.20	-1250.0	0222	PS
8.0	1.0	38.0	.10	-1375.0	0223	PS
6.0	1.0	12.0	.10	-1200.0	0224	PS
26.0	2.0	152.0	.10	-1300.0	0225	PS
14.0	1.0	86.0	.20	-1325.0	0226	PS
10.0	1.0	50.0	.20	-1225.0	0227	PS
16.0	1.0	78.0	.10	-1225.0	0228	PS
18.0	1.0	112.0	.30	-1225.0	0229	PS
22.0	1.0	84.0	.10	-1250.0	0230	PS
20.0	1.0	106.0	.10	-1250.0	0231	PS
22.0	1.0	68.0	.10	-1275.0	0232	PS
22.0	1.0	205.0	.60	-1025.0	0233	PS
16.0	1.0	118.0	.10	-1025.0	0234	PS
20.0	1.0	96.0	.30	-920.0	0235	PS
50.0	5.0	310.0	.10	-790.0	0236	PS
28.0	1.0	124.0	.40	-310.0	0237	PS
30.0	1.0	172.0	.00	300.0	0238	PS
24.0	1.0	106.0	.00	-40.0	0239	PS
24.0	2.0	90.0	.70	20.0	0240	PS
24.0	1.0	106.0	.10	-240.0	0241	PS
18.0	1.0	72.0	.10	-1325.0	0242	PS

APPENDIX B (contd.)

Raw Geochemical and Magnetic Data

Cu (ppm)	Mo (ppm)	Zn (ppm)	Ag (ppm)	MAG (gammas)	ID	Code
28.0	1.0	110.0	.20	-1300.0	0243	PS
46.0	1.0	106.0	.30	-1100.0	0244	PS
62.0	1.0	60.0	.10	-1150.0	0245	PS
14.0	1.0	114.0	.10	-1175.0	0246	PS
16.0	1.0	66.0	.30	-1225.0	0247	PS
20.0	1.0	122.0	.20	-1200.0	0248	PS
16.0	1.0	140.0	.20	-1225.0	0249	PS
14.0	1.0	112.0	.30	-1250.0	0250	PS
16.0	1.0	150.0	.80	-1250.0	0251	PS
14.0	1.0	82.0	.30	-1275.0	0252	PS
14.0	1.0	60.0	.10	-1275.0	0253	PS
46.0	1.0	320.0	.20	-860.0	0254	PS
10.0	1.0	38.0	.20	-830.0	0255	PS
20.0	1.0	104.0	.20	-730.0	0256	PS
10.0	1.0	42.0	.30	-820.0	0257	PS
16.0	1.0	68.0	.30	-130.0	0258	PS
16.0	1.0	84.0	.30	230.0	0259	PS
18.0	1.0	68.0	.50	220.0	0260	PS
18.0	1.0	58.0	.10	940.0	0261	PS
22.0	1.0	66.0	.10	60.0	0262	PS
22.0	1.0	60.0	.20	-180.0	0263	PS
118.0	1.0	56.0	.50	-780.0	0264	PS
36.0	3.0	62.0	.50	-1275.0	0265	PS
22.0	3.0	84.0	.50	-950.0	0266	PS
18.0	2.0	72.0	.20	-380.0	0267	PS
20.0	1.0	106.0	.00	-450.0	0268	PS
16.0	1.0	174.0	.20	-1125.0	0269	PS
18.0	1.0	270.0	.40	-1100.0	0270	PS
18.0	1.0	116.0	.30	-1125.0	0271	PS
16.0	1.0	128.0	.20	-1150.0	0272	PS
12.0	1.0	66.0	.10	-1150.0	0273	PS
22.0	1.0	68.0	.10	-1150.0	0274	PS
28.0	1.0	202.0	.10	-1025.0	0275	PS
18.0	1.0	110.0	.50	-1050.0	0276	PS
20.0	1.0	128.0	.50	-1050.0	0277	PS
24.0	1.0	124.0	.30	-1100.0	0278	PS
22.0	1.0	122.0	.50	-900.0	0279	PS
22.0	1.0	98.0	.30	-1200.0	0280	PS
20.0	1.0	74.0	.20	-500.0	0281	PS
32.0	1.0	74.0	.20	-420.0	0282	PS
20.0	1.0	86.0	.10	-330.0	0283	PS
36.0	1.0	92.0	.20	-570.0	0284	PS
20.0	1.0	36.0	.10	-820.0	0285	PS
12.0	1.0	52.0	.20	-800.0	0286	PS
20.0	3.0	64.0	.20	-1025.0	0287	PS
14.0	6.0	110.0	.10	-840.0	0288	PS

APPENDIX B (contd.)

Raw Geochemical and Magnetic Data

Cu (ppm)	Mo (ppm)	Zn (ppm)	Ag (ppm)	MAG (gammas)	ID	Code
22.0	2.0	125.0	.50	-680.0	0289	PS
24.0	1.0	186.0	.60	-1175.0	0290	PS
18.0	1.0	150.0	.50	-1200.0	0291	PS
14.0	1.0	68.0	.60	-1200.0	0292	PS
12.0	1.0	88.0	.10	-1175.0	0293	PS
14.0	1.0	72.0	.10	-1150.0	0294	PS
14.0	1.0	74.0	.10	-1150.0	0295	PS
26.0	1.0	136.0	.40	-1050.0	0296	PS
28.0	1.0	72.0	.30	-1200.0	0297	PS
16.0	1.0	74.0	.10	-1300.0	0298	PS
16.0	1.0	82.0	.40	-1275.0	0299	PS
20.0	1.0	80.0	.10	-1250.0	0300	PS
22.0	1.0	88.0	.10	-1175.0	0301	PS
20.0	1.0	80.0	.10	-1150.0	0302	PS
24.0	1.0	78.0	.10	-670.0	0303	PS
18.0	1.0	64.0	.10	-390.0	0304	PS
20.0	1.0	72.0	.10	-230.0	0305	PS
20.0	1.0	76.0	.10	-200.0	0306	PS
18.0	1.0	102.0	.20	-230.0	0307	PS
12.0	1.0	66.0	.10	120.0	0308	PS
16.0	1.0	88.0	.10	100.0	0309	PS
12.0	1.0	80.0	.10	90.0	0310	PS
20.0	1.0	66.0	.10	-760.0	0311	PS
16.0	1.0	88.0	.30	-1325.0	0312	PS
16.0	1.0	126.0	.30	-1200.0	0313	PS
12.0	1.0	100.0	.20	-1400.0	0314	PS
8.0	1.0	74.0	.20	-1350.0	0315	PS
14.0	1.0	112.0	.80	-1350.0	0316	PS
18.0	1.0	66.0	.20	-1275.0	0317	PS
16.0	1.0	64.0	.10	-1600.0	0318	PS
22.0	1.0	72.0	.60	-1300.0	0319	PS
16.0	1.0	72.0	.40	-1250.0	0320	PS
20.0	1.0	82.0	.40	-1225.0	0321	PS
22.0	1.0	86.0	.30	-1200.0	0322	PS
12.0	1.0	54.0	.30	-1125.0	0323	PS
18.0	2.0	106.0	.40	-1025.0	0324	PS
16.0	1.0	60.0	.10	230.0	0325	PS
28.0	1.0	82.0	.20	50.0	0326	PS
20.0	1.0	78.0	.10	350.0	0327	PS
14.0	1.0	74.0	.10	580.0	0328	PS
22.0	1.0	92.0	.10	340.0	0329	PS
22.0	1.0	104.0	.20	490.0	0330	PS
18.0	1.0	96.0	.20	-146.0	0331	PS
8.0	1.0	88.0	.10	-1450.0	0332	PS
18.0	1.0	94.0	.20	-1400.0	0333	PS
22.0	1.0	100.0	.20	-1525.0	0334	PS

APPENDIX B (contd.)

Raw Geochemical and Magnetic Data

Cu (ppm)	Mo (ppm)	Zn (ppm)	Ag (ppm)	MAG (gammas)	ID	Code
14.0	1.0	78.0	.10	-1425.0	0335	PS
10.0	1.0	96.0	.50	-1400.0	0336	PS
16.0	1.0	92.0	.20	-1375.0	0337	PS
18.0	1.0	80.0	.10	-1250.0	0338	PS
42.0	1.0	72.0	.20	-1300.0	0339	PS
16.0	1.0	66.0	.10	-1300.0	0340	PS
18.0	1.0	46.0	.30	-1225.0	0341	PS
50.0	8.0	158.0	.50	-1225.0	0342	PS
14.0	1.0	50.0	.10	-1250.0	0343	PS
16.0	1.0	51.0	.10	-1100.0	0344	PS
22.0	1.0	86.0	.10	-1075.0	0345	PS
24.0	2.0	138.0	.30	-1050.0	0346	PS
6.0	1.0	30.0	.10	-950.0	0347	PS
16.0	1.0	80.0	.20	200.0	0348	PS
14.0	1.0	58.0	.10	10.0	0349	PS
16.0	2.0	106.0	.10	200.0	0350	PS
16.0	1.0	40.0	.10	-250.0	0351	PS
16.0	2.0	150.0	.10	-1325.0	0352	PS
16.0	1.0	42.0	.10	-1000.0	0353	PS
8.0	1.0	12.0	.10	-1200.0	0354	PS
28.0	1.0	68.0	.10	-1325.0	0355	PS
30.0	1.0	96.0	.10	-1550.0	0356	PS
42.0	1.0	68.0	.10	-1350.0	0357	PS
24.0	1.0	72.0	.10	-1375.0	0358	PS
20.0	1.0	62.0	.10	-1125.0	0359	PS
62.0	1.0	86.0	.20	-1125.0	0360	PS
40.0	1.0	54.0	.60	-1075.0	0361	PS
30.0	1.0	60.0	.20	-1300.0	0362	PS
28.0	1.0	70.0	.20	-1225.0	0363	PS
20.0	1.0	92.0	.20	-1175.0	0364	PS
24.0	1.0	56.0	.10	-1175.0	0365	PS
26.0	1.0	74.0	.10	-1200.0	0366	PS
14.0	1.0	58.0	.10	-1225.0	0367	PS
16.0	1.0	104.0	.10	-1225.0	0368	PS
18.0	1.0	60.0	.10	-910.0	0369	PS
20.0	1.0	80.0	.10	-1275.0	0370	PS
12.0	1.0	66.0	.10	-1300.0	0371	PS
14.0	1.0	62.0	.10	-1350.0	0372	PS
20.0	1.0	86.0	.10	-1275.0	0373	PS
20.0	1.0	62.0	.10	-1275.0	0374	PS
12.0	1.0	50.0	.10	-1300.0	0375	PS
6.0	1.0	12.0	.10	-1275.0	0376	PS
14.0	1.0	74.0	.10	-1325.0	0377	PS
38.0	1.0	88.0	.10	-1375.0	0378	PS
18.0	2.0	62.0	.10	ND	23211	RR
8.0	1.0	45.0	.10	ND	23212	RR

APPENDIX B (contd.)

Raw Geochemical and Magnetic Data

Cu (ppm)	Mo (ppm)	Zn (ppm)	Ag (ppm)	MAG (gammas)	ID	Code
22.0	1.0	110.0	.10	ND	23215	RR
15.0	1.0	80.0	.10	ND	23219	RR
5.0	1.0	26.0	.10	ND	23220	RR
6.0	1.0	128.0	.20	ND	23223	RR
7.0	1.0	18.0	.20	ND	23225	RR
14.0	1.0	78.0	.20	ND	23226	RR
10.0	4.0	130.0	.10	ND	23228	RR
13.0	1.0	40.0	.10	ND	23231	RR
4.0	1.0	20.0	.10	ND	23235	RR
14.0	1.0	70.0	.10	ND	23237	RR
6.0	1.0	20.0	.10	ND	23261	RR
12.0	1.0	76.0	.10	ND	23263	RR
6.0	1.0	20.0	.10	ND	23265	RR
22.0	1.0	44.0	.10	ND	23277	RR
8.0	2.0	114.0	.20	ND	23674	RR
15.0	1.0	80.0	.10	ND	23683	RR
10.0	1.0	92.0	.10	ND	23690	RR
2.0	3.0	12.0	.40	ND	23691	RR
2.0	1.0	40.0	.10	ND	23692	RR
9.0	1.0	430.0	.80	ND	23694	RR
12.0	1.0	122.0	.20	ND	23695	RR
5.0	1.0	40.0	.10	ND	23696	RR
340.0	1.0	99.0	.60	ND	23700	RR
6.0	7.0	80.0	.20	ND	23851	RR
14.0	2.0	70.0	.10	ND	23852	RR
12.0	1.0	72.0	.10	ND	23853	RR
12.0	3.0	50.0	.10	ND	23854	RR
4.0	4.0	62.0	.10	ND	23855	RR
3.0	2.0	66.0	.10	ND	23856	RR
4.0	7.0	60.0	.10	ND	23858	RR
12.0	2.0	80.0	.10	ND	23860	RR
4.0	1.0	50.0	.10	ND	23862	RR
7.0	2.0	70.0	.10	ND	24028	RR
60.0	2.0	84.0	.10	ND	24159	RR
4.0	2.0	110.0	.10	ND	24326	RR
10.0	1.0	10.0	.10	ND	24327	RR
60.0	1.0	26.0	.10	ND	24330	RR
6.0	1.0	20.0	.10	ND	24342	RR
2.0	1.0	10.0	.10	ND	24358	RR
5.0	1.0	10.0	.10	ND	24362	RR
16.0	1.0	34.0	.10	ND	24372	RR
18.0	1.0	108.0	.20	ND	24373	RR
24.0	1.0	144.0	.00	ND	24375	RR
16.0	1.0	56.0	.10	ND	24939	RR
106.0	1.0	40.0	.10	ND	25259	RR
52.0	1.0	32.0	.10	ND	25270	RR

APPENDIX B (contd.)

Raw Geochemical and Magnetic Data

Cu (ppm)	Mo (ppm)	Zn (ppm)	Ag (ppm)	MAG. (gammas)	ID	Code
10.0	1.0	34.0	.10	ND	25282	RR
50.0	3.0	62.0	.60	ND	25314	RR
2.0	1.0	86.0	.10	ND	25347	RR
8.0	1.0	74.0	.10	ND	25348	RR
375.0	1.0	29.0	.10	ND	27612	RR
9.0	1.0	56.0	.10	ND	27613	RR
14.0	1.0	50.0	.10	ND	27614	RR
7.0	54.0	4.0	.10	ND	27615	RR
2850.0	2.0	110.0	.80	ND	27616	RR
33.0	14.0	84.0	.00	ND	27617	RR
12.0	8.0	86.0	.20	ND	27618	RR
3100.0	14.0	76.0	.50	ND	27621	RR
7.0	3.0	20.0	.20	ND	7450	RR
22.0	1.0	45.0	.50	ND	7551	RR
90.0	2.0	37.0	.80	ND	7584	RR
6.0	2.0	12.0	.20	ND	7589	RR
7.0	2.0	12.0	.20	ND	7590	RR
5.0	1.0	17.0	.10	ND	7752	RR
6.0	1.0	36.0	.10	ND	7753	RR
4.0	1.0	44.0	.10	ND	7754	RR
8.0	1.0	14.0	.60	ND	7760	RR
38.0	1.0	525.0	.80	ND	9180	RR
17.0	2.0	168.0	.00	ND	9186	RR
8.0	1.0	32.0	.10	ND	9190	RR
6.0	1.0	9.0	.10	ND	9192	RR
4.0	1.0	13.0	.10	ND	9193	RR
10.0	1.0	62.0	.10	ND	9196	RR
6.0	1.0	86.0	.10	ND	9199	RR
4.0	1.0	18.0	.20	ND	9200	RR
12.0	2.0	70.0	.10	ND	9201	RR
28.0	5.0	86.0	.30	ND	9202	RR
6.0	1.0	78.0	.10	ND	9203	RR
13.0	1.0	33.0	.10	ND	9204	RR
6.0	1.0	40.0	.10	ND	9206	RR
12.0	1.0	60.0	.10	ND	9208	RR
9.0	1.0	29.0	.10	ND	9210	RR
4.0	1.0	21.0	.10	ND	9211	RR
10.0	4.0	124.0	.10	ND	9212	RR
42.0	2.0	166.0	.20	ND	9213	RR
14.0	1.0	82.0	.10	ND	9217	RR
9.0	1.0	37.0	.10	ND	9218	RR
9.0	1.0	102.0	.20	ND	9219	RR
6.0	1.0	13.0	.10	ND	9221	RR
4.0	1.0	120.0	.10	ND	9224	RR
4.0	1.0	12.0	.10	ND	9226	RR
7.0	1.0	34.0	.10	ND	9227	RR

APPENDIX B (contd.)

Raw Geochemical and Magnetic Data

Cu (ppm)	Mo (ppm)	Zn (ppm)	Ag (ppm)	MAG (gammas)	ID	Code
88.0	23.0	230.0	.60	ND	9230	RR
17.0	2.0	11.0	.10	ND	9234	RR
420.0	1.0	17.0	.20	ND	9238	RR
22.0	1.0	148.0	.10	ND	23210	RS
18.0	1.0	68.0	.10	ND	23213	RS
18.0	1.0	58.0	.10	ND	23214	RS
21.0	1.0	60.0	.10	ND	23216	RS
15.0	1.0	65.0	.10	ND	23217	RS
18.0	1.0	95.0	.30	ND	23218	RS
12.0	2.0	48.0	.10	ND	23221	RS
16.0	1.0	120.0	.30	ND	23224	RS
29.0	2.0	176.0	.20	ND	23227	RS
22.0	2.0	125.0	.10	ND	23229	RS
28.0	1.0	128.0	.20	ND	23230	RS
14.0	1.0	162.0	.40	ND	23232	RS
22.0	1.0	48.0	.10	ND	23233	RS
12.0	2.0	70.0	.10	ND	23234	RS
38.0	1.0	60.0	.10	ND	23236	RS
7.0	2.0	10.0	.10	ND	23238	RS
30.0	2.0	60.0	.10	ND	23239	RS
37.0	1.0	90.0	.10	ND	23260	RS
22.0	1.0	60.0	.10	ND	23262	RS
58.0	2.0	90.0	.10	ND	23264	RS
11.0	2.0	98.0	.10	ND	23266	RS
14.0	4.0	65.0	.60	ND	23267	RS
38.0	2.0	97.0	.10	ND	23268	RS
47.0	1.0	109.0	.20	ND	23269	RS
38.0	2.0	82.0	.10	ND	23270	RS
46.0	4.0	120.0	.20	ND	23271	RS
67.0	3.0	146.0	.20	ND	23272	RS
74.0	3.0	120.0	.10	ND	23273	RS
138.0	3.0	150.0	.10	ND	23274	RS
54.0	1.0	98.0	.10	ND	23275	RS
86.0	5.0	230.0	.30	ND	23276	RS
35.0	2.0	85.0	.10	ND	23278	RS
80.0	1.0	98.0	.10	ND	23279	RS
21.0	1.0	47.0	.10	ND	23280	RS
21.0	1.0	75.0	.10	ND	23385	RS
20.0	2.0	55.0	.10	ND	23393	PS
26.0	1.0	80.0	.10	ND	23394	RS
18.0	1.0	58.0	.10	ND	23395	RS
18.0	1.0	74.0	.10	ND	23396	RS
18.0	1.0	102.0	.20	ND	23397	RS
15.0	1.0	120.0	.30	ND	23398	RS
26.0	1.0	84.0	.40	ND	23400	RS
46.0	1.0	86.0	.10	ND	23548	RS

APPENDIX B (contd.)

Raw Geochemical and Magnetic Data

Cu (ppm)	Mo (ppm)	Zn (ppm)	Ag (ppm)	MAG (gammas)	ID	Code
35.0	1.0	72.0	.10	ND	23549	RS
20.0	1.0	110.0	.70	ND	23680	RS
18.0	1.0	110.0	.30	ND	23681	RS
8.0	1.0	45.0	.20	ND	23685	RS
15.0	1.0	65.0	.20	ND	23686	RS
10.0	1.0	92.0	.10	ND	23688	RS
12.0	1.0	115.0	.10	ND	23689	RS
22.0	1.0	78.0	.20	ND	23693	RS
17.0	1.0	78.0	.20	ND	23697	RS
13.0	1.0	98.0	.40	ND	23698	RS
34.0	5.0	255.0	.10	ND	24027	RS
11.0	1.0	62.0	.10	ND	24151	RS
27.0	1.0	76.0	.10	ND	24152	RS
25.0	1.0	74.0	.10	ND	24153	RS
35.0	1.0	72.0	.10	ND	24155	RS
26.0	1.0	72.0	.10	ND	24156	RS
32.0	1.0	47.0	.10	ND	24157	RS
29.0	1.0	42.0	.10	ND	24160	RS
31.0	1.0	62.0	.20	ND	24161	RS
23.0	1.0	63.0	.10	ND	24162	RS
21.0	1.0	62.0	.10	ND	24164	RS
12.0	1.0	58.0	.10	ND	24165	RS
32.0	1.0	58.0	.10	ND	24166	RS
19.0	1.0	22.0	.10	ND	24168	RS
50.0	2.0	125.0	.10	ND	24245	RS
32.0	1.0	40.0	.10	ND	24247	RS
28.0	2.0	58.0	.10	ND	24249	RS
56.0	1.0	112.0	.10	ND	24323	RS
38.0	1.0	60.0	.10	ND	24324	RS
98.0	1.0	194.0	.10	ND	24325	RS
82.0	1.0	78.0	.10	ND	24328	RS
94.0	1.0	54.0	.10	ND	24329	RS
84.0	2.0	150.0	.10	ND	24331	RS
40.0	1.0	54.0	.10	ND	24332	RS
64.0	4.0	170.0	.20	ND	24333	RS
64.0	2.0	188.0	.20	ND	24334	RS
124.0	7.0	220.0	.10	ND	24335	RS
84.0	3.0	174.0	.30	ND	24336	RS
44.0	1.0	130.0	.60	ND	24338	RS
32.0	1.0	112.0	.40	ND	24339	RS
66.0	1.0	108.0	.10	ND	24341	RS
54.0	5.0	118.0	.80	ND	24343	RS
52.0	1.0	150.0	.40	ND	24344	RS
34.0	1.0	84.0	.20	ND	24345	RS
72.0	6.0	126.0	.80	ND	24346	RS
84.0	4.0	192.0	.80	ND	24348	RS

APPENDIX B (contd.)

Raw Geochemical and Magnetic Data

Cu (ppm)	Mo (ppm)	Zn (ppm)	Ag (ppm)	MAG (gammas)	ID	Code
32.0	1.0	78.0	.10	ND	24349	RS
24.0	1.0	58.0	.10	ND	24350	RS
32.0	1.0	68.0	.10	ND	24351	RS
98.0	1.0	160.0	.20	ND	24352	RS
18.0	1.0	42.0	.20	ND	24353	RS
22.0	1.0	70.0	.10	ND	24354	RS
30.0	1.0	64.0	.10	ND	24355	RS
46.0	1.0	70.0	.10	ND	24356	RS
26.0	1.0	76.0	.10	ND	24359	RS
10.0	1.0	48.0	.10	ND	24361	PS
8.0	1.0	18.0	.10	ND	24364	RS
18.0	1.0	134.0	.10	ND	24365	RS
14.0	1.0	46.0	.10	ND	24366	RS
6.0	1.0	30.0	.10	ND	24367	RS
10.0	1.0	102.0	.20	ND	24369	RS
14.0	1.0	104.0	.10	ND	24370	RS
16.0	1.0	80.0	.10	ND	24371	RS
28.0	1.0	182.0	.10	ND	24891	RS
30.0	1.0	96.0	.10	ND	24892	RS
18.0	1.0	40.0	.10	ND	24893	RS
20.0	1.0	168.0	.10	ND	24894	RS
20.0	1.0	168.0	.10	ND	24894	RS
14.0	1.0	76.0	.30	ND	24896	RS
10.0	1.0	68.0	.40	ND	24898	RS
12.0	1.0	52.0	.10	ND	24900	RS
14.0	1.0	80.0	.10	ND	24940	RS
14.0	1.0	70.0	.10	ND	24941	RS
14.0	1.0	60.0	.10	ND	24943	RS
14.0	1.0	58.0	.10	ND	24944	RS
24.0	1.0	52.0	.10	ND	24945	RS
20.0	1.0	72.0	.10	ND	24947	RS
18.0	1.0	60.0	.10	ND	24948	RS
22.0	1.0	60.0	.10	ND	24950	PS
18.0	1.0	62.0	.10	ND	24951	RS
30.0	1.0	54.0	.10	ND	24952	RS
22.0	1.0	50.0	.10	ND	24953	RS
22.0	1.0	40.0	.10	ND	24954	RS
24.0	1.0	54.0	.10	ND	24955	RS
24.0	1.0	60.0	.10	ND	24956	PS
28.0	1.0	60.0	.00	ND	24957	RS
36.0	2.0	40.0	.00	ND	24958	RS
22.0	2.0	52.0	.10	ND	24959	RS
22.0	1.0	58.0	.10	ND	24960	RS
18.0	1.0	50.0	.20	ND	24961	RS
18.0	1.0	108.0	.00	ND	24962	RS
20.0	1.0	76.0	.10	ND	24963	RS

APPENDIX B (contd.)

Raw Geochemical and Magnetic Data

Cu (ppm)	Mo (ppm)	Zn (ppm)	Ag (ppm)	MAG (gammas)	ID	Code
24.0	1.0	68.0	.10	ND	24964	RS
28.0	1.0	60.0	.10	ND	24965	RS
20.0	1.0	36.0	.20	ND	24966	RS
18.0	1.0	64.0	.20	ND	25251	RS
10.0	1.0	48.0	.10	ND	25253	RS
18.0	1.0	82.0	.10	ND	25254	RS
16.0	1.0	40.0	.10	ND	25255	RS
16.0	1.0	58.0	.10	ND	25256	RS
52.0	1.0	84.0	.10	ND	25258	RS
40.0	1.0	54.0	.10	ND	25260	RS
14.0	1.0	80.0	.10	ND	25261	RS
38.0	2.0	98.0	.20	ND	25262	RS
42.0	1.0	116.0	.10	ND	25263	RS
20.0	1.0	106.0	.10	ND	25264	RS
30.0	1.0	70.0	.10	ND	25265	RS
58.0	1.0	84.0	.10	ND	25266	RS
32.0	1.0	68.0	.10	ND	25267	RS
32.0	1.0	68.0	.10	ND	25268	RS
50.0	1.0	42.0	.20	ND	25269	RS
30.0	1.0	62.0	.10	ND	25272	RS
50.0	1.0	42.0	.10	ND	25273	RS
40.0	1.0	42.0	.10	ND	25274	RS
24.0	1.0	54.0	.10	ND	25275	RS
60.0	1.0	70.0	.10	ND	25276	RS
44.0	1.0	62.0	.10	ND	25277	RS
22.0	1.0	64.0	.10	ND	25278	RS
30.0	1.0	62.0	.10	ND	25279	RS
26.0	1.0	64.0	.10	ND	25280	RS
20.0	1.0	50.0	.10	ND	25281	RS
42.0	1.0	22.0	.20	ND	25283	RS
50.0	1.0	58.0	.10	ND	25284	RS
54.0	1.0	160.0	.10	ND	25286	RS
22.0	1.0	68.0	.10	ND	25287	RS
30.0	1.0	78.0	.10	ND	25299	RS
66.0	1.0	88.0	.10	ND	25300	RS
20.0	1.0	66.0	.10	ND	25310	RS
68.0	1.0	78.0	.10	ND	25311	RS
24.0	1.0	54.0	.10	ND	25312	RS
22.0	1.0	44.0	.10	ND	25313	RS
36.0	1.0	56.0	.50	ND	25315	RS
44.0	1.0	104.0	.10	ND	25316	RS
26.0	1.0	90.0	.10	ND	25317	RS
46.0	1.0	84.0	.30	ND	25318	RS
38.0	2.0	98.0	.40	ND	25319	RS
48.0	1.0	72.0	.10	ND	25320	RS
36.0	1.0	74.0	.10	ND	25321	RS

APPENDIX B (contd.)

Raw Geochemical and Magnetic Data

Cu (ppm)	Mo (ppm)	Zn (ppm)	Ag (ppm)	MAG (gammas)	ID	Code
30.0	1.0	80.0	.10	ND	25323	RS
18.0	1.0	66.0	.10	ND	25324	RS
16.0	1.0	58.0	.10	ND	25325	RS
46.0	1.0	72.0	.10	ND	25326	RS
112.0	1.0	96.0	.10	ND	25327	RS
36.0	2.0	108.0	.20	ND	25328	RS
40.0	1.0	98.0	.20	ND	25329	RS
46.0	3.0	136.0	.50	ND	25330	RS
42.0	1.0	70.0	.10	ND	25332	RS
40.0	1.0	84.0	.10	ND	25333	RS
50.0	1.0	142.0	.10	ND	25334	RS
30.0	1.0	62.0	.10	ND	25336	RS
42.0	1.0	88.0	.10	ND	25337	RS
32.0	1.0	84.0	.10	ND	25339	RS
36.0	1.0	92.0	.10	ND	25341	PS
24.0	2.0	64.0	.10	ND	25342	RS
200.0	3.0	106.0	.10	ND	25343	RS
16.0	1.0	108.0	.10	ND	25344	RS
28.0	1.0	90.0	.10	ND	25345	RS
18.0	1.0	62.0	.10	ND	25346	RS
20.0	1.0	56.0	.10	ND	25349	RS
22.0	1.0	58.0	.10	ND	25350	RS
20.0	2.0	44.0	.20	ND	25614	PS
22.0	1.0	52.0	.10	ND	25615	RS
18.0	1.0	86.0	.10	ND	25616	RS
20.0	1.0	84.0	.10	ND	25617	RS
6.0	1.0	38.0	.10	ND	25618	RS
36.0	1.0	50.0	.10	ND	25702	RS
42.0	1.0	100.0	.10	ND	25704	RS
38.0	1.0	54.0	.10	ND	25705	RS
30.0	1.0	54.0	.10	ND	25706	RS
34.0	1.0	76.0	.10	ND	25707	RS
46.0	1.0	66.0	.10	ND	25709	RS
38.0	1.0	120.0	.10	ND	25710	RS
34.0	1.0	92.0	.10	ND	25712	RS
23.0	1.0	66.0	.10	ND	27842	RS
22.0	1.0	96.0	.10	ND	27843	RS
24.0	1.0	56.0	.10	ND	27844	RS
26.0	5.0	52.0	.10	ND	27845	RS
305.0	4.0	96.0	.20	ND	27846	RS
80.0	7.0	92.0	.30	ND	27847	RS
60.0	2.0	64.0	.10	ND	27848	PS
36.0	1.0	70.0	.20	ND	27849	RS
25.0	1.0	120.0	.30	ND	27850	RS
25.0	1.0	64.0	.10	ND	27978	RS
31.0	3.0	80.0	.10	ND	27979	RS

APPENDIX B (contd.)

Raw Geochemical and Magnetic Data

Cu (ppm)	Mo (ppm)	Zn (ppm)	Ag (ppm)	MAG (gammas)	ID	Code
80.0	8.0	60.0	.80	ND	27980	RS
21.0	1.0	120.0	.20	ND	27981	RS
18.0	1.0	87.0	.60	ND	7581	RS
18.0	1.0	76.0	.60	ND	7588	RS
23.0	3.0	71.0	.90	ND	7758	RS
23.0	1.0	205.0	.70	ND	9179	RS
26.0	1.0	78.0	.20	ND	9181	RS
24.0	1.0	140.0	.80	ND	9182	RS
16.0	1.0	190.0	.60	ND	9183	RS
17.0	2.0	168.0	.00	ND	9184	RS
18.0	2.0	118.0	.20	ND	9185	RS
14.0	1.0	215.0	.10	ND	9187	RS
19.0	1.0	70.0	.10	ND	9188	RS
16.0	1.0	104.0	.10	ND	9189	RS
21.0	1.0	160.0	.60	ND	9191	RS
20.0	1.0	74.0	.20	ND	9194	RS
19.0	1.0	56.0	.10	ND	9195	RS
24.0	1.0	132.0	.30	ND	9197	RS
20.0	1.0	124.0	.40	ND	9198	RS
22.0	1.0	74.0	.20	ND	9205	RS
25.0	4.0	116.0	.30	ND	9207	RS
36.0	1.0	120.0	.20	ND	9209	RS
52.0	6.0	138.0	.30	ND	9214	RS
24.0	2.0	90.0	.10	ND	9215	RS
21.0	1.0	100.0	.50	ND	9216	RS
31.0	1.0	100.0	.20	ND	9220	RS
15.0	3.0	60.0	.30	ND	9222	RS
4.0	1.0	120.0	.10	ND	9223	RS
15.0	2.0	62.0	.10	ND	9225	RS
8.0	2.0	19.0	.10	ND	9228	RS
44.0	3.0	70.0	.20	ND	9229	RS
64.0	3.0	144.0	.10	ND	9231	RS
38.0	1.0	84.0	.10	ND	9232	RS
28.0	1.0	60.0	.10	ND	9233	RS
83.0	2.0	84.0	.30	ND	9235	RS
92.0	1.0	54.0	.20	ND	9236	RS
51.0	1.0	86.0	.20	ND	9237	RS
37.0	1.0	88.0	.10	ND	9239	RS
78.0	2.0	30.0	.10	ND	9240	RS
11.0	1.0	32.0	.10	ND	9241	RS
90.0	1.0	90.0	.10	ND	9242	RS
16.0	1.0	118.0	.10	ND	23222	RW
28.0	1.0	98.0	.10	ND	23301	RW
12.0	1.0	65.0	.10	ND	23387	RW
15.0	1.0	82.0	.20	ND	23391	PW
14.0	1.0	120.0	.20	ND	23392	RW

APPENDIX B (contd.)

Raw Geochemical and Magnetic Data

Cu (ppm)	Mo (ppm)	Zn (ppm)	Ag (ppm)	MAG (gammas)	ID	Code
8.0	1.0	104.0	.30	ND	23399	RW
25.0	1.0	140.0	.10	ND	23550	RW
10.0	1.0	98.0	.10	ND	23676	RW
26.0	3.0	139.0	.40	ND	23679	RW
14.0	1.0	100.0	.60	ND	23682	RW
15.0	2.0	134.0	.20	ND	23684	RW
9.0	1.0	120.0	.20	ND	23687	RW
15.0	1.0	120.0	.40	ND	23699	RW
10.0	2.0	68.0	.10	ND	23857	RW
16.0	3.0	110.0	.10	ND	23859	RW
19.0	2.0	200.0	.10	ND	23861	RW
6.0	1.0	45.0	.10	ND	24154	RW
19.0	1.0	52.0	.10	ND	24158	RW
11.0	1.0	57.0	.10	ND	24163	RW
9.0	1.0	76.0	.20	ND	24167	RW
4.0	1.0	30.0	.10	ND	24246	RW
9.0	1.0	61.0	.10	ND	24248	RW
15.0	2.0	46.0	.10	ND	24250	RW
68.0	1.0	184.0	.60	ND	24337	RW
20.0	1.0	134.0	.20	ND	24340	RW
52.0	3.0	174.0	.50	ND	24347	RW
14.0	1.0	60.0	.10	ND	24357	RW
24.0	1.0	110.0	.20	ND	24360	RW
16.0	1.0	64.0	.10	ND	24363	RW
14.0	1.0	66.0	.20	ND	24368	RW
4.0	4.0	96.0	.10	ND	24374	RW
16.0	1.0	510.0	.40	ND	24895	RW
14.0	1.0	144.0	.30	ND	24897	RW
10.0	1.0	86.0	.10	ND	24899	RW
16.0	1.0	110.0	.10	ND	24942	RW
10.0	1.0	48.0	.10	ND	24946	RW
20.0	1.0	78.0	.10	ND	24949	RW
16.0	1.0	96.0	.20	ND	25252	RW
12.0	1.0	78.0	.10	ND	25257	RW
32.0	1.0	134.0	.20	ND	25271	RW
34.0	1.0	92.0	.10	ND	25285	RW
36.0	1.0	124.0	.40	ND	25322	RW
40.0	1.0	88.0	.10	ND	25331	RW
16.0	1.0	70.0	.10	ND	25335	RW
10.0	1.0	68.0	.10	ND	25338	RW
26.0	1.0	64.0	.10	ND	25340	RW
70.0	1.0	60.0	.10	ND	25701	RW
20.0	1.0	108.0	.10	ND	25703	RW
32.0	1.0	90.0	.10	ND	25708	RW
24.0	1.0	46.0	.10	ND	25711	RW
17.0	1.0	48.0	.60	ND	7280	RW

APPENDIX B (contd.)

Raw Geochemical and Magnetic Data

Cu (ppm)	Mo (ppm)	Zn (ppm)	Ag (ppm)	MAG (gammas)	ID	Code
3.0	1.0	42.0	.70	ND	7281	RW
9.0	1.0	65.0	.60	ND	7282	RW